Three-Dimensional Echocardiography for the Assessment of Congenital and Acquired Heart Disease

BY

Aleksandra Lange

Doctor of Medicine

The University of Edinburgh

1999

ABSTRACT

Although conventional two-dimensional and Doppler blood-flow echocardiography are the standard imaging approaches in the assessment of heart disease they do not provide anatomic reconstructions in a form that resembles the cardiac morphology as visualized by the surgeon.

The work presented in this thesis has explored the hypotheses that three-dimensional echocardiography facilitates spatial recognition of intracardiac structures and therefore enhances the diagnostic confidence of echocardiography in congenital and acquired heart disease. The accuracy of three-dimensional reconstructions has been validated *in vitro* using two different phantoms and *in vivo* comparing the results with other established diagnostic techniques or surgical findings. Additionally, as the main limitation of transthoracic three-dimensional echocardiography is poor image quality in a substantial proportion of adult patients, Doppler myocardial imaging has been tested as a potentially superior method to conventional grey-scale imaging for transthoracic three-dimensional image acquisition.

In vitro, using a virtual computer-generated phantom and a dynamic tissue-mimicking phantom, the accuracy of both linear measurements and volume computation obtained from three-dimensional images was established. For both grey-scale and Doppler myocardial imaging, a detail of 1.0 mm dimension and two details separated from each other by a distance of 1.0 mm were the smallest structures and distances identified from a three-dimensional image. When testing the accuracy of volume measurements it appeared that both techniques marginally underestimated the true phantom volume (by approximately 1.0 ml for Doppler myocardial imaging and 4.0 ml for grey-scale imaging), but the systematic error was

smaller and more constant in the case of Doppler myocardial imaging over the range of different true volumes.

In vivo, the study was designed to compare the accuracy of grey-scale and Doppler myocardial imaging three-dimensional left ventricular volume measurements and cineventriculography. The differences were significantly smaller for the Doppler technique during both end-diastole and end-systole. A series of congenital heart lesions has also been studied. It has been shown that dynamic surgical reconstruction of the secundum atrial septal defect is feasible from the transthoracic approach in all patients. However, in adults, Doppler myocardial imaging proved more effective than grey-scale imaging in the accuracy of three-dimensional defect reconstruction. In patients with sinus venosus atrial septal defect, transthoracic three-dimensional echocardiography was more accurate than standard echocardiography in diagnosing the defect including a detailed description of the abnormal pulmonary venous drainage. Finally, in children with atrio-ventricular septal defects, the 'unroofed' atrial reconstruction of the common valve accurately displayed dynamic valve morphology *en face* and the mechanism of valve reflux.

F A I T H

Faith is in you whenever you look

At a dewdrop or a floating leaf

And know that they are because they have to be.

Even if you close your eyes and dream up things

The world will remain as it has always been

And the leaf will be carried by the waters of the rivers.

You have faith also when you hurt your foot

Against a sharp rock and you know

That rocks are here to hurt our feet.

See the long shadow that is cast by the tree?

We and the flowers throw shadows on the earth.

What has no shadow has no strength to live.

Czesław Miłosz

'But it is hardly a consolation,

that I will be read by doctoral

candidates - what they do not read!

One would like to do something

not only for library dust.'

Czesław Miłosz

CONTENTS

DECLARATION

This thesis describes research undertaken in the Department of Cardiology at the Western General Hospital from my position as Clinical Research Fellow in the Cardiovascular Research Unit of Edinburgh University during the period from 1994 to 1998. I have been fortunate in having the advice and help of several colleagues who are formally acknowledged. The substantial part of the work in this thesis has been my own and the writing of this thesis has been entirely my own undertaking. Part of the work presented has been published in peer reviewed academic journals and copies of these publications and other relevant publications of my own constitute the Appendix.

ACKNOWLEDGEMENTS

The work presented in this thesis was carried out whilst I was Clinical Research Fellow in the Cardiovascular Research Unit of Edinburgh University and Honorary Registrar in the Department of Cardiology at the Western General Hospital in Edinburgh.

I would like to express special gratitude to Dr Michael J Godman who was instrumental in generating the hypotheses I have sought to test and who has provided crucial support for the work I have carried out. I am also grateful to him for his helpful comments on the text of this thesis.

Throughout these studies I have had great good fortune in working with colleagues whose commitment to our projects has ensured their success and, in particular, I am grateful to Dr Mohammed Walayat for help and enthusiasm in carrying out studies with children.

For the original impetus to start on this work I am very grateful to Professor George Sutherland, who supported the initial stages of my work.

I am indebted to Mr Pankaj Mankad, cardiothoracic surgeon, for much needed help in understanding complex spatial morphology of different congenital heart defects.

I would like to thank Professor Keith Fox who has provided invaluable encouragement and constructive advice when it was most needed.

It would not have been possible to carry out these studies without the financial support of the Scottish Office and the Chest, Heart and Stroke Association of Scotland.

More than any others I thank my husband Przemek and my parents Teresa and Andrzej for their sacrifices and patience. I dedicate this work to them.

PREFACE

Three-dimensional echocardiography is an imaging technique that is in active evolution. Since 1974 the technique has evolved from potentially interesting but crude, and limited for practical use, to the user friendly and almost clinically practical where the acquisition of dynamic and high-resolution three-dimensional images of heart structures takes no longer than a couple of minutes. Although three-dimensional echocardiography is potentially seen as the most informative method of assessing complex heart malformations, the experience of using it in clinical practice is limited and requires further validation in a series of clinical studies.

The aim of this thesis was to assess the feasibility of transthoracic three-dimensional echocardiography in the assessment of congenital and acquired heart disease.

Previous studies on three-dimensional ultrasound image reconstruction have been carried out using standard grey-scale (B-mode) imaging technique. In these reports, due to poor transthoracic image quality, standard grey-scale images were frequently acquired from a transoesophageal approach. In this thesis the additional value of Doppler myocardial imaging as potentially superior to grey-scale imaging technique for three-dimensional transthoracic echocardiography has been assessed.

After a general overview, provided in Chapter 1, the methodology of three-dimensional image acquisition used in this thesis is presented in Chapter 2.

Chapter 3 deals with the *in vitro* validation of the spatial resolution of reconstructed three-dimensional images. Also, the *in vitro* accuracy of three-dimensional volume computation has been assessed in this chapter. These *in vitro* studies have been performed using the two imaging techniques of standard grey-scale and Doppler myocardial imaging.

In the next four chapters the potential clinical applications of three-dimensional echocardiography were evaluated in various heart conditions.

Volume measurements by three-dimensional echocardiography allow the elimination of geometrical assumptions. This is addressed in Chapter 4 where a clinical study has been designed to compare the accuracy of standard grey-scale and Doppler myocardial imaging three-dimensional volume measurements by comparing them to the clinically accepted method of left ventricular volume measurement, cineventriculography.

Chapter 5 evaluates the usefulness of three-dimensional echocardiography in the imaging of secundum atrial septal defect. With the growing interest in new techniques of atrial septal defect closure, the precise assessment of the defect size, morphology and its spatial relations to other cardiac structures is crucial for optimum patient selection. Therefore, in Chapter 5 the feasibility of transthoracic three-dimensional echocardiography in the assessment of size and morphology of secundum atrial septal defect was studied. The diagnostic information obtained from three-dimensional reconstructed images (both grey-scale and Doppler myocardial images) has been compared to Magnetic Resonance Imaging and intraoperative findings.

In Chapter 6 the role of transthoracic three-dimensional echocardiography in the diagnosis of sinus venosus atrial septal defect was evaluated. Sinus venosus is an uncommon but also an underdetected congenital cardiac anomaly. Because of the extraseptal location of the interatrial communication it is often not readily diagnosed by two-dimensional transthoracic echocardiography. Therefore, an accurate transthoracic technique to diagnose this heart defect would be of great value.

Chapter 7 describes the feasibility of transthoracic three-dimensional echocardiography in the pre-operative assessment of atrio-ventricular septal defect. Although, the presence of the defect can readily be diagnosed by transthoracic two-dimensional echocardiography, three-dimensional reconstruction of the exact morphology of the common atrio-ventricular valve and the display of the mechanism of valve reflux should enhance preoperative information and potentially improve surgical reconstruction.

Finally, Chapter 8 provides a summary and states the conclusions of the thesis.

Separate studies are described in each of the data chapters. A similar layout is employed in each, consisting of the background, study aims, methods, results, discussion and conclusions. To avoid the risk of introducing a degree of repetition in the methods section, Chapter 1 describes the protocol for image acquisition in detail and the consecutive methodology sections of each chapter therefore emphasise the important differences that exist between the studies.

CHAPTER 1

Three-dimensional echocardiography

An overview

1.1. Introduction

Echocardiography has evolved over the last four decades from single beam imaging to sophisticated three-dimensional and Doppler techniques which allow us to study cardiac structure, function and haemodynamics in detail.

It was in the early 1950s that the collaboration of a cardiologist, Inge Edler and a physicist, Hellmuth Hertz resulted in the recording of the first M-mode echocardiogram [Edler and Hertz, 1954]. A few years later, in 1957, the first paper was published in English by Satomura about the feasibility of the Doppler phenomenon in detecting moving cardiac structures [Satomura, 1957]. This publication laid the foundations to another important development that was reported in 1969 independently by Baker in the USA, Peronneau in France and Wells in Britain and which demonstrated the clinical feasibility of the range-gated pulsed Doppler principle [Baker, 1969; Peronneau et al., 1969; Wells, 1969]. Almost in parallel, in 1972, Bom and colleagues constructed the first practical two-dimensional real-time scanner and demonstrated the potential of this technique in diagnosing heart disease [Bom, 1972]. Duplex scanning, which meant that two-dimensional imaging could be used to identify the anatomical position of the Doppler beam, was invented in the USA in 1980 by Phillips and colleagues [Phillips et al., 1980]. The introduction of Doppler colour flow mapping can be regarded as a natural extension of duplex scanning. In 1981 Eyer and colleagues described a colour flow mapping system operating at an image frame rate of four per second [Eyer et al., 1981]. This was regarded too slow for diagnostic cardiac investigation. Four years later, in 1985, a Japanese engineer Kasai and co-workers developed real-time colour flow mapping [Kasai et al., 1985].

Thus, echocardiography in the form that is used today in clinical practice was born effectively in 1985.

1.2. Basic concepts of three-dimensional echocardiography

One of the chief goals of cardiac imaging is to display the anatomy of the heart throughout its cycle. From the assessment of cardiac morphology the size, shape, and function of the chambers and valves, as well as the spatial relationships of these structures can be evaluated. The latter information is of the most obvious importance in congenital cardiac disorders, where complex morphology is commonly seen. Most cardiac imaging methods attempt to depict the details of cardiac geometry by offering several individual projection views (e.g. angiography) or topographic sections (e.g. echocardiography, computed tomography, or magnetic resonance) through the heart. A mental reconstruction of these views into a three-dimensional image of the heart is then required. The usual method of achieving this mental picture is qualitative, based on experience examining images of many normal and abnormal hearts. Another alternative is to utilise a computer-reconstructed three-dimensional image or model of the heart. The purpose of such computer-based three-dimensional images is to replace the mental picture of cardiac geometry with a computer generated image that can be displayed in various orientations and even 'sliced' by the computer to delineate better the complexities of cardiac anatomy.

Two main approaches are used for the display of three-dimensional cardiac images: (1) wire-frame displays that in general are associated with acoustic transducer position registration systems and (2) shaded surface (volume-rendered) displays usually associated with mechanical transducer position registration systems.

The general steps in performing three-dimensional ultrasound reconstruction include: (1) acquiring each two-dimensional image along with the information on its position and orientation relative to other images acquired; (2) interpolation of data between original two-dimensional images in order to complete the three-dimensional data-set for display and analysis; (3) reconstructing the several two-dimensional cut-planes into a three-dimensional data structure with a global, three-dimensional co-ordinate system; (4) display of the three-dimensional data; and (5) computing of quantitative variables from the three-dimensional reconstruction, such as distances, angles, and volumes at any phase of the cardiac cycle.

These steps differ slightly between the volume-rendered and wire-frame three-dimensional echocardiography.

1.2.1. Image acquisition and registration

Recording of echocardiographic data for reassembly into a three-dimensional data-set requires the use of a spatial registration device to record the position and orientation of the transducer as each individual two-dimensional image is obtained. This problem has been solved in a variety of ways, including the use of acoustic, mechanical and laser-based position registration devices. So far, most experience has been achieved with acoustic and mechanical transducer position registration systems and these will be summarised below.

Acoustic transducer position registration systems

To acquire a three-dimensional data-set, a conventional real-time ultrasound scanner is linked to an acoustical three-dimensional spatial locating system that associates spatial co-ordinate information with each acquired two-dimensional image. The first

three-dimensional spatial locator was designed by King et al. as an acoustical position-tracking system composed of an array of four point microphone receivers plus electronic circuitry [King et al., 1976]. Using the system of King et al., three sound emitters need to be fixed in a small triangle on a metal plate attached to the ultrasound transducer. The four acoustic point microphone receivers are mounted in a square array on a frame suspended from a stand. The sound emitters, energised in a rapid sequence, produce 60-kHz sound waves that travel to each of the four overhead microphones. The time of flight of the sound from each emitter to each microphone is being measured, corrected for environmental conditions, and used to calculate a slant range between the two points. From these slant ranges the X,Y,Z co-ordinates of the transducer and subsequently its image are computed in a spatial co-ordinate system defined by the microphone array. The ultrasound images and their spatial co-ordinate data are combined in the computer video display to produce a three-dimensional data-set. Any ultrasound scanner may be used if its video image signal is accessible for transmission to the computer and the sound emitter array may be attached to the transducer head. The *in vitro* analysis of the potential accuracy of this system showed that (1) the three-dimensional scanner per se does not introduce significant new errors into echocardiographic measurements; (2) the measurement of dimensions, angles, and volumes can be achieved with a very high degree of accuracy; and (3) the principal source of error in echocardiographic measurement is related to the poor lateral resolution caused by the ultrasound beam width [King et al., 1991].

Several similar three-dimensional scanners based on the same principle of using acoustic spatial locator have been developed by others. [Brinkley et al., 1982; Moritz et al., 1983; Levine et al., 1989].

Mechanical transducer position registration systems

Dynamic three-dimensional echocardiographic reconstruction of the left ventricle using a mechanical type of locator system was first described in 1974 by Dekker et al. [Dekker et al., 1974]. Later, in 1982 this approach was used again in an improved form by Geiser et al. and Ghosh et al. [Geiser et al., 1982; Ghosh et al., 1982].

Geiser and colleagues have used a special mechanical arm with five 'degrees of freedom'. The method described allowed for a three-dimensional reconstruction of the contracting left ventricle from five two-dimensional short-axis cross-sections and the parasternal and apical long-axis views. The three-dimensional reconstruction was carried out using measurements from a mechanical arm which had five degrees of freedom and which allowed spatial registration of two-dimensional planes with respect to a fixed external reference point. The rotational or linear motion of the probe was recorded by five calibrated high precision potentiometers. With the information from this arm, the X, Y, and Z co-ordinates of each of twelve points on the epicardial and endocardial borders in each video field of each of the five cross-sections was calculated for one cardiac cycle. The indices that could be calculated from these three-dimensional data-sets were muscle volume/mass, chamber volume, stroke volume, cardiac output and volume dynamics i.e. systolic ejection rate and diastolic filling rate. The approximate time of data acquisition was between thirty minutes and over one hour. Cycle selection, stop-frame photography, printing border

selection, and digitising took from four to seven days of interaction between technician and the echocardiographer.

The difference between the report of Geiser et al. [Geiser et al., 1982] and that of Ghosh et al. [Ghosh et al., 1982] is that Ghosh used an apical transthoracic window rather than a parasternal for three-dimensional image acquisition. Once the transducer was applied to the chest (either in parasternal or apical view) it was then rotated in 30° increments from 0° to 180° to obtain different two-dimensional cross-sections. The acquisition was electrocardiographically triggered, and both end-diastolic and end-systolic frames were obtained at every angular increment. 0° and 180° images were exact mirror images of each other. For three-dimensional reconstruction, two mutually orthogonal cursors were used to digitise two-dimensional data with respect to a fixed co-ordinate system with its origin at the transducer position. The left and right points of each view, were plotted at the specified angle. The final area was reconstructed at a specified location along the apical axis. Finally, integrating these areas along the axis, the desired volume was calculated. A spatial averaging technique was used over all boundary data near the extremities of the apical axis because of lack of continuity of data in these regions caused by large (30°) angular rotation. Although this approach allowed observation of a three-dimensional reconstructed image at any desired angle and from any desired distance, it had a few major limitations. First of all, the transducer was rotated in large (30°) increments. Secondly, the echocardiographic images were traced from the oscilloscope using X-ray transparencies and this technique introduces parallax error as well as obfuscation of the faint endocardial boundary by the

superimposed X-ray film. Thirdly, the technique was very tedious and therefore not practical for clinical use.

In 1991 Kuroda et al. published the first report on mechanical rotation scanning using the transoesophageal approach [Kuroda et al., 1991]. In this study they used only a longitudinal plane of the biplane transoesophageal probe to compare the *in vitro* accuracy of parallel and rotational scanning in volume measurements. Although pull-back parallel scanning intuitively appeared easy for three-dimensional reconstruction it was concluded to be impractical because of the anatomic relationship between heart and chest or oesophagus.

Volume-rendered dynamic three-dimensional imaging based on mechanical transducer position registration system became feasible for clinical use in 1991 when the first commercial three-dimensional mechanical acquisition system was developed (TomTec Echo-Scan, Munich Germany). Using this system, a three-dimensional data-set can be obtained within a couple of minutes by a mechanical movement of the ultrasound transducer controlled by electrocardiographic and respiratory gating [Pini et al., 1991]. There are three ways of acquiring a volume-rendered three-dimensional data-set using the Echo-Scan: parallel scanning, rotational scanning, and sweep (fan) scanning. During parallel scanning the ultrasound probe is mounted on a parallel shift carriage device. The acquired image planes are always parallel and equidistant to each other. The usual slice distance varies between 0.5 mm to 1.0 mm. Using the same three-dimensional acquisition system one can obtain a three-dimensional data-set using sweep (fan) scanning or rotational scanning. For an arc-like fan scanning a step angle between image planes is between 1° and 3°. The maximum sweep angle is 90°. For rotational scanning, the rotational carriage device

is used with ultrasound probes to perform a 180° rotation. The step angle between image planes is usually 1° to 3°. The known relationship between images as the transducer and the imaging plane are rotated aids in desired spatial registration of the images. All these approaches are used in specific situations. While fan-like scanning may be suitable for transoesophageal imaging, it is not a desirable transthoracic approach in adults. Similarly, although rotational scanning may find application in transoesophageal and transthoracic three-dimensional imaging, it is not preferable in intravascular ultrasound imaging where parallel scanning is most frequently used. Pandian et al. first reported on clinical feasibility of reconstructing dynamic three-dimensional images of a beating heart. In addition to dynamic three-dimensional display, they have been able to cut and visualise the heart in dynamic mode in any desired plane and also in multiple planes [Pandian et al., 1992].

1.2.2. Three-dimensional image reconstruction

The exact methods of assembling individual two-dimensional images into a three-dimensional reconstruction of the heart vary between techniques, depending on the type of transducer position registration system used. Nonetheless, all methods essentially consist of placing the individual cross-sectional images into a common three-dimensional co-ordinate system based on the position and orientation information relating the tomographic planes to one another or relative to an external reference system. Once all individual image slices have been registered in the global three-dimensional co-ordinate system, the spaces between the individual image slices are interpolated.

As mentioned earlier on, two general approaches have been widely used for the display of three-dimensional cardiac images: (1) wire-frame displays that in general are associated with acoustic transducer position registration systems and (2) shaded surface (volume-rendered) displays usually associated with mechanical transducer position registration systems.

(1) A wire-frame display exhibits the epicardial and endocardial contours from individual images along with a series of lines calculated to connect each image to the next and does not allow to display grey-scale information on cardiac tissue in three-dimensions. The advantages of wire-frame displays include their relative simplicity and the facilitation of calculation of volumes, mass, and regional volumes, since contours dividing the reconstruction into subregions are already present. The main disadvantage of wire-frame display is the difficulty appreciating complex structure because of the presence of many, sometimes confusing lines in the display.

(2) Shaded surface displays (volume-rendered) produce a rendering of the three-dimensional reconstruction that appears as an opaque object with appropriate shading effects. These displays have the advantage of ease of visual qualitative interpretation because of their closer resemblance to actual anatomy compared to the somewhat artificial appearance of the wire-frame displays.

In both wire-frame and shaded surface displays, three-dimensional reconstructions throughout the heart cycle may be used to produce a cine loop, leading to an animated rendition of cardiac contraction and filling.

1.3. Clinical applications of three-dimensional echocardiography

One of the main advantages of three-dimensional reconstruction is the ability to precisely calculate physiological variables of interest. As will be discussed below, calculations of simple parameters such as mass and volume have been accurately performed using three-dimensional reconstructions. Furthermore, the precise depiction of cardiac morphology and geometry provided by a three-dimensional reconstruction permits the calculation of more complex variables in congenital and acquired heart disease (**Figure 1**).

1.3.1. Assessment of cardiac geometry and function

The primary reason for attempting three-dimensional reconstruction to analyse cardiac geometry and function was based on the hypothesis that more accurate estimates will be obtained if they are calculated on the basis of realistic geometry instead of assumed geometric models.

Analysis of volume

One of the first attempts to use three-dimensional echocardiography in the assessment of heart function was to measure left ventricular systolic and diastolic volume without making assumptions about its spatial geometry. Until 1991 all reports from this area were based exclusively on acoustic transducer registration systems and a wire-frame display of three-dimensional information. In 1983, three-dimensional cardiac reconstruction proved to be an accurate method of assessing ventricular mass and volume. Moritz and co-workers, using three-dimensional echocardiography, with a wire-frame display, calculated volumes of excised formalin-fixed canine ventricles and found an extremely good correlation between

computer-predicted and actual volumes [Moritz et al., 1983]. Similar work on volume calculation was published in 1984 by Ariet et al. [Ariet et al., 1984]. In this *in vitro* experiment, an acoustic transducer position registration system was used to acquire five non-triggered short-axis views and to combine them into a wire-frame display of the left ventricle. It was calculated that the error of measurement of the left ventricular volume and mass volume was ± 10 ml as compared to the true volume measurements. These two studies were followed by studies of others in which three-dimensional echocardiography was used to calculate left ventricular volume *in vitro* and *in vivo* against other established techniques [Sawada et al., 1983; Fazzalari et al., 1984; Stickels et al., 1984]. Slightly later, in 1986, three-dimensional echocardiography was used to calculate right ventricular volume. Linker et al. have validated *in vitro* the right ventricular volume measurement using also an acoustic transducer position registration system and a wire-frame display of three-dimensional data [Linker et al., 1986]. Their results showing good accuracy in right ventricular volume measurement by three-dimensional echocardiography have been confirmed by Jiang et al. *in vivo* using the same three-dimensional system, and by Vogel et al. *in vitro* who used a mechanical transducer position registration system and volume-rendered display [Jiang et al., 1994; Vogel et al., 1995a]. In 1989, Martin et al. published an interesting paper in which for the first time a transoesophageal approach was used to acquire wire-frame (acoustic transducer position registration system) three-dimensional data in order to calculate *in vivo* the left ventricular end-systolic and end-diastolic volume in a group of ten anaesthetised dogs [Martin et al., 1989]. In this study, three-dimensional transoesophageal data were based on a triggered (end-diastolic and end-expiration based) acquisition of

twelve to fifteen consecutive two-dimensional images using mechanical transducer position registration systems. As an end-point of the acquisition process, a wire-frame of the left ventricle was calculated by the computer from which stroke volume (end-systolic and end-diastolic volumes) was calculated and compared to the stroke volume calculated using a thermodilution method. Although, excellent agreement was obtained between these two techniques (standard error 4.1 ml), the time of data acquisition lasted from two to seven hours and therefore was not feasible for a clinical use. This acquisition time has been shortened substantially by the release of first commercial three-dimensional acquisition system for volume-rendered (shaded surface) display.

The first comparison of three-dimensional, two-dimensional echocardiography and cineventriculography in volume computation was published in 1993 by Sapin et al. [Sapin et al., 1993]. Using an acoustic transducer position registration system and a wire-frame display, fifteen excised pig hearts were studied for volume measurements using two-, three-dimensional echocardiography and cineventriculography. It was calculated that three-dimensional echocardiography provides accuracy comparable to that of biplane cineventriculography. Two-dimensional echocardiographic volume computation was significantly less accurate than three-dimensional echocardiography and cineventriculography. The same three-dimensional system and the same study protocol was used again by Sapin et al. in 1994, but this time in a clinical setting, to perform the first comparison in patients of left ventricular volume computation by three-dimensional echocardiography, two-dimensional echocardiography and cineventriculography [Sapin et al., 1994]. Three-dimensional echocardiography correlated highly with cineventriculography for estimation of left

ventricular volume and had approximately half the variability of two-dimensional echocardiography for volume measurements. The improvement of three-dimensional over two-dimensional echocardiography was attributed to eliminating the use of geometric assumptions and improved image positioning by use of the 'line of intersection display'. The advantage of volume and mass computation by three-dimensional reconstruction over two-dimensional echocardiography has recently been reported in children with functionally single left ventricles. Accurate assessment of these parameters is particularly important in this group of patients as the mass to volume ratio is recognised as strong predictor of postoperative outcome and long term prognosis [Altmann et al., 1997]. The conclusion of that paper was that not only three-dimensional echocardiographic volume measurements were more accurate than corresponding measurements obtained from two-dimensional echocardiography but also that the interobserver and intraobserver variability for mass and volume measurements derived from three-dimensional reconstructions were significantly lower than those derived from two-dimensional echocardiography.

Analysis of regional cardiac motion

There are still little data in the literature dealing with the use of three-dimensional echocardiography to measure regional cardiac motion. The pioneering work in this field belongs to McPherson et al. who have analysed acute ischaemia by three-dimensional echocardiography [McPherson et al., 1987]. In 1993 King et al. showed that using an acoustic transducer position registration system and a wire-frame display of three-dimensional data it is possible to accurately measure *in vitro* the surface area of an irregular shape by studying the total and infarcted surface area of the left ventricle [King et al., 1993]. A similar approach using an acoustic transducer

position registration system and a wire frame display of three-dimensional data to quantify the extent of myocardial damage after acute myocardial infarction was published recently by Sapin et al. [Sapin et al., 1996]. In that report, an open chest canine model of acute myocardial infarction was studied to test the ability of three-dimensional echocardiography to quantify the extent of regional dyssynergy and thereby to estimate infarct size. Using a polyhedral surface reconstruction algorithm [Cook et al., 1980], end-diastolic left ventricular endocardial surface area was computed by three-dimensional echocardiography from the traced endocardial boundaries of each short-axis section. The extent of abnormal wall motion was assessed subjectively from wall thickening and endocardial excursion, observed when a cine loop was played forward. To determine total endocardial surface area and dyssynergic surface area, the operator first traced each endocardial outline using mouse-driven cursor and then used the cursor to delineate the segment showing abnormal wall motion. For each image, the traced endocardial border was divided by interpolation into 180 equally spaced co-ordinate points. The surface between adjacent images was defined by lines connecting two consecutive points on one slice with a single point on the adjacent slice, forming a series of triangular 'tiles'. The area of all surface 'tiles' was summed to yield total endocardial surface area. The area within the regions demarcated as showing abnormal wall motion were also totalled to yield the surface area of the abnormal region, which was then expressed as a percentage of total surface area. The percent of left ventricular mass showing abnormal wall motion was calculated by assuming that the wall motion abnormality extended uniformly through the thickness of the left ventricle and that wall thickness in each image was uniform. The results obtained from three-dimensional

echocardiography were correlated with those obtained from standard two-dimensional images. Three different methods were used to quantitfy the extent of abnormal wall motion from two-dimensional images: (1) summation-of-discs, (2) summation-of-conical sections, and (3) summed endocardial lengths. The three-dimensional echocardiographic quantification of the extent of regional wall motion abnormality provided more accurate estimates of infarct size than all three techniques used in two-dimensional echocardiography. The results of Sapin et al. were confirmed in another open chest canine myocardial infarction model reported by Yao et al. [Yao et al., 1997]. In the paper of Yao et al., as opposed to that of Sapin et al., a mechanical transducer position registration rather than an acoustic system was used before and three hours after coronary occlusion in sixteen dogs. Again, it was shown that three-dimensional echocardiography accurately displays regional dysfunction of infarcted left ventricle. Three-dimensional echocardiography measured the dysfunctional mass accurately as compared to the anatomic infarct mass. There was an excellent correlation between the mass of dysfunctional myocardium and pathological infarct mass without systemic over- or under-estimation. The advantage of the volume-rendered three-dimensional echocardiography over a wire frame display is that dynamic three-dimensional images can be reconstructed without any tracing of the cardiac silhouettes on two-dimensional images and have the characteristic appearance of cardiac tissue. This allows visual appraisal of global and regional left ventricular function, detection of wall motion abnormalities, and aneurysmal deformations.

It is likely that the absolute accuracy of the results obtained in both studies, that were discussed above, will not be replicated in clinical myocardial infarction studies.

However, the relative improvement of three-dimensional echocardiography will probably be retained, as it has been in other human studies.

1.3.2. Assessment of cardiac structures

The ultimate goal of three-dimensional reconstruction of the heart relies on the potential of the objective display of the anatomy and the complex relationships among the different structures. It has been shown that with an integrated system for three-dimensional acquisition of ultrasound data, this goal can be achieved both with the transoesophageal and precordial approach. In general, mechanical transducer position registration systems (shaded volume-rendered display) and the rotational approach of data acquisition has many advantages over other acquisition techniques [Roelandt et al., 1994a&b]. The possibility of obtaining unrestricted two-dimensional images coupled with the shaded (volume-rendered) dynamic display of cardiac tissue allows us to explore fully the morphologic features of a given structure.

Congenital heart disease

Because of the low attenuation factor of the ultrasound signal in children, three-dimensional studies can be performed successfully using in a majority of cases a transthoracic approach. Shaded display (volume-rendered echocardiography) of the images and a rotational acquisition technique remains the most popular. To date, ventricular septal defects [Rivera et al., 1994] and atrial septal defects [Belohlawek et al., 1993b; Franke et al., 1997] have been studied. Both transthoracic and transoesophageal three-dimensional images accurately displayed the varying morphology, dimensions, and spatial relations of atrial/ventricular septal defects. The

three-dimensional reconstruction of the mitral valve allows us to demonstrate the nonplanarity of the mitral annulus [Levine et al., 1987] and to enhance the criteria for the diagnosis of mitral valve prolapse [Levine et al., 1989]. Salustri and co-workers studied a group of adult patients (age range sixteen to fifty seven years) with various congenital heart defects (mitral valve anomalies in five patients, aortic valve anomalies in nine, subaortic membrane in five, ventricular septal defect in four, other defects in ten patients) using transthoracic volume-rendered three-dimensional echocardiography [Salustri et al., 1995]. The unroofed cut plane of the left atrium (equivalent to the 'surgical view' of the mitral valve) and visualisation of the mitral valve from above allowed comprehensive assessment of leaflet motion, area orifice and shape, and commissure morphology. Different cut planes of the left ventricle allowed visualisation of the left ventricular outflow tract from below, with adequate evaluation of this area. The three-dimensional reconstruction of the aortic cusps from above or below was difficult and feasible only in two of the five patients studied. In patients with ventricular septal defects, the relation between the ventricular septum and the aortic valve was assessed easily and with confidence. The three-dimensional reconstruction to view the defect *en face* was not feasible only in two patients in whom defects were very small. In general, the additional information obtained by transthoracic three-dimensional echocardiography was provided for 36% of patients. The additional data provided by three-dimensional echocardiography were mostly for the mitral valve, aortoseptal continuity and atrial septum. A similar study in which a wide variety of congenital cardiac disorders have been studied in a group of forty five children (age range 3 days to seventeen years) by transthoracic volume-rendered three-dimensional echocardiography was reported by Vogel and co-workers

[Vogel et al., 1994]. Good quality transthoracic volume-rendered three-dimensional reconstructions were obtained in forty three of the forty five patients studied. The study group consisted of eleven patients with ventricular septal defects, nine with subaortic stenosis, seven with atrio-ventricular septal defects, four with atrial septal defects and fourteen others. Image acquisition took between three and five minutes and the three-dimensional reconstruction of the images took between twenty and ninety minutes, depending on the complexity of the underlying anatomy. The various heart defects were displayed in a view that is similar to that seen by a surgeon during repair of the defect. The authors concluded that transthoracic three-dimensional echocardiography is feasible in most paediatric patients. It is easy to use and enhances the information on intracardiac anatomy to that available from standard two-dimensional echocardiography.

Acquired heart disease

In acquired heart disease, a mechanical transducer positioning registration system and shaded surface display (volume rendering) of reconstructed data is also the most successful way of image acquisition and display by three-dimensional echocardiography. However, because of the mainly adult patient population being dealt with, a transoesophageal approach is the most commonly used to acquire a data-set. It provides high resolution images in virtually all patients by reducing the effect of ultrasound signal attenuation by chest wall structures and by the use of higher transducer frequencies. There is no doubt that two-dimensional transoesophageal echocardiography provides excellent morphological and functional information in a variety of disorders. However, to evaluate the abnormalities in a three-dimensional heart, the examiner often performs a mental three-dimensional

reconstruction of the pathology from multiple two-dimensional image. If a method were available that provided objective three-dimensional images of the heart, proper assessment of the cardiac morphology would be easier.

In 1994, Kupferwasser and co-workers evaluated the clinical applicability of three-dimensional volume-rendered transoesophageal echocardiography in the assessment of acquired heart disease [Kupferwasser et al., 1994]. A group of fifteen patients with known varies heart defects (endocarditis in five, abscesses in five, heart tumours in three, heart failure in two patients) and five patients with no apparent abnormalities on standard transoesophageal echocardiograms were studied. The mean time for three-dimensional data acquisition was twelve minutes (12 ±4 minutes). Approximately thirty five minutes was needed (35 ±14 minutes) to complete three-dimensional reconstruction of acquired images. The longest reconstruction times were required in patients with perivalvular abscesses. The main advantage of three-dimensional transoesophageal echocardiography over standard two-dimensional transoesophageal echocardiography was in more comprehensive rendition of cardiac anatomy. Consequently, a better differentiation between artefacts and structures-of-interest was achieved from three-dimensional reconstructed images. Additionally, distance measurements of mass lesions obtained from three-dimensional data were shown to be more accurate then corresponding measurements obtained from two-dimensional images.

The experience of three-dimensional visualisation of aneurysms and psedoaneurysms of the aorta using a multiplane transoesophageal approach to acquire volume-rendered three-dimensional images was reported by Roelandt et al. [Roelandt et al., 1994b]. The image acquisition time was essentially the same in the study of

Kupferwasser et al. [Kupferwasser et al., 1994] - twelve minutes and that of Roelandt et al. - seven minutes. The time required to complete a three-dimensional acquisition remained also the same (between thirty to sixty minutes). It was concluded that qualitative and quantitative assessment of both geometry and pathologic aspects of the thoracic aorta, including aneurysm and dissection, are facilitated by three-dimensional imaging. Their experience in the evaluation of aortic disorders by three-dimensional imaging was repeated later by Sugeng et al. [Sugeng et al., 1997]. Using the same rotational multiplanar imaging system as Roelandt et al., a group of twenty eight pigs with aortic disorders (fifteen aortic dissections, five saccular aneurysms, five coarctations of the aorta, five atheromas, and five clots within dissections) and thirty six patients with aortic lesions on a routine two-dimensional echocardiographic examination were studied. Again as in previous studies, dynamic three-dimensional reconstruction of the aorta have been performed in all study subjects. The aortas were displayed in numerous views to demonstrate the lesions in various perspectives. These lesions were projected in several cut planes and observed in different phases of the cardiac cycle. The location of thrombus, atheromas, and mobile plaques were easily noted on a three-dimensional reconstruction. Also, a closer observation of structural relationships was possible in the reconstructions of aortic dissections. The true and false lumens were observed as well as intimal flaps. The length and width of the intimal flap were observed, and in dynamic form the motion of this structure was appreciated. In one case it was also possible to note the origin of the intimal flap arising near the coronary artery ostium. Unique perspectives of the dissection from the ascending aorta, looking down towards the aortic valve, allowed observation of the valve leaflets and location of the intimal tear. In cases of aortic coarctations, it

was possible to reconstruct in three-dimensions most of the aortic arch and narrowed descending aorta. The advantage of three-dimensional echocardiography in the quantification of aortic valve area by using a rotational method was also reported by Nanda et al. and Kasprzak et al. [Nanda et al., 1994; Kasprzak et al., 1998a&b].

Mitral stenosis and both mitral and aortic regurgitation were also studied by three-dimensional echocardiography (**Figures 2, 3 & 4**). Chen et al. have studied a group of fifteen patients with mitral valve stenosis [Chen et al., 1997]. The purpose of that study was to determine the feasibility and the reproducibility of three-dimensional echocardiography for calculating mitral valve area. In addition, the accuracy of mitral valve area measurement from three-dimensional and two-dimensional images was compared with values obtained by Doppler pressure half-time. Despite interesting results and a clear potential advantage of three-dimensional over two-dimensional imaging this study failed to prove the superior role of the three-dimensional technique in the assessment of mitral stenosis. Firstly, no differences were found between techniques in the assessment of mitral valve area, and the interobserver and intraobserver variability were essentially the same for all studied techniques. Also, in order to measure the mitral valve area only, in half of the group studied three-dimensional data-sets were acquired using a transoesophageal approach. No attempt was made to analyse the morphology of mitral commissures or to reconstruct the stenotic mitral Doppler inflow. In the report of Delabays et al. it has been shown that three-dimensional echocardiography has the potential to depict not only the anatomic abnormalities of the mitral valve apparatus but also to characterise mitral regurgitant jets in greater detail than with conventional imaging [Delabays et al., 1995]. With respect to the analysis of the mitral valve morphology

by three-dimensional echocardiography, their results were similar to the report of Salustri et al. which was published one year later (see section on the congenital heart disease) [Salustri et al., 1996]. The new information from the report of Delabays et al. was that three-dimensional echocardiography was accurate in the assessment of mitral reflux and particularly useful in cases with multiple or eccentric jets, which were difficult to assess using conventional two-dimensional imaging. Also, three-dimensional reconstruction of flow jets allowed display of the flow convergence zone in a unique fashion. As this region of convergence zone can be viewed from different perspectives, it allowed for accurate assessment of the global shape. This is very important, as the initial results of the experimental work of Utsunomiya and co-workers indicated that the proximal flow convergence zones are not perfect hemispheres or hemiellipses as assumed in the calculation of regurgitant volume using the proximal isovelocity surface area method [Utsunomiya et al., 1991]. Also, the use of three-dimensional reconstruction of valvular structure was very helpful in the determination of the most suitable therapeutic modality for each individual patient. The accurate measurement of left ventricular function, surface area of the leaflets and regurgitant orifice area available from a three-dimensional data-set was particularly valuable when pre-operative assessment of mitral valve morphology was performed. In the same report they have also looked at usefulness and potential superiority of dynamic three-dimensional echocardiography in reconstructing abnormal intracardiac blood flow jets in aortic regurgitation, tricuspid regurgitation, mitral stenosis, and also shunts in atrial and ventricular septal defects. As in patients with mitral regurgitation, also in patients with aortic and tricuspid regurgitation the flow convergence zone could also be reconstructed in three-dimensions. The

supporting results showing the feasibility of three-dimensional echocardiography in reconstructing correctly the flow convergence zone and demonstrating its curved geometry in valve insufficiency was published recently by Shiota et al. [Shiota et al., 1997]. Using the same volume-rendered three-dimensional acquisition system as Delabays et al. [Delabays et al., 1995], direct measurement of the three-dimensional reconstructed flow convergence areas as well as measurements of flow convergence areas estimated with two-dimensional methods with hemispherical and hemielliptical assumptions were performed in six open-chest sheep with surgically induced chronic aortic regurgitation. Although, in both studies, direct measurements of three-dimensionally reconstructed proximal isovelocity flow convergence surface areas provided more accurate regurgitant flows than conventional two-dimensional colour Doppler methods it is important to mention the limitations of this technique. In general, limitations inherent to the colour Doppler flow mapping for imaging the flow convergence, including instrument factors such as colour gain, wall filter settings, and variability of aliasing velocities, are carried into the three-dimensionally reconstructed flow convergence images. Low frame rates (12 to 17 frames per second) may cause underestimation of the maximal flow convergence size. Especially important is the loss of velocity information for flows at the edges of the flow convergence region induced by the angle between Doppler interrogation and the actual direction of blood flow. Because of these problems, in the study of Shiota et al. [Shiota et al., 1997], portions of the imaged flow convergence surface adjacent to the valves did not correspond strictly to true isovelocity surfaces. Thus, the technique still needs correction for flow constraint, competing flows, and Doppler angle dependency.

Until the autumn 1998 three-dimensional reconstructions of colour Doppler blood flow jets were possible only in grey-scale (black & white). The first reports on the clinical applications of three-dimensional Doppler in original colour coding in patients with mitral regurgitation were presented only recently during the XXth Congress of the European Society of Cardiology [De Simone et al., 1998; Coisne et al., 1998] (**Figure 5**).

1.4. Real-time three-dimensional echocardiography

In parallel to volume-rendered three-dimensional imaging systems described already in this Chapter, a real-time volumetric three-dimensional echocardiography is being developed by the Duke University Medical Center in Durham, USA [Snyder et al., 1986; von Ramm et al., 1990; Fleishman et al., 1996a; Shiota et al., 1998]. The acquisition time is short and neither electrocardiographic nor respiratory gating is necessary because the three-dimensional data is obtained essentially in real-time. The data are not displayed in a conical form as in three-dimensional systems based on mechanical registration of transducer position but as two orthogonal B-scans and two or three C-scan images (images parallel to the transducer face) simultaneously. Although the C-scans can be moved towards or away from the transducer and angled relative to the transducer face to display various parts of the data set on-line, three-dimensional reconstructions can only be displayed off-line and require a considerable amount of data interpolation thus reducing its accuracy. Despite on-going validation of the system, including the recent study by Fleishman et al. [Fleishman et al., 1996b] in a group of fifteen children with various congenital heart defects, the technique is still in its early stages and the wide-spread acceptance of the system is

limited, not only because of the sub-optimal image quality but also due to its very high cost and the ability to acquire only transthoracic images with no colour Doppler flow mapping.

1.5. Conclusions

During the last two decades three-dimensional echocardiography has undergone intensive development. Several different approaches have been used to acquire and to reconstruct ultrasound data in three-dimensions. However, the technique has not yet been widely applied clinically and there has been a paucity of validative studies. Volume-rendered three-dimensional imaging obtained from either transthoracic or transoesophageal approach would seem the best method of reconstructing heart structures in three-dimensions. We know already that such three-dimensional reconstructions provide views of heart chambers and intracardiac structures that strongly resemble the views seen during cardiac surgery. The accuracy of these reconstructed images has been tested by several investigators *in vitro* and *in vivo* but these studies involved mainly volume and area measurements. Not much is known on the feasibility and the accuracy of this technique in the assessment of congenital and acquired lesions of the atrio-ventricular junction. Also the preliminary studies on reconstruction of colour Doppler jets, although promising and interesting, need to be further validated. It remains to be established whether three-dimensional echocardiography simply improves our way of diagnosing heart disease or contributed also to a better understanding of the underlying mechanism of some disorders.

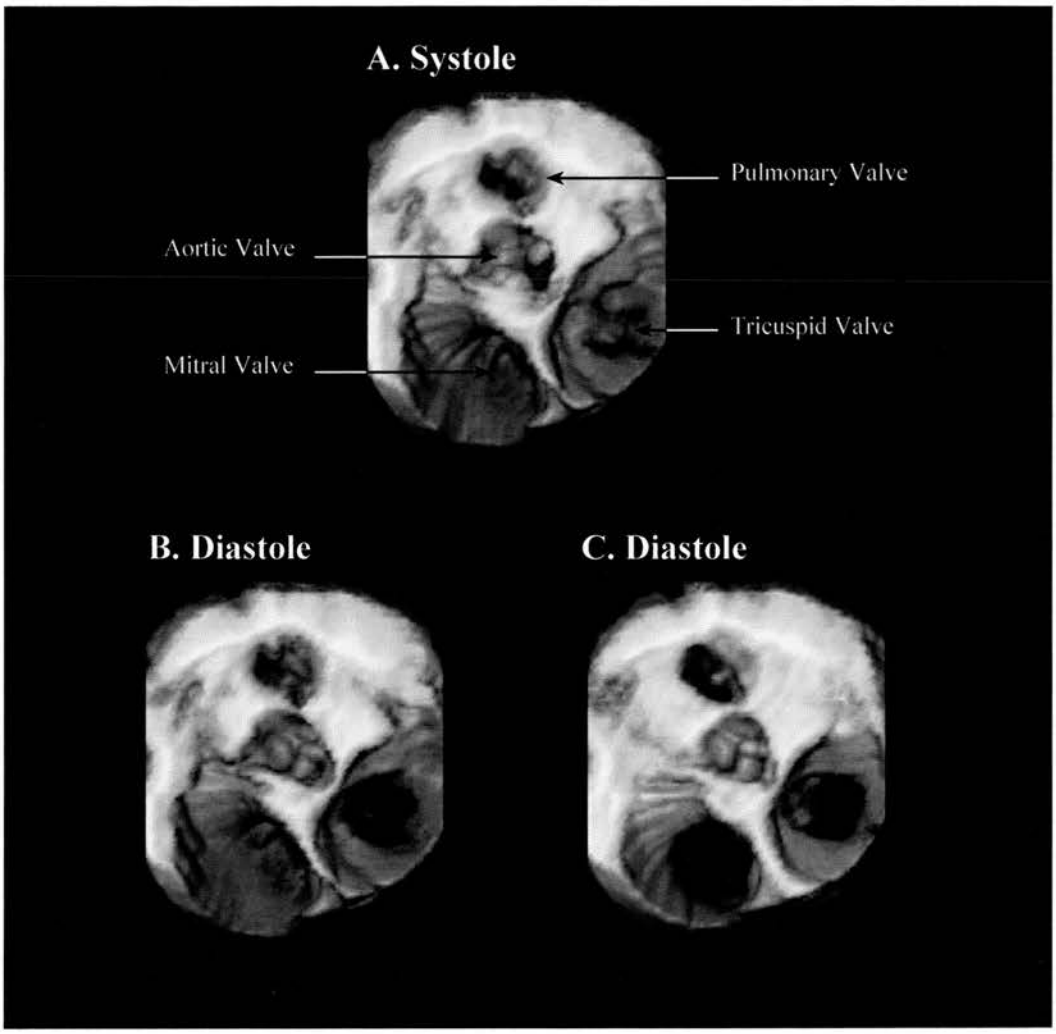

Figure 1. Examples of volume-rendered transoesophageal three-dimensional reconstruction of the heart: short-axis view at the level of atrio-ventricular valves directed from above (an atrial perspective). During systole **(A)** and diastole **(B, C)** two vegetations are seen in the ascending aorta, just in front of the aortic valve corresponding to acute bacterial endocarditis of the aortic valve. Elevated right heart pressure with mild tricuspid and pulmonary valves regurgitation.

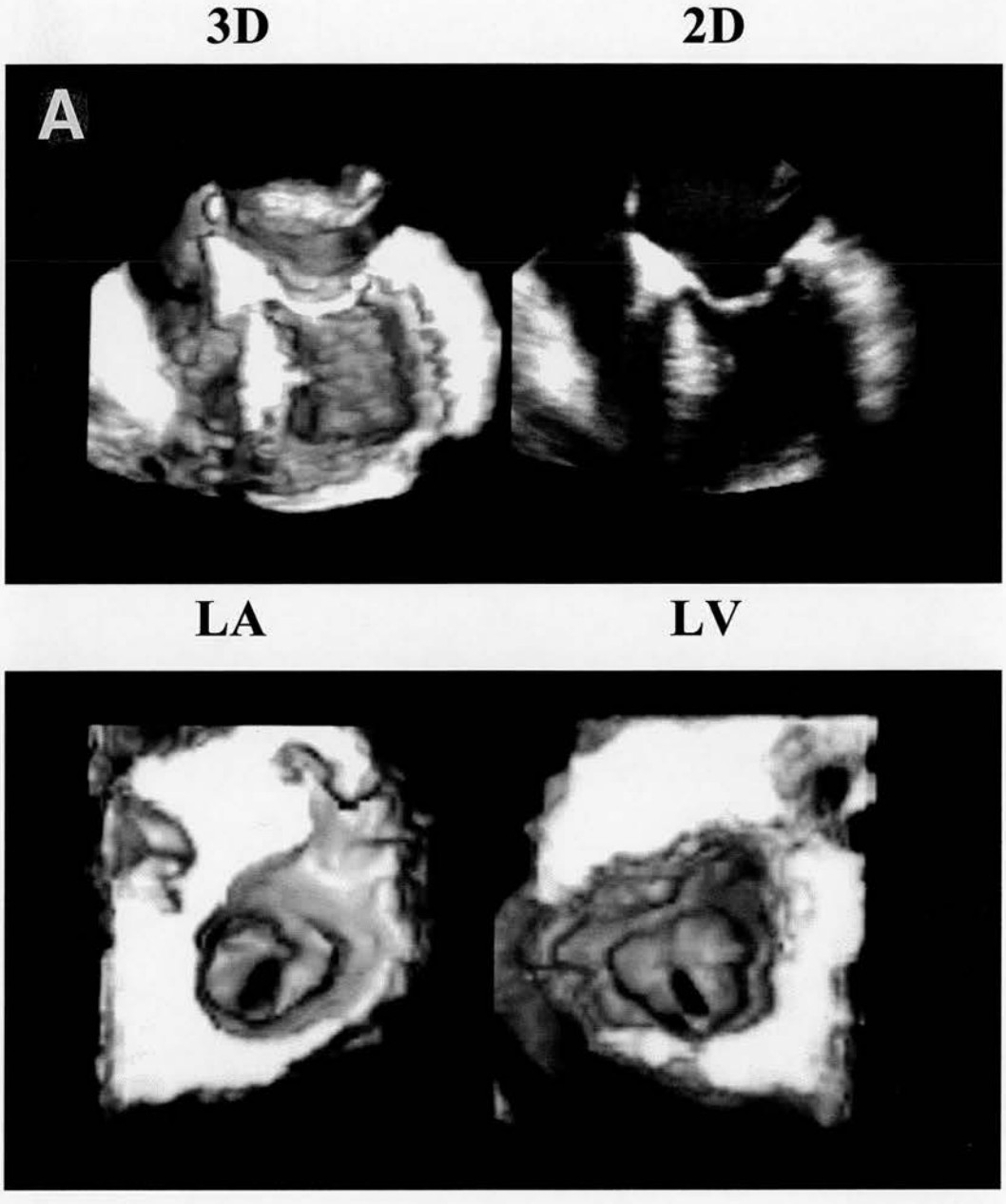

Figure 2. Examples of transoesophageal three-dimensional (3D) reconstruction of a stenotic mitral valve. **(A), top** - long-axis view with the corresponding two-dimensional (2D) image on the right hand side; **bottom** - reconstruction of the mitral valve *en face*, corresponding left atrial - (LA) and left-ventricular perspective (LV). Small central orifice with well visualized outline of the extent of commissural fusion from both perspectives.

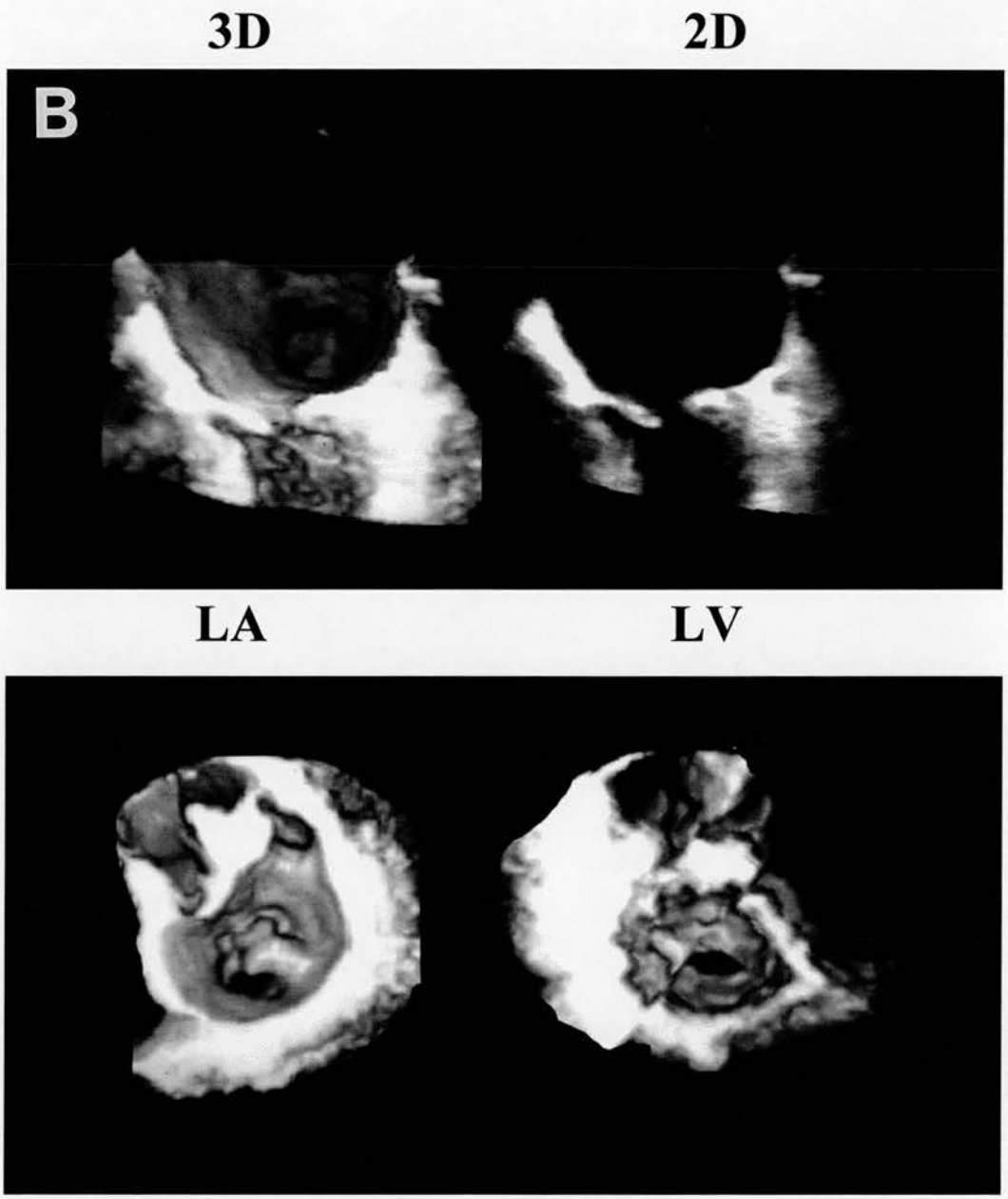

Figure 2 (cont'd). Examples of transoesophageal three-dimensional (3D) reconstruction of a stenotic mitral valve. **(B), top** - long-axis view with the corresponding two-dimensional (2D) image on the right hand side; **bottom** - reconstruction of the mitral valve *en face*, corresponding left atrial - (LA) and left-ventricular perspective (LV). Small slightly eccentric orifice. Extensively thickened and irregular surface of the anterior leaflet suggesting the presence of calcification. From the atrial perspective, the ouline of commissural fusion is difficult to trace. Well visualised outline of the extent of commissural fusion from the ventricular perspective.

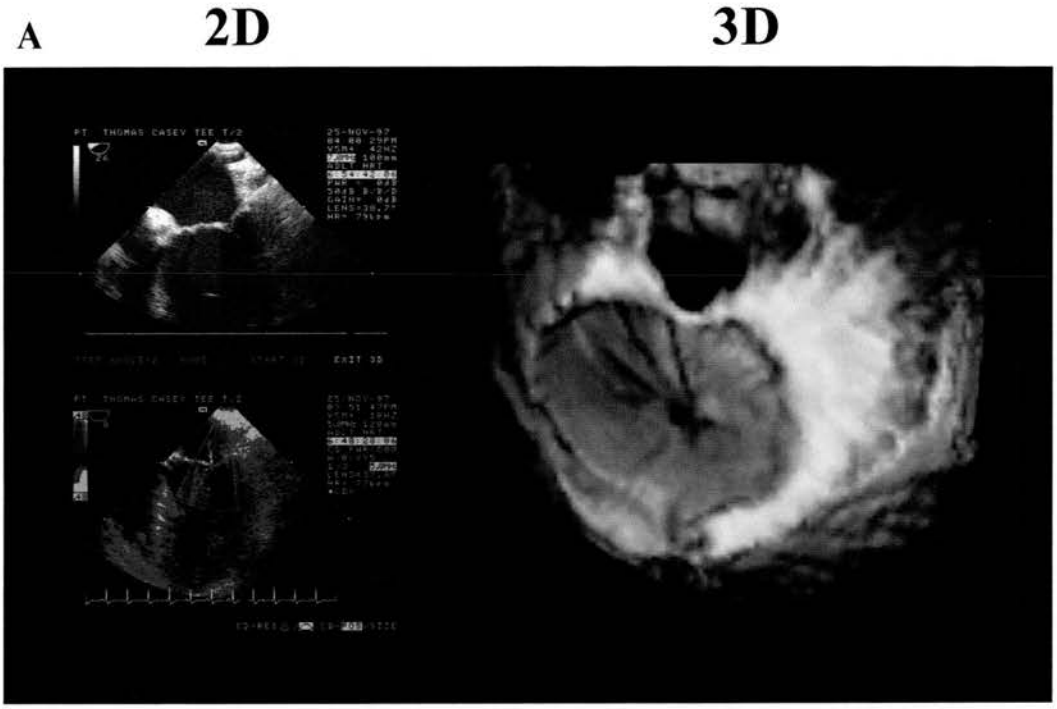

Figure 3. Examples of transoesophageal three-dimensional (3D) reconstruction of a regurgitant mitral valve. **(A),** *en face* (short-axis) view of the mitral valve reconstructed from an atrial perspective with corresponding two-dimensional (2D) long-axis views (grey-scale and with colour Doppler flow) on the left hand side. Mild central mitral regurgitation caused by dilated atrio-ventricular junction and poor central leaflet coaptation.

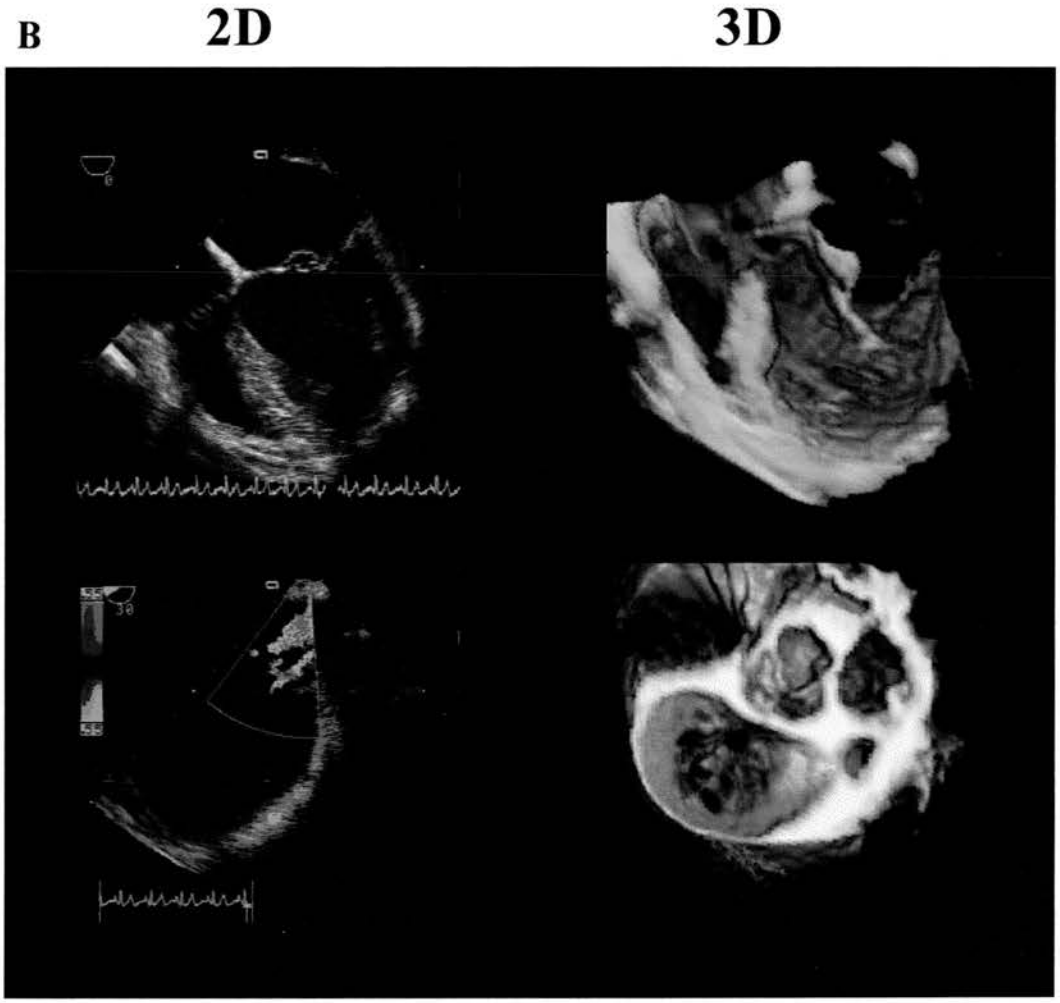

Figure 3 (cont'd). Examples of transoesophageal three-dimensional (3D) reconstruction of a regurgitant mitral valve. **(B), top -** long-axis view with the corresponding two-dimensional (2D) image on the left hand side; **bottom -** reconstruction of the mitral valve *en face* from an atrial perspective with 2D image and colour Doppler flow on the left hand side. Moderate/severe mitral regurgitation. Marked prolaps of the anterior mitral leaflet. Degenerative mitral valve with complex mechanism of reflux originating from the closure line (one jet) and from perforated anterior mitral leaflet (two jets).

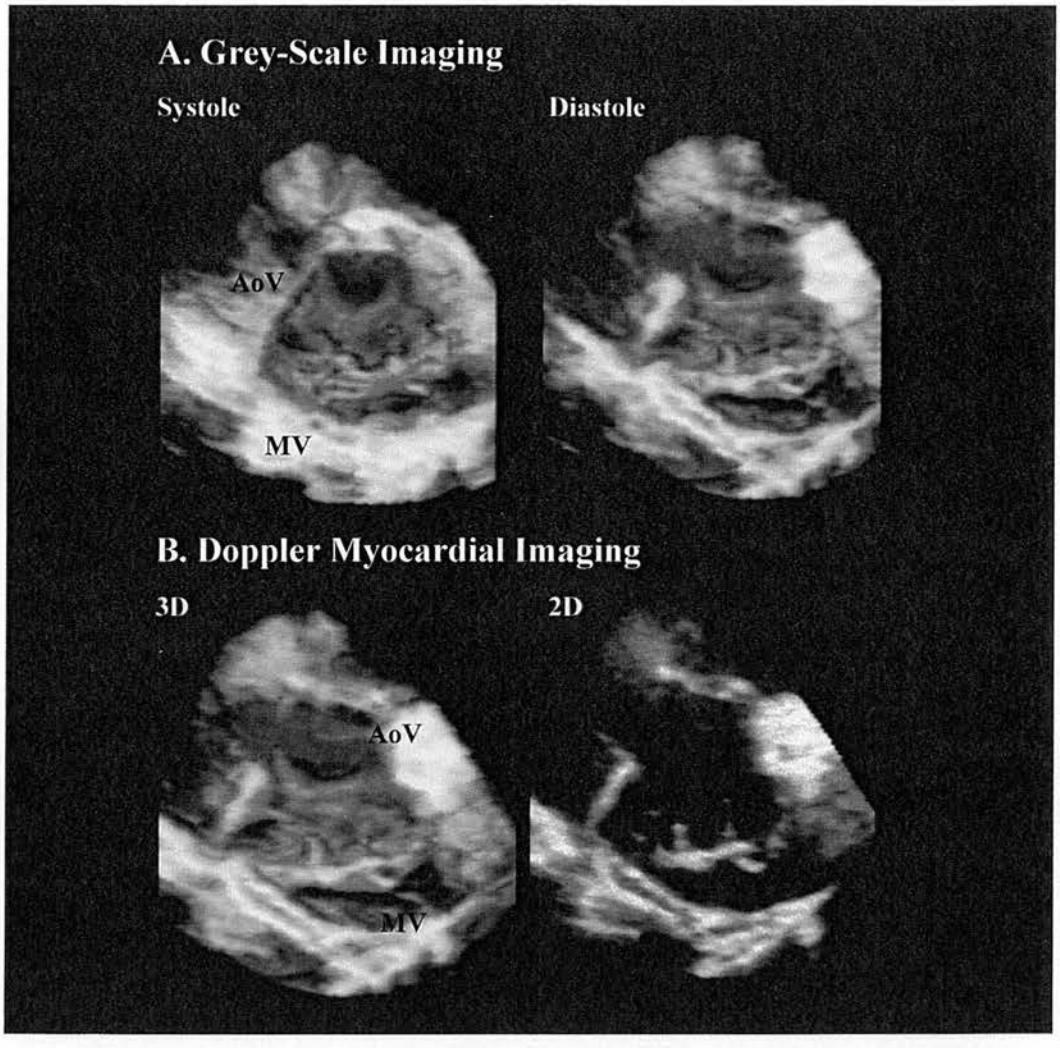

Figure 4. Example of transthoracic three-dimensional (3D) reconstruction of a regurgitant aortic valve. **(A)**, Grey-scale imaging - reconstruction of mitral and aortic valves en face from left ventricular perspective. On the right hand side, marked spontaneous contrast refluxing from the ascending aorta to the left ventricular outflow tract during diastole. Heavily calcified mitral valve. **(B)**, Doppler myocardial imaging technique - reconstruction of mitral and aortic valves *en face* from left ventricular perspective with corresponding two-dimensional image on myocardial imaging technique

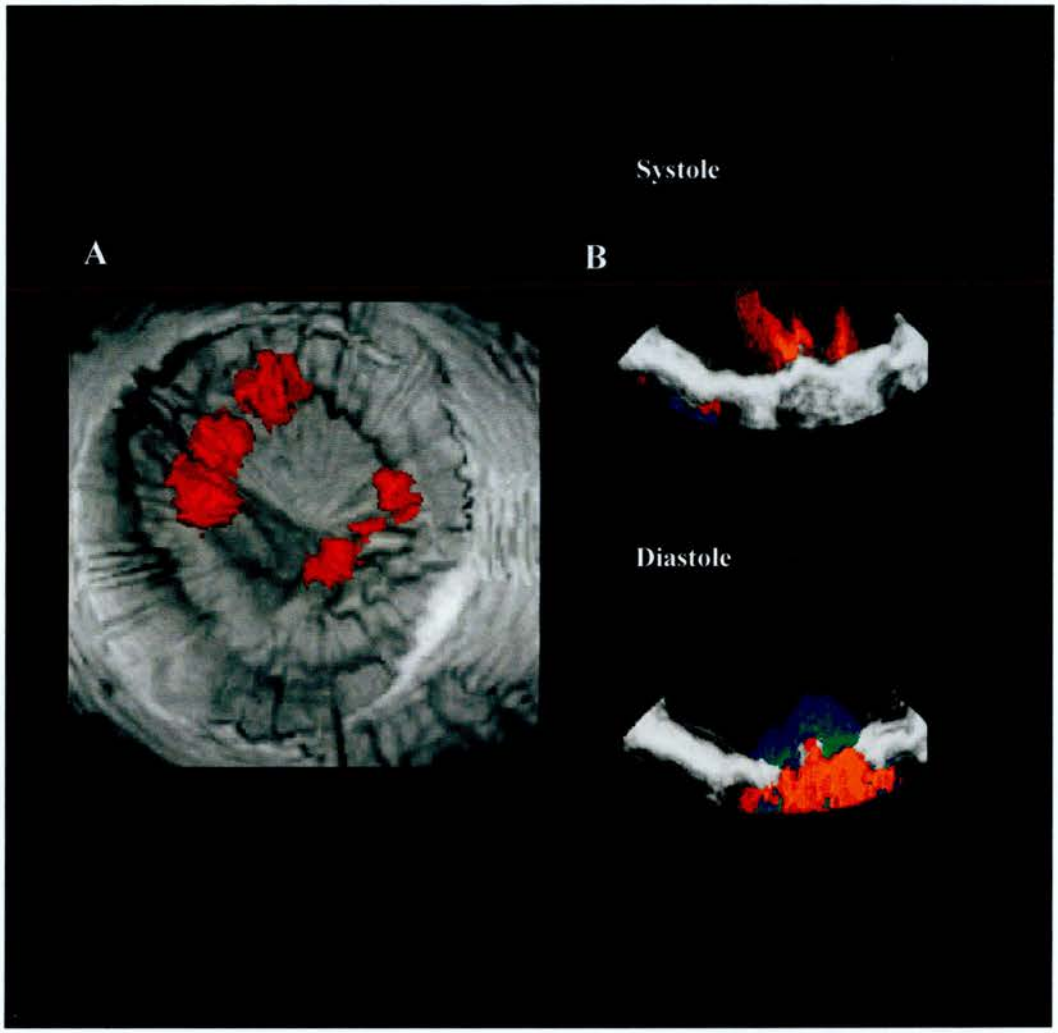

Figure 5. Example of transthoracic three-dimensional (3D) reconstruction of a regurgitant prosthetic mitral valve. **(A)**, *en face* (short-axis) view of the prosthetic mitral valve reconstruction from an atrial perspective with corresponding **(B)** long-axis views during systole **(top)** and diastole **(bottom)**. 3D reconstructions contain both grey-scale data and colour Doppler jets displaying a complex mechanism of valve insufficiency. (courtesy of Dr Andreas Franke & Dr Harald Kühl, University Hospital Aachen, Germany).

CHAPTER 2

A Review of Methods of Three-Dimensional Image Acquisition Used in this Thesis

2.1. Background

As already described in Chapter 1, two different transducer position registration systems are currently used to acquire a three-dimensional data-set. These are based on either acoustic or mechanical registration of the spatial position of the transducer.

The acoustic transducer position registration system was introduced in 1976 by King et al. [King et al., 1976]. A conventional ultrasound scanner is linked to an acoustical three-dimensional spatial locating system. The acquired two-dimensional images and their X, Y, Z spatial co-ordinates are combined in the computer to produce a three-dimensional data-set and displayed in a wire-frame form.

The mechanical transducer position registration system was first described by Dekker et al. [Dekker et al., 1974]. Other than the first few reports, where a three-dimensional data set was acquired and then displayed in a wire-frame form, this system is now always associated with the volume-rendered (shaded surface) display of three-dimensional data. Dynamic volume-rendered three-dimensional imaging based on the mechanical transducer position registration system became feasible for clinical use in 1991 when the first commercial three-dimensional mechanical acquisition system was released (TomTec Echo-Scan, Munich Germany). Volume-rendered three-dimensional reconstructions appear as an opaque object with appropriate shading effects. These displays closely resemble the actual anatomy compared to the somewhat artificial appearance of the wire-frame displays. The first report on the clinical feasibility of reconstructing heart structures using this new system was by Pandian and co-workers [Pandian et al., 1992]. Encouraged by these

results, other centres in Europe and the United States began work with volume-rendered three-dimensional echocardiography.

In Edinburgh, we have designed and undertaken our first project on three-dimensional echocardiography in December 1994. After validating the system *in vitro*, the complexity of the studies undertaken has increased so that the more difficult diagnostic problems of paediatric and adult cardiology have been tackled.

Throughout this thesis, the methodology and the protocol of image acquisition remains the same.

2.2. Image acquisition

In this thesis, the mechanical (rotational) transducer position registration system and volume- rendered display was used to acquire and reconstruct the data in three-dimensions.

The instrumentation used for the three-dimensional imaging protocol consists of an ultrasound scanner and a three-dimensional acquisition system (TomTec Echo-Scan, TomTec Imaging Systems; Munich, Germany).

One of the following ultrasound scanners was used to acquire images: Acuson XP10 or Acuson Sequoia (Mountain View California, USA). Both scanners had additional software which allowed the use of Doppler myocardial imaging.

It was envisaged that Doppler myocardial imaging, based on the Doppler principle to visualise heart structures rather than blood flow, should give better quality transthoracic two-dimensional images than the standard grey-scale (B-mode) imaging technique for three-dimensional reconstruction. Full details of the physical principles of the technique that potentially make Doppler myocardial imaging

superior to standard grey-scale transthoracic imaging for three-dimensional transthoracic echocardiography are given in Chapter 3.

The scanner modifications and software enabling acquisition of the ultrasound images in the Doppler myocardial imaging mode included: Lower Doppler velocity range settings to encode myocardial velocities (0-16 cm/s) than those typically used for blood flow. The display of Doppler information was therefore enabled for tissue instead of blood. Image persistence was turned off to eliminate blurring of the moving cardiac structures. Doppler receive gain was set to achieve maximum colour Doppler information of the heart structures while limiting colour information within the blood pool.

Figure 1 shows schematically how three-dimensional images were acquired.

The three-dimensional acquisition system used (TomTec Echo-Scan) consisted of a 486, 66 MHz computer with 64 Mbytes of storage system memory, steering logic for image acquisition, processing and presentation.

For transthoracic image acquisition a standard apical window was used in most cases. The two-dimensional ultrasound images were obtained using a 2.5- 4.0 MHz phased array transducer steered by the transducer mechanical rotational device supplied with the Echo-Scan. In each patient the appropriate transducer frequency was selected to obtain the best quality two-dimensional grey-scale image.

During the image acquisition, the Echo-Scan was connected to the ultrasound video output of the scanner via a black/white video cable. Thus, when Doppler myocardial images were acquired, the colour Doppler signal was transferred as a black and white video signal to the Echo-Scan. During the acquisition electrocardiographic and respiration gating was used. A standard three-lead electrocardiogram cable was used

to monitor the electrocardiogram while the patient's respiration was monitored by measuring skin impedance. Using this information the system created an on-line histogram based on the patient's heart rate and respiration. This enabled the setting of a gating window based on the RR intervals of the electrocardiogram. The expiratory phase was used for gating respiration.

During the acquisition procedure, the transducer placed in the transthoracic apical position was rotated by the mechanical rotational device at 2^{o} steps over 180^{o}. Based on the gating parameters, the computer acquired one complete cardiac cycle at the acquisition start position and recorded it at 25 frames/sec. When one cardiac cycle had been stored in the computer's RAM, the steering control advanced the transducer by one step. A total of 90 cardiac cycles were stored during one acquisition.

The same acquisition protocol was used for the acquisition of grey-scale and Doppler myocardial images. When relevant, the acquisition started with grey-scale data and then Doppler myocardial images were collected.

The acquisition time was approximately three minutes for both the grey-scale and Doppler myocardial imaging technique.

Patients undergoing transthoracic three-dimensional echocardiograms were not routinely given a sedative. Most of the children who did require mild sedation were from the group of atrio-ventricular septal defects which in most cases co-existed with Down's syndrome and even for routine standard ultrasound examination these children required a mild sedation using Triclofos Elixir BP.

After acquisition, the data was stored on the system hard drive and then analysed off-line.

2.3. Image processing

Image processing was performed off-line after the data was stored on the system's hard-drive. The post-processing of images is automatic and takes approximately ten to thirty minutes depending on the size of a data-set. During this time the recorded images are converted from polar to Cartesian co-ordinates and the gaps between adjacent two-dimensional cross-sections in the far field are electronically filled with a trilinear cylindrical interpolation. Several algorithms are used to minimise signal noise and potential artefacts created by patient and/or transducer movement.

2.4. Image display

From the post-processed data-set, any desired cross-section can be computed and displayed in a dynamic two-dimensional format. This so-called any-plane echocardiography allows unlimited two-dimensional cross-sections not dependent on the ultrasound window. After selection of an appropriate two-dimensional cross-section, a polyhedral surface algorithm allows dynamic three-dimensional reconstruction of tissue data behind the chosen two-dimensional plane. Three different shading functions (distance, gradient and texture) are mixed automatically to create a three-dimensional image. In the distance-shading, the distance from the observer to the surface of the object is converted into grey values, with light grey values indicating proximity and the darker ones indicating increasing distance between the surface of the object and the observer. The role of gradient-shading is to create a more realistic appearance of three-dimensional images by correlating grey

values of neighbouring pixels. With texture-shading, the perception of depth is further enhanced and the characteristic appearance of ultrasound images can be retained. These three functions can also be adjusted manually after the data is post-processed however because of its high susceptibility to artefacts is not recommended. In this thesis different views were used to reconstruct heart structures in three-dimensions. In general, for each studied cardiac malformation the view selected for three-dimensional reconstruction was similar to that seen by a surgeon during the defect repair. The time required to complete a reconstruction varied between five minutes to ninety minutes depending on the complexity of the malformation.

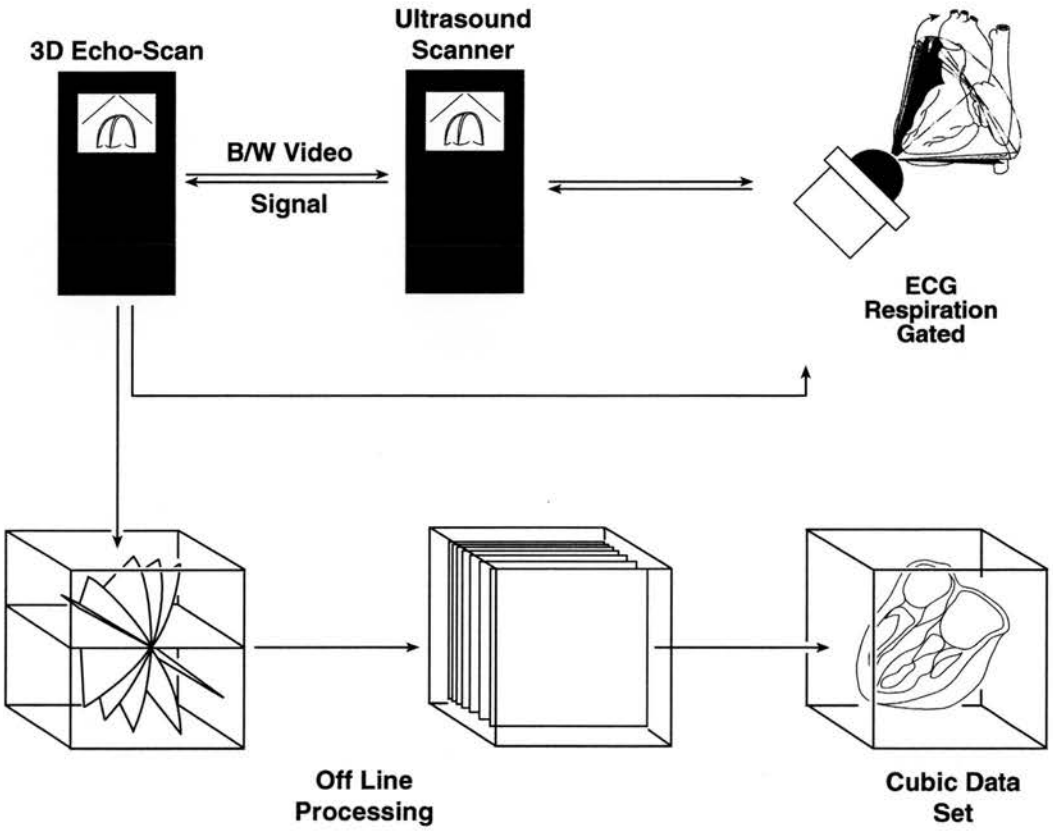

Figure 1. Steps taken to acquire three-dimensional data-set. Diagram shows an ECG and respiration gated acquisition of two-dimensional cross-sections obtained from the transthoracic apical window by rotating the transducer by the mechanical device at 2^0 steps over 180^0. Once the acquisition was completed, off-line processing based on interpolation of the missing information between the acquired two-dimensional images at 2^0 steps and conversion of the images from polar to Cartesian co-ordinates was carried out.

CHAPTER 3

An in Vitro Validation of the Accuracy of Measurements and Volume Computation Derived by Three-Dimensional Echocardiography: a Comparison of Grey-Scale and Doppler Myocardial Imaging Acquisition Techniques Using Dynamic Phantoms

3.1. Background

Several three-dimensional ultrasound systems have been developed which allow three-dimensional images to be constructed from either the transthoracic or transoesophageal approach. However, the accuracy of each system has to be independently validated because the design, calibration techniques, and computer algorithms vary between the systems. Three-dimensional acoustic position registration systems (wire-frame display of three-dimensional images) have been validated in a series of *in vitro* experiments [Brinkley et al., 1982; Moritz et al., 1983; Levine et al., 1989; King et al., 1991]. It has been shown that dimensions, angles and volumes can be obtained from a wire-frame three-dimensional data-set with a very high accuracy. The *in vitro* analysis of the acoustic system of King et al. showed that the mean error in distance measurements is not bigger that 0.4% of the true value, and for volume measurement this does not exceed 1.6%. [King et al., 1991]. However, in that *in vitro* experiment, only a static model constructed of several strong acoustic reflectors (steel pin heads) mounted on a metal base was tested. It is possible that the results of King et al., would not be achieved if tested in a dynamic setting and tissue mimicking structure rather than strong acoustic reflectors was used.

No data have been available on the accuracy of volume-rendered dynamic three-dimensional reconstructions. As a basis for a series of clinical studies an *in vitro* model was established to test the accuracy of the three-dimensional system in computing linear measurements and volumes. Additionally, two different imaging techniques (standard grey-scale and Doppler myocardial imaging) were tested as

acquisition techniques for three-dimensional echocardiography. Currently, grey-scale is the standard imaging technique used to acquire three-dimensional data. The limitation of the use of grey-scale imaging technique in three-dimensional transthoracic echocardiography is that the quality of the acquired images is directly related to the amplitude of the ultrasound signal returning from the heart which is, in a substantial number of patients, markedly attenuated by chest wall structures. In order to obtain good quality three-dimensional data in these patients, it is necessary to use a transoesophageal approach. Doppler myocardial imaging is a new ultrasound technique, based on the Doppler principle, in which special algorithms are applied to detect heart structure instead of blood flow [McDicken et al., 1992; Sutherland et al., 1994; Miyatake et al., 1995]. As opposed to grey-scale technique, the quality of Doppler myocardial images is dependent on two factors: the amplitude of the returning signal, and the frequency shift of this signal which is relatively independent of the attenuation factor. Thus, it is the latter factor which gives rise to the potential of the Doppler myocardial imaging technique to provide more complete images of the heart than the standard grey-scale technique from the transthoracic approach [Fleming et al., 1996].

The aim of this study was to validate the accuracy of measurements taken from three-dimensional ultrasound images acquired using two different imaging techniques: grey-scale and Doppler myocardial imaging.

3.2. Methods

To validate the accuracy of measurements taken from three-dimensional ultrasound images, a computer-generated virtual phantom and a dynamic tissue mimicking phantom were tested. In the preparation of the virtual phantom I was fortunate to have a support of Mr Thomas Anderson and Professor W Norman McDicken from the Department of Medical Physics and Medical Engineering, the Royal Infirmary of Edinburgh in Edinburgh. Tissue mimicking phantom was designed and made by Professor Andrzej Nowicki's group from the Institute of Fundamental Technological Research, Polish Academy of Sciences in Warsaw, Poland [Nowicki et al., 1996].

The virtual phantom was constructed to assess the potential accuracy of the three-dimensional system. Also, the aim was to establish whether the three-dimensional system does introduce a measurement error which is not observed in two-dimensional scanner. The layout for the virtual phantom was prepared on a computer aided drawing package (KeyCad). This allowed precise positioning and relative sizing of the phantom components. The actual scale or size of the phantom was determined by comparing the virtual phantom image on the three-dimensional capture system with markers from the ultrasound system. To capture the virtual phantom as an image, the monitor output was fed to a commercially available interface box which provided RGB signals to the three-dimensional acquisition system (TomTec Echo-Scan) (**Figure 1**).

Also, a one chamber contracting tissue-mimicking phantom was constructed to simulate left ventricle contraction. The phantom consisted of a latex balloon (acting

as endocardium) placed inside one centimetre thick tissue-equivalent expandable foam (acting as myocardium) of a shape and size of the left ventricle. In order to mimic left ventricular contractions, the phantom was connected to an electrocardiogram gated water pump and de-gassed water was pumped into the phantom at a rate 50 times/min. A specially constructed valve between the phantom and the pump allowed the water from the phantom chamber to be returned back to the pump.

To validate the accuracy of the changes in volume measurements, by both techniques grey-scale imaging and Doppler myocardial imaging, with changes in size of the measured volume, varying known amounts of water were pumped into the phantom (from 24 ml to 190 ml).

In addition, in order to define the minimum size of an isolated reflector which could be accurately identified in a three-dimensional reconstruction by this system, rings of resin crystals of known differing dimension were implanted on the surface of the scanned phantom.

Three-dimensional imaging protocol

The instrumentation used for the three-dimensional imaging protocol consisted of an ultrasound scanner (Acuson XP 10 Mountain View, California) with Doppler myocardial imaging software connected to a three-dimensional acquisition system (TomTec Echo-Scan, Munich, Germany). The scanner modifications enabling Doppler myocardial imaging and the steps for three-dimensional image acquisition have been described in Chapter 2.

For grey-scale imaging, the gain was adjusted to optimise the clarity of the phantom 'endocardial' boundaries. In Doppler myocardial imaging, 'endocardial' boundary was defined as the line of interface between the layer of the latex connected to the sponge and the cavity of the phantom.

Briefly, during the image acquisition consecutive two-dimensional imaging frames were acquired from the contracting phantom using electrocardiographic gating. A mechanical device rotated the transducer at 2° steps over 180° (**Figure 2**). Using a polyhedral volume algorithm, the minimum and maximum volumes (systolic and diastolic) of the contracting phantom were calculated from consecutive 1.0 millimetre thick short-axis slices. In order to validate the accuracy of both imaging techniques in three-dimensional volume measurements, seventeen different volumes of a tested object were measured during maximum and minimum contraction of the phantom. This was achieved by pumping differing known amounts of water into the chamber of the contracting phantom.

The same protocol was used for grey-scale and Doppler myocardial image acquisition.

Statistical analysis

The error of inaccuracy of both grey-scale and Doppler myocardial imaging three-dimensional volume estimation was assessed by calculating two different parameters: bias (systematic error), and imprecision (random error) [Bishop et al., 1975].

The differences between both grey-scale and Doppler myocardial imaging volume measurements taken during minimum and maximum phantom contraction and true

volume were compared with the true volume of the phantom. This allowed us to assess whether the two tested ultrasound techniques have a tendency to underestimate or overestimate the measured volume. In order to determine whether the changes in the magnitude of the systematic error varied according to the changes in the volume size, seventeen different volumes were measured and these values were compared using linear regression analysis. The systematic error was also expressed as a percentage of the volume being measured [percentage error = (measured volume - true volume) / true volume x 100%], and the mean percentage error ± one standard deviation was calculated for each method. Finally, the mean percent error was compared by nonparametric methods using analysis of variance (Friedman ANOVA).

To assess the accuracy of each method, each measurement was adjusted for systematic error by applying a correcting factor based on the linear regression of the measured three-dimensional grey-scale and Doppler myocardial imaging volumes with the respective true volume. In these calculations a predicted true volume was substituted for each measured volume. After this adjustment, the difference between the predicted true volume and the true volume was calculated, and the percentage error was expressed as an absolute value. The accuracy of each technique was compared by applying the Friedman ANOVA test.

3.3. Results

Analysis of three-dimensional images of the virtual phantom showed that 1.0 millimetre dimension structure can still be reconstructed by the three-dimensional

system and the smallest distance between the two structures is of 1.0 millimetre (**Figure 1**).

Analysis of three-dimensional images of the dynamic phantom showed that both imaging techniques (grey-scale and Doppler myocardial imaging) underestimated the true volume of the phantom but the systematic error (bias) was significantly smaller for Doppler myocardial imaging than for grey-scale imaging technique (-1.2 ±1.5 % versus -4.3 ±3.1 %; $p<0.01$). **Figure 3** shows that the systematic error for three-dimensional Doppler myocardial imaging was more constant ($r = -0.40$; $p<0.02$) than GSI ($r = -0.79$; $p<0.001$) over the range of different sizes of true volume. Thus, the magnitude of the bias was smaller in Doppler myocardial imaging than in grey-scale imaging when the measurements were taken from bigger volumes.

Figure 4 shows that the random error was low in both three-dimensional ultrasonic techniques: for grey-scale imaging 2.1 ± 2.2 % and for Doppler myocardial imaging 1.2 ± 1.0; $p=0.086$.

Finally, we have shown that a 1.0 millimetre isolated crystal may be correctly identified and measured in a three-dimensional grey-scale and Doppler myocardial imaging reconstruction (**Figure 5**).

3.4. Discussion

In this study, both phantoms (the virtual phantom and the dynamic tissue mimicking phantom) were created to validate the *in vitro* accuracy of the three-dimensional reconstructions and also the accuracy of measurements obtained from these three-dimensional images reconstructed using the TomTec three-dimensional

acquisition system. This was undertaken as, despite the general agreement that three-dimensional echocardiography enhances the understanding of cardiac anatomy, no validation of the accuracy of dynamic three-dimensional volume-rendered images has been performed.

The analysis of the three-dimensional reconstruction of the virtual phantom showed excellent potential accuracy of the three-dimensional capture system (TomTec Echo-Scan). It has been demonstrated that using this system it is possible to reconstruct a detail of 1.0 millimetre dimension and two details separated from each other by a distance of 1.0 millimetre.

In the second part of the study, three-dimensional volumes of a single chamber contracting tissue mimicking phantom were measured independently by the two techniques (grey-scale imaging and Doppler myocardial imaging) and then the results were correlated with the true volume of the tested object. Previous studies which were based only on grey-scale imaging and acoustic transducer position registration systems (wire-frame display of three-dimensional images) have demonstrated a high degree of accuracy *in vitro* three-dimensional volume computation [Gopal et al., 1994; Kuroda et al., 1991; Sapin et al., 1993]. *In vivo*, although grey-scale three-dimensional echocardiography was shown to slightly underestimate the measured volume, it has been found to be superior to grey-scale two-dimensional echocardiography [Schroeder et al., 1993; Gopal et al., 1993; Sapin et al., 1994]. A major potential problem in transthoracic grey-scale imaging three-dimensional echocardiography is the poor image quality obtained in a substantial number of patients [Pearlman et al., 1993]. Superimposed lungs and chest wall

structures attenuate the ultrasound signal reducing the signal to noise ratio making it difficult to acquire a sufficient number of clear images to represent the left ventricular cavity accurately. Therefore, another imaging technique that would give us clear transthoracic images in a substantial part of adult patient population would be of great value. Doppler myocardial imaging offers clear advantages over the standard grey-scale imaging technique for transthoracic data acquisition. Unlike grey-scale imaging, the quality of Doppler myocardial images is dependent on two parameters: the amplitude of the ultrasound signal, which is directly affected by chest wall attenuation, and the frequency shift of ultrasound signal, which is relatively independent of the attenuation. Thus, where ultrasound attenuation produced by overlying tissues is a problem, Doppler myocardial imaging could provide better quality transthoracic images in a substantial number of patients. In this study, we have demonstrated that *in vitro*, both techniques slightly underestimated the true volume of tissue mimicking phantom, and although there was no significant difference in the percentage of accuracy between the two, the systematic error was not only significantly smaller for Doppler myocardial imaging but also remained fairly constant over the range of volumes tested. Although, a spatial resolution of two-dimensional Doppler myocardial imaging technique is slightly lower than a grey-scale imaging technique [Fleming et al., 1994], we have shown that for all studied gain and depth settings, the minimum size of a relatively strong isolated reflector which may be correctly distinguished and measured in a three-dimensional Doppler myocardial reconstruction is 1.0 millimetre. This gives a guide to how potentially accurate measurements taken from three-dimensional images can be.

3.5. Conclusions

Analysis of the three-dimensional reconstruction of the virtual phantom showed excellent accuracy of the three-dimensional capture system. It has been shown that using this system it is possible to reconstruct a detail of 1.0 millimetre dimension and two details separated from each other by a distance of 1.0 millimetre.

Both techniques slightly underestimated the true volume of the tissue mimicking phantom, and although there was no significant difference in the percentage of accuracy between the two, the systematic error was not only significantly smaller for Doppler myocardial imaging but also remained fairly constant over the range of volumes tested.

The spatial resolution of the *in vitro* acquired three-dimensional ultrasound images using both grey-scale and Doppler myocardial imaging data has been shown to be virtually identical. Thus, the advantage of three-dimensional Doppler myocardial imaging over three-dimensional grey-scale images is that the Doppler technique should provide good quality transthoracic three-dimensional images in 'poorly echogenic' patients with the spatial resolution inherent in standard grey-scale images.

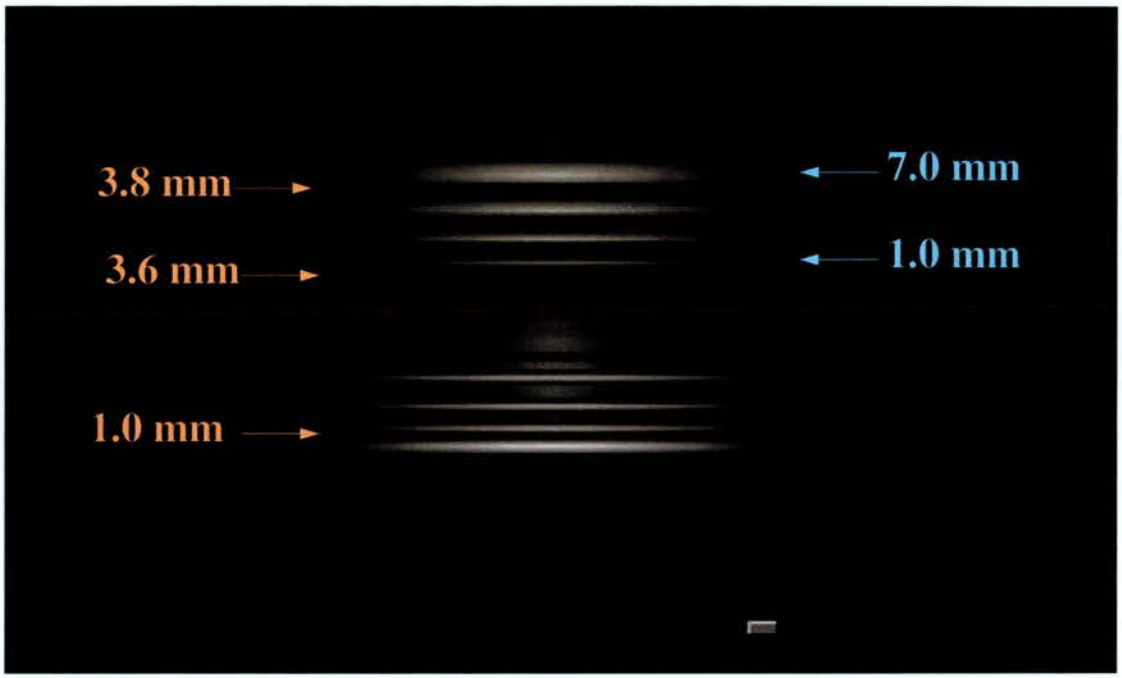

Figure 1. Three-dimensional reconstruction of the virtual phantom.
On the right side of the image, the thickness of the consecutive reconstructed disks is displayed. On the left side of the image, the distances between disks is displayed.

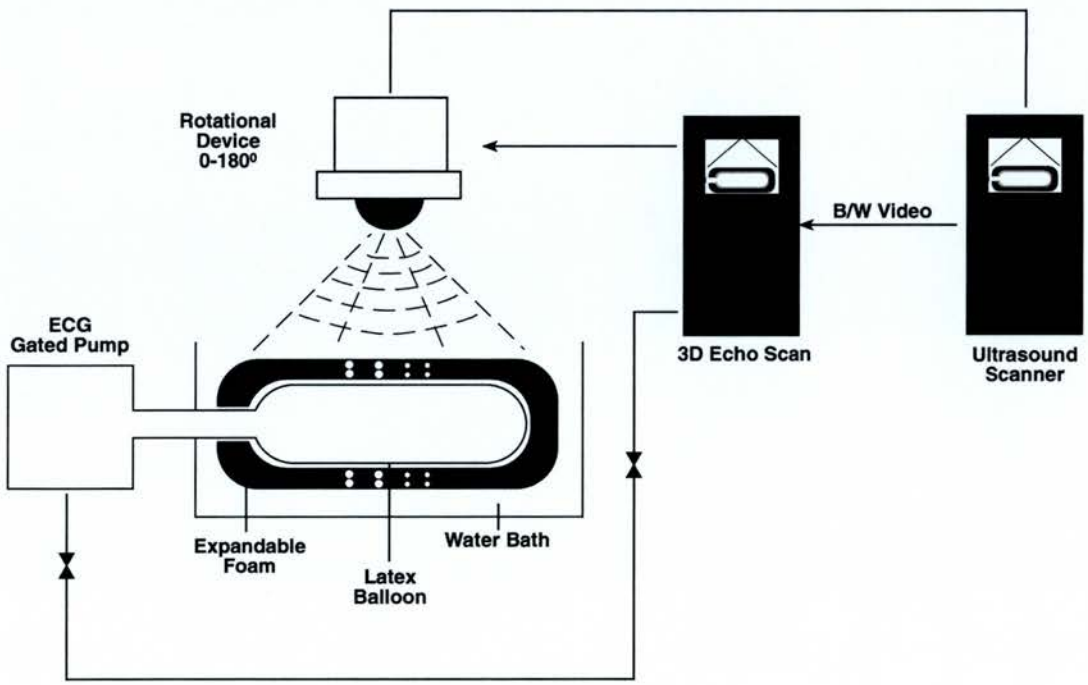

Figure 2. Schematic diagram presenting the set-up of the in vitro study.
An ECG gated acquisition of two-dimensional cross-sections of the phantom at 2° steps over 180°. After the completion of the acquisition: off-line processing based on the interpolation of the missing information between the acquired two-dimensional images at 2^0 steps and conversion of the images from polar to cartesian co-ordinates.

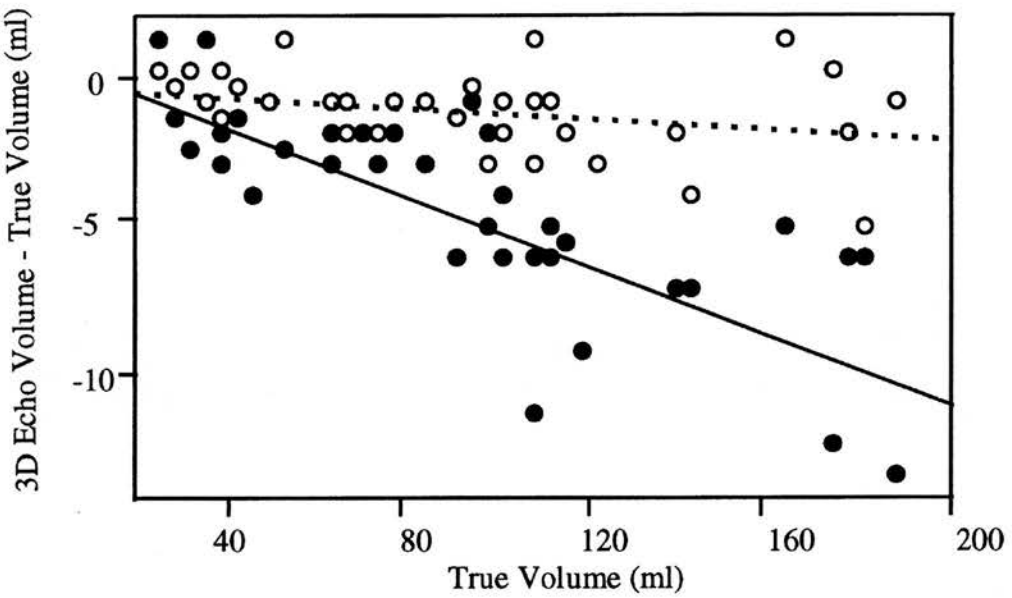

Figure 3. Scatterplot illustrating the *in vitro* relation between the magnitude and direction of systematic error (bias) and size of the volume being measured. The differences between estimated and true volume is plotted against the true volume. The systematic error for Doppler myocardial imaging (**open circles**) remains relatively constant over the range of volumes measured, whereas for grey-scale imaging (**solid circles**) is greater at larger volumes.

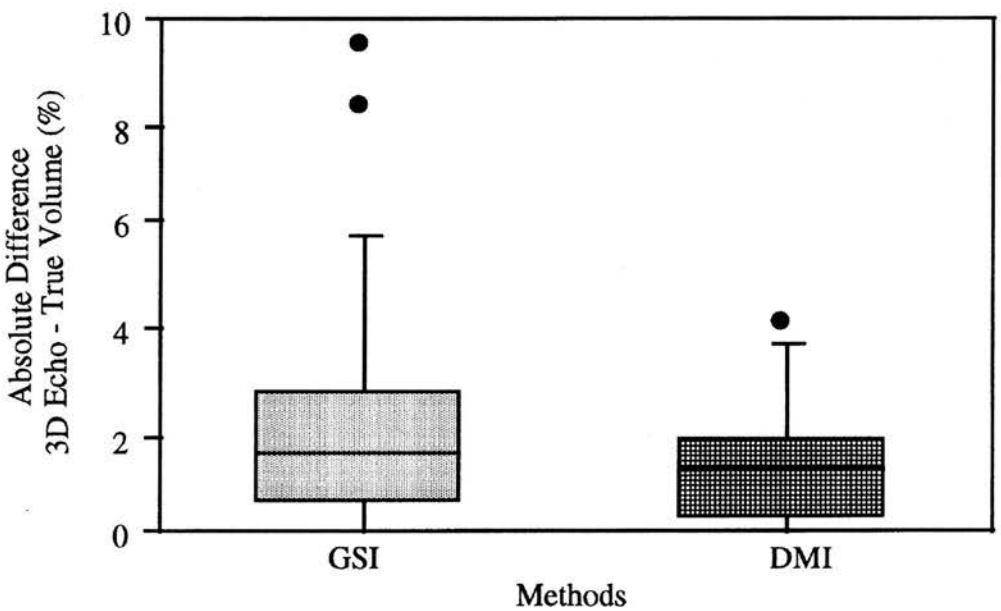

Figure 4. Box plot illustrating the *in vitro* systematic error and imprecision of both ultrasound techniques.
The position of the box in relation to the zero line is an indicator of systematic error.
The vertical height of the box and its error bars are an indicator of imprecision.
GSI, grey-scale imaging; DMI, Doppler myocardial imaging

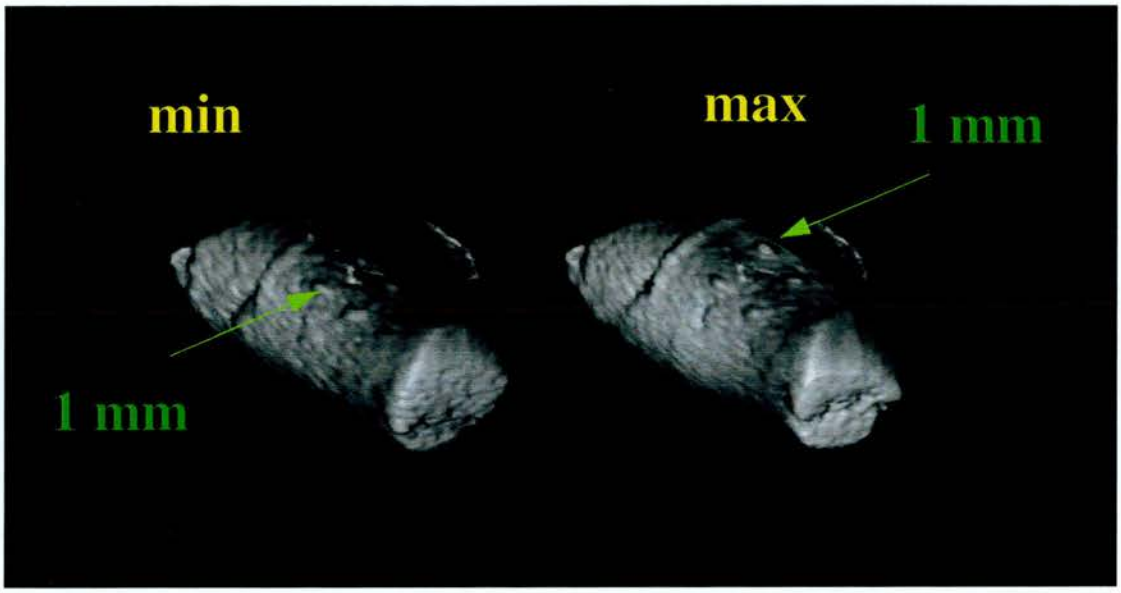

Figure 5. Three-dimensional Doppler myocardial imaging reconstruction of the tested tissue mimicking phantom during minimum (min) and maximum (max) contraction. Arrows indicate the reconstructed resin crystals of 1mm dimension.

CHAPTER 4

Three-Dimensional Echocardiographic Evaluation of Left Ventricular Volume: Comparison of Doppler Myocardial Imaging and Standard Grey-scale Imaging with Cineventriculography

4.1. Background

The measurement and monitoring of left ventricular volume is an important clinical tool in patients with cardiac disease. Although cineventriculography has been accepted as a clinical standard for left ventricular volume determination, the invasive nature of the technique and the inherent assumptions concerning the geometry of the left ventricle limit its application in repeated assessments [Dodge et al., 1960; Vas et al., 1981; Wyme et al., 1978; Schnittger et al., 1982]. Radionuclide methods offer an alternative, non-invasive approach [Levy et al., 1992] but are subject to other limitations. These are mainly related to the detection of edges and end planes as well as the determination of the level of background activity [Starling et al., 1981]. Previous attempts using standard two-dimensional echocardiographic techniques have also demonstrated several important limitations, particularly in patients with regions of left ventricular asynergy. Factors contributing to the low predictive accuracy of two-dimensional echocardiographic volume measurements include geometric assumptions, image plane positioning errors and imprecise endocardial boundary detection [Wyatt et al., 1980; Tortoledo et al., 1982]. Recently, a number of three-dimensional echocardiographic scanners have been developed which address the issue of geometric assumptions [Geiser et al., 1982; Nixon et al., 1983; Ghosh et al., 1982; Sawada et al., 1983; Snyder et al., 1986]. These allow three-dimensional images to be constructed from either transthoracic or transesophageal data-sets. Using different three-dimensional acquisition systems it has been shown that standard grey-scale imaging three-dimensional echocardiography is superior to two-dimensional echocardiography in measuring left ventricular volume [Schroeder et al.,1993; Gopal et al., 1993] and that the three-dimensional measurements correlate

well with cineventriculography and magnetic resonance imaging [Sapin et al., 1994; Pini et al., 1997]. However a major limitation of the transthoracic approach in acquiring a three-dimensional data-set is the poor quality of grey-scale images obtained in a substantial proportion of patients [Lange et al., 1995; Azevedo et al., 1996; Lange et al., 1996]. This is because the quality of grey-scale images is related to the amplitude of the ultrasound signal returning from the interrogated myocardium which is markedly attenuated by chest wall structures in a substantial number of patients. Doppler myocardial imaging is a new ultrasound technique, based on Doppler principles, in which special algorithms are applied to detect myocardial wall motion instead of intracardiac blood flow [McDicken et al., 1992; Sutherland et al., 1994; Miyatake et al., 1995]. The quality of Doppler myocardial images is dependent on two factors as opposed to one factor in grey-scale imaging: the amplitude of the returning signal, which is in turn directly dependent on the attenuation, and the frequency shift of this signal which is relatively independent of the attenuation factor. Thus, it is this latter factor which gives rise to the potential of the Doppler technique to provide more complete images of the myocardium than the standard grey-scale technique. The potential clinical application of Doppler myocardial imaging in quantifying regional left ventricular function [Donovan et al., 1995; Miyatake et al., 1995; Palka et al., 1995&1996; Gorcsan et al., 1996&1997; Uematsu et al., 1996] and also in differentiating left ventricular hypertrophy of different aetiology [Rodgriguez et al., 1996; Palka et al., 1997] has been previously validated in a series of studies. Also, Doppler myocardial imaging has been reported to be a superior technique to grey-scale imaging in displaying the endocardial boundary [Lange et al., 1997] and providing better quality three-dimensional reconstructions of

heart structures when using the transthoracic approach [Lange et al.,1996; Azevedo et al., 1996].

This study was designed to compare the accuracy of standard grey-scale imaging and Doppler myocardial imaging three-dimensional left ventricular volume measurements by comparing them to the clinically accepted method of left ventricular volume measurement, cineventriculography.

4.2. Methods

Sixteen randomly selected patients with ischaemic heart disease undergoing coronary angiography (eight females, mean age 63 ± 11 years) were studied. All of the sixteen patients selected had localised regional wall motion abnormalities as assessed by standard two-dimensional echocardiography. Prior to entry into the study, informed consent was obtained from all volunteers.

Although, computer tomography or magnetic resonance imaging would seem to be a more appropriate technique against which to compare three-dimensional echocardiographic volume measurements, cineventriculography was chosen consciously for practical reasons. All our patients planned for a surgical revascularization had their left ventricles assessed by cineventriculography and therefore we have used the results already available for the comparison with three-dimensional echocardiographic measurements.

Three-dimensional imaging protocol

The instrumentation used for the three-dimensional imaging protocol consisted of an ultrasound scanner (Acuson XP10 Mountain View, California) with Doppler myocardial imaging software connected to a three-dimensional acquisition system (TomTec Echo-Scan; Munich, Germany). The scanner modifications enabling Doppler myocardial imaging have been described in Chapter 2. In brief, the velocity range settings used to encode myocardial velocities (0.2-24 cm/s) were lower than those typically used for blood flow. No filters were used. Image persistence was turned off to eliminate blurring of the moving myocardium. Doppler receive gain was also set to achieve maximum colour Doppler information in the myocardium.

Although the Doppler information is angle dependent, the angle insonation needs to be taken into account when measuring myocardial velocities only [Fleming et al., 1994]. In previously reported cases where Doppler myocardial imaging was used as an acquisition technique to visualise cardiac structures, the incident angle of the ultrasonic beam did not affect the completeness of the image [Lange et al., 1995&1996; Azevedo et al., 1996]. This is because even very low myocardial velocities with approximate values of around 0 to 0.2 m/s are also colour coded by Doppler myocardial imaging as a mosaic of red and blue colour [Fleming et al., 1996]. For grey-scale imaging, the gain was adjusted to optimise the clarity of the endocardial boundaries. In the grey-scale imaging, images endocardial boundary was defined as the "speckle line" near the myocardial borders. Often the lines were not continuous: in some instances, they would fade and then completely disappear. In such cases, the trace was terminated. However, if another speckle line was present at

a slightly different depth which appeared to be the continuation of the first line then the trace was continued from the first to the second line across the region of "drop-out". In Doppler myocardial imaging, endocardial boundary was defined as the line of interface between myocardial wall and blood pool.

The detailed protocol for image acquisition has been described in Chapter 2. The ultrasound images (both grey-scale and Doppler myocardial images) were obtained using 2.5 MHz phased array transducer driven by the transducer mechanical rotational device supplied with the TomTec Echo-Scan. Electrocardiographic and respiration gating were used. During the acquisition procedure the transducer was placed in the standard apical position and was rotated by the mechanical rotational device at 2^{o} steps over 180^{o}. A total of 90 cardiac cycles were stored during one acquisition. In order to create the three-dimensional data-set, additional points needed to be interpolated (off-line post-processing) between the acquired 2^{o} step two-dimensional images. The same protocol was used for grey-scale imaging and Doppler myocardial imaging acquisition.

Left ventricular volumes were calculated at end-diastole and end-systole from both grey-scale and Doppler myocardial data-sets. The protocol for left ventricular volume computation was similar to that described in Chapter 3 where maximum and minimum volumes of the contracting phantom were computed. The endocardial boundary was manually traced in a series of short-axis 5 millimetre thick images, which were acquired with reference to the pre-defined apical long-axis of the image. The papillary muscles were excluded from the chamber volume.

The results obtained from three-dimensional ultrasound images were then compared to those obtained from cineventriculography.

Cineventriculography

Within two hours after the three-dimensional echocardiograms were performed, the patients underwent diagnostic coronary angiography and cineventriculography. All cineventriculograms were recorded at 30 frames/s during the power injection of 30 to 40 ml of iopamidol at 10 ml/s through a 6 F pigtail catheter. In all patients, two views 30° right anterior oblique (RAO) and 60° left anterior oblique (LAO) views were obtained. The first three sinus beats recorded after the contrast injection that did not follow a premature beat were used for volume calculation. Because of the lack of software to automatically calculate left ventricular volume from two views, we measured left ventricular volumes separately for 30° RAO and 60° LAO views and then the average value was taken from both measurements. Papillary muscles were excluded in the volume calculation. End-diastole was defined as the visually estimated largest silhouette, and end-systole as the smallest silhouette of the left ventricle. The contours were then hand-traced and the volumes calculated using the disc-summation method as previously described and validated by others [Dodge et al., 1960; Erbel et al., 1983].

Statistical analysis

End-systolic and end-diastolic volumes of the left ventricle were assessed by both three-dimensional echocardiography (grey-scale and Doppler myocardial imaging) and cineventriculography and are presented as mean values and a standard deviation (mean $\pm$ SD). As we did not have a true value of the measured left ventricular

volume but a value obtained from an accepted clinical standard, both grey-scale and Doppler myocardial imaging three-dimensional volume measurements were correlated using linear regression analysis to the volumes obtained by cineventriculography. To assess the level of agreement between grey-scale imaging versus cineventriculography and Doppler myocardial imaging versus cineventriculography and to test the reproducibility of both three-dimensional ultrasound techniques, Bland and Altman's test was used [Bland et al., 1986]. The 95% limits of agreement were calculated as twice the standard deviation and the results were compared by Friedman ANOVA test. Interobserver variability and intraobserver variability were assessed in a group of ten randomly selected patients. Finally, the endocardial boundary definition obtained by grey-scale imaging and Doppler myocardial imaging was compared using McNemars test for marginal homogeneity. This expresses the percentage of a clearly defined endocardial boundary to the circumference of the inner dimension for each measured slice of the ventricle [Bishop et al., 1975]. A p value < 0.05 was considered to be significant.

4.3. Results

The mean end-systolic volumes for three-dimensional echocardiography were: for grey-scale imaging 70 ±15 ml, for Doppler myocardial imaging 75 ±18 ml; and for cineventriculography 77 ±18 ml. For end-diastole these values were: 127 ±18 ml, 140 ± 20 ml and 144 ± 22 ml, respectively.

There was a good correlation between both three-dimensional ultrasonic techniques and cineventriculography: grey-scale imaging ($r = 0.98$, $p<0.0001$), Doppler

myocardial imaging ($r = 0.99$, $p<0.0001$). The standard error of estimates for grey-scale imaging was ±7 ml and for Doppler myocardial imaging ±5 ml.

In three-dimensional echocardiography the mean difference for end-diastole using grey-scale imaging was -12.6 ml, the limits of agreement being ± 18 ml. For end-systole these values were -6.5 ± 10.6 ml, respectively. Using Doppler myocardial imaging the mean difference for end-diastole was -4.2 and ± 10.6 ml and for end-systole -1.5 ± 10 ml (**Figure 1**). The magnitude of the difference between three-dimensional echocardiography and cineventriculography in volume measurement was significantly smaller for Doppler myocardial imaging than for grey-scale imaging for both end-diastole and end-systole ($p<0.01$).

Finally, Doppler myocardial imaging proved to be significantly more efficient than the standard grey-scale imaging in endocardial boundary detection at both end-diastole (80 ± 8% versus 67 ± 16% respectively, $p< 0.05$) and end-systole (85 ± 7% versus 71 ± 13% respectively, $p<0.05$) (McNemars test).

Table 1 shows the intraobserver and interobserver variability which was slightly lower for Doppler myocardial imaging.

4.4. Discussion

Although grey-scale three-dimensional echocardiography slightly underestimates the measured volume, it has been found to be superior to grey-scale two-dimensional echocardiography [Schroeder et al., 1993; Gopal et al., 1993; Sapin et al., 1994]. A major potential problem in transthoracic grey-scale imaging three-dimensional echocardiography is the poor image quality obtained in a substantial

number of patients [Pearlman et al., 1993]. Superimposed lungs and chest wall structures attenuate the ultrasound signal reducing the signal to noise ratio making it difficult to acquire a sufficient number of clear images to represent the left ventricular cavity accurately. It is possible to overcome this problem by using a transoesophageal approach. Although it has been documented that this can be performed with a low level of accompanying risk, it still remains a semi-invasive technique, poorly tolerated by a significant number of patients [Daniel et al., 1991]. Doppler myocardial imaging offers clear advantages over the standard grey-scale imaging technique for transthoracic data acquisition (see Chapter 3). Unlike grey-scale imaging, the quality of Doppler myocardial images is dependent on two parameters: the amplitude of the ultrasound signal, which is directly affected by chest wall attenuation, and the frequency shift of ultrasound signal, which is relatively independent of the attenuation. Thus, where ultrasound attenuation produced by overlying tissues is a problem, Doppler myocardial imaging could provide better quality transthoracic images in a substantial number of patients (**Figure 2**). In the previous chapter (Chapter 3), it was demonstrated that *in vitro*, both imaging techniques slightly underestimated the true volume of tissue mimicking phantom. Although there was no significant difference in the percentage of accuracy between the two, the systematic error was not only significantly smaller for Doppler myocardial imaging but also remained fairly constant over the range of volumes tested. *In vivo*, the correlation between volume measurements by three-dimensional echocardiography and those obtained by cineventriculography was very good. However, three-dimensional volume measurements obtained by Doppler myocardial

imaging had significantly closer agreement with those generated by cineventriculography than did those from grey-scale imaging.

Additionally, using McNemars test for marginal homogeneity we have shown the superior boundary definition provided by Doppler myocardial imaging. This is also in agreement with our previous study in which we have shown that endocardial boundary is more reliably displayed and visually easier to detect using Doppler myocardial imaging than grey-scale imaging [Lange et al., 1997].

4.5. Limitations

A potential source of error was the small differences in frame rate of the studied techniques. This was approximately 20 frames/sec for Doppler myocardial imaging, as opposed to 25 frames/sec for grey-scale imaging and 30 frames/sec for cineventriculography. As a consequence, end-systolic and end-diastolic volume measurements could have been measured in slightly different time periods of the heart cycle. Echocardiography and cineventriculography detect different endocardial outlines and additionally cineventriculography still makes assumptions about left ventricular shape. Finally, the changes in the heart rate and expanded circulating volume during cineventriculography may have contributed to differences between the left ventricular volume measurements and three-dimensional echocardiography.

4.6. Conclusions

The results of this study indicate that if three-dimensional echocardiography is to be used to estimate left ventricular volume, Doppler myocardial imaging is the ultrasound technique of choice.

Table 1. Interobserver and Intraobserver Variability

	Interobserver Variability		Intraobserver Variability	
ml	Mean ± SD	%	Mean ± SD	%
EDV				
DMI	1.9 ±5.8	9.7	1.2 ± 3.0	5.3
GSI	2.2 ±5.9	10.9	1.8 ± 4.4	8.7
ESV				
DMI	0.9 ± 2.3	7.1	0.7 ± 2.0	6.8
GSI	1.3 ± 3.0	9.8	1.1 ± 2.9	9.2

EDV, end-diastolic volume; ESV, end-systolic volume; DMI, Doppler myocardial imaging; GSI, grey-scale imaging.

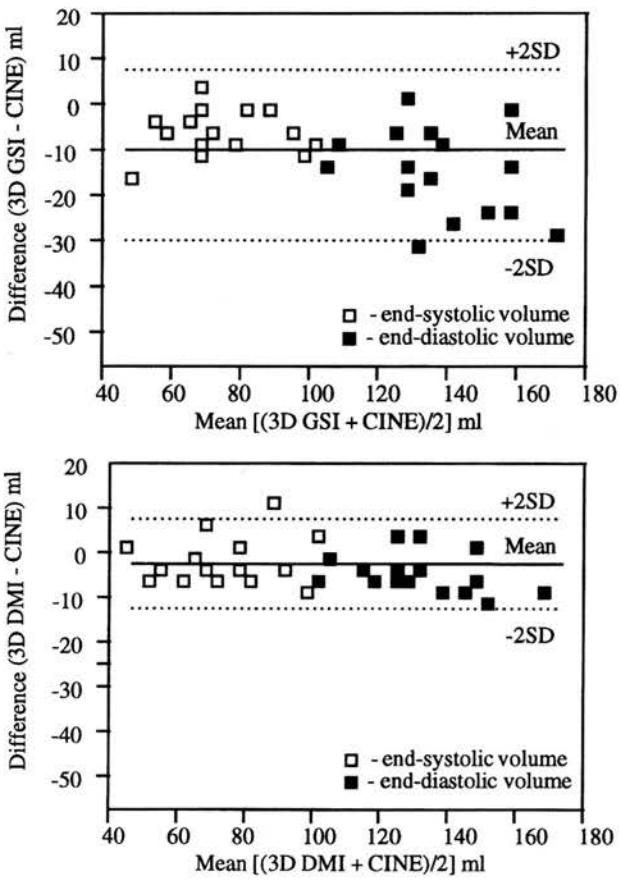

Figure 1. Difference between three-dimensional grey-scale imaging (**top**), Doppler myocardial imaging (**bottom**) and cineventriculography plotted against the mean value.

Results are shown for end-diastolic volumes (**solid squares**) and end-systolic volumes (**open squares**). The solid lines show the mean difference; the dotted lines show the 95% limit of agreement.

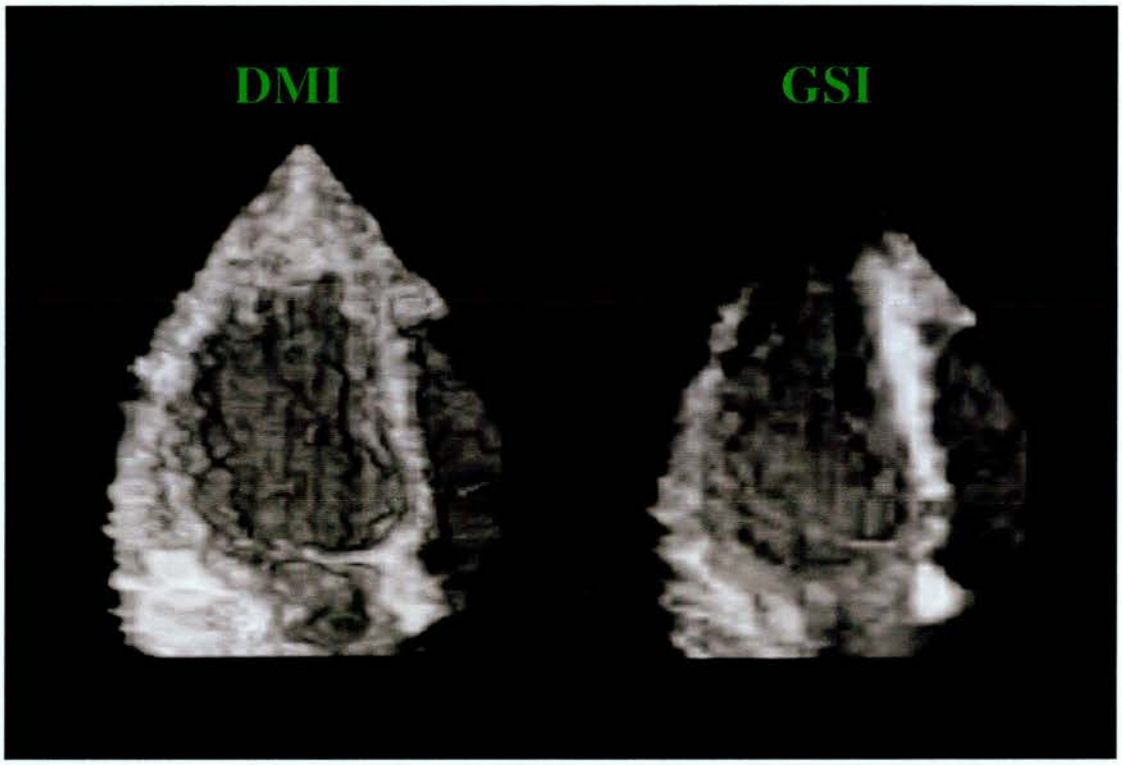

Figure 2. An example of a transthoracic three-dimensional reconstruction of the left ventricle obtained from a 54 year old male with coronary artery disease. Doppler myocardial imaging (DMI) technique on the left side and grey-scale imaging (GSI) technique on the right side of the picture.

CHAPTER 5

Assessment of Atrial Septal Defect Morphology by Transthoracic Three-Dimensional Echocardiography Using Standard Grey-Scale and Doppler Myocardial Imaging Techniques: Comparison with Magnetic Resonance Imaging and Intraoperative Findings

5.1. Background

The development of new techniques of secundum atrial septal defect closure including minimal access surgery [Burke et al., 1994; Schwartz et al., 1996] and percutaneous catheter closure [Rome et al., 1990; Boutin et al., 1993; Lloyd et al., 1994] has increased the need for accurate assessment not only of atrial septal defect size but also defect morphology and its spatial relations to other cardiac structures [Boutin et al., 1993; Chan et al., 1993; Magni et al., 1996]. Currently, several techniques are used to image or size atrial septal defects - echocardiography [Schapira et al., 1979; Morimoto et al., 1990; Hellenbrand et al., 1990; Mehta et al., 1991; Scott et al., 1992], magnetic resonance imaging (MRI) [Holmvang et al., 1995; Diethelm et al., 1987] or balloon sizing during heart catheterisation. Two-dimensional echocardiography is probably the most commonly used imaging technique and with standard precordial imaging, the sensitivity in detecting secundum and primum atrial septal defects is greater than 90% [Mehta et al., 1991; Reeder et al., 1983]. A potentially superior role for three-dimensional echocardiography in atrial septal defect sizing was claimed recently in a comparative study between guided three-dimensional and conventional two-dimensional - examinations [King et al., 1992].

Previous studies on three-dimensional atrial septal defect reconstruction have been carried out using standard grey-scale images [Magni et al., 1996; Belohlavek et al., 1993b; Marx et al., 1995]. In these reports, due to poor transthoracic image quality, grey-scale images were frequently acquired from a transoesophageal approach. In this study therefore we have looked not only at the potential of transthoracic three-

dimensional grey-scale image reconstruction but at the additional value of three-dimensional reconstruction using Doppler myocardial imaging technique.

The principles of Doppler myocardial imaging have been described in previous chapters. In brief, this technique is based on a colour Doppler principle that is applied to detect heart structures rather than a blood flow. As the quality of two-dimensional Doppler myocardial images is not directly affected by the chest wall attenuation, as it is in grey-scale imaging, it should provide better quality images than standard grey-scale imaging for transthoracic three-dimensional echocardiography [Azevedo et al., 1996; Lange et al., 1996].

In order to correlate the two ultrasound techniques in a three-dimensional setting, patients with diagnosed secundum atrial septal defects were studied.

5.2. Methods

A prospective study of the transthoracic three-dimensional echocardiographic definition of atrial septal defect morphology and its dynamic changes during the cardiac cycle was performed. Two different imaging techniques: grey-scale and Doppler myocardial imaging were used to acquire three-dimensional data-sets from each patient. The information obtained from three-dimensional Doppler myocardial images and grey-scale images was compared with that obtained by phase-contrast cine Magnetic Resonance Imaging or surgery.

Patient Selection

Thirty four patients (age 20 ±17 years) with secundum atrial septal defect have been studied. In eighteen patients (age 23 ±18 years) the measurements obtained from

three-dimensional grey-scale and Doppler myocardial images were correlated with phase-contrast cine Magnetic Resonance Imaging and in the remaining sixteen patients the three-dimensional measurements were correlated with these taken during surgical atrial septal defect repair (age 10 ±7 years). The three-dimensional echocardiogram and Magnetic Resonance Imaging scans were performed on the same day in sixteen patients and in two patients there was a four days interval between the three-dimensional echocardiogram and Magnetic Resonance Imaging scan. The average time between three-dimensional echocardiogram and surgery was 30 ±25 days. All but two patients were in sinus rhythm. These two patients were excluded from the analysis of changes in atrial; septal defect size during the cardiac cycle. All patients were informed about the purpose of the study and gave informed consent to be enrolled in the study.

Three-dimensional echocardiography

The instrumentation used for the three-dimensional imaging protocol consisted of an ultrasound scanner (Acuson XP10 Mountain View, California) with implemented Doppler myocardial imaging software and a three-dimensional acquisition system (TomTec Echo-Scan, TomTec Imaging Systems; Munich, Germany).

The scanner modifications which enable Doppler myocardial images to be acquired have been described in previous chapters. Figure 1 in Chapter 2 shows schematically how the three-dimensional images were acquired. The detailed protocol for three-dimensional image acquisition has also been described in Chapter 2. The ultrasound images were obtained using a 2.5- 4.0 MHz phased array transducer steered by the transducer mechanical rotational device supplied with the Echo-Scan. During the

acquisition, the Echo-Scan was connected to the ultrasound video output of the Acuson scanner via a black/white video cable. Thus, when Doppler myocardial images were acquired, the colour Doppler signal was transferred as a black and white video signal to the Echo-Scan. The transducer was placed in the standard apical position and was rotated by the mechanical rotational device at 2^{o} steps over 180^{o}. A total of 90 cardiac cycles were stored during one acquisition. The same acquisition protocol was used for the acquisition of grey-scale and Doppler myocardial images. The acquisition time was approximately three minutes for both techniques. As the patient needs to be immobile, during the image acquisition, seven patients (age from 2 to 3.5 years) required mild sedation using Triclofos Elixir BP.

After acquisition, the data were stored on the system hard drive and then analysed off-line. In each patient, three-dimensional reconstruction of the atrial septal defect was carried out from the right atrium. Firstly, an apical four chamber view was reconstructed. Secondly, the acquired data-set was cut vertically by a longitudinal plane through the right atrial free wall, tricuspid valve and anterior right ventricular free wall. Finally, the reconstruction was orientated anterior to posterior. These manoeuvres provided us with an 'en face' view of the atrial septal defect from which the following parameters were measured: minimum and maximum of horizontal (H) and vertical (V) atrial septal defect dimensions (D) during the cardiac cycle, distances to: coronary sinus (CS), vena cava inferior (IVC), vena cava superior (SVC) and tricuspid valve (TV) during late left ventricular systole (maximum atrial septal defect dimension). (**Figure 1**)

Out of the thirty four defects which were reconstructed using both grey-scale and Doppler myocardial imaging, thirty were single secundum defects and four were multiple (from two to four defects).

From all three-dimensional atrial septal defect reconstructions, the feasibility of detecting right atrial structures and undertaking measurements was assessed for both techniques Doppler myocardial imaging and grey-scale imaging.

Magnetic Resonance Imaging

The Magnetic Resonance Imaging studies were performed on a 1.5 T Siemens Magneton SP system. Fast acquisition 'Turboflash' localizer images (TR 4.9 ms, TE 2 ms, FA 8^{o}) were obtained in the coronal and transverse planes through the ventricles, followed by a single angulated plane through the ventricles, followed by a single angulated plane through the interventricular and interatrial septa to give a right anterior oblique (RAO) two chamber plane localizer. Multiple, contiguous, six mm slice width, sixteen cardiac phases, gated, cine gradient echo images (TR 560 ms, TE 6 ms, FA 30^{o}) were then obtained perpendicular to the interatrial septum in the four chamber projection, using the angulated RAO two chamber localizer.

Gated, velocity encoded, phase contrast imaging with a maximum velocity sensitivity of 120 cm/sec was then performed using a four chamber cine image with the imaging plane proscribed to lie parallel to, and contiguous with the right atrial side of the interatrial septum, to provide an en face view of the defect.

The maximum dimensions of the defects were measured from the images on an independent operating console using electronic callipers.

Surgical data

All operations were performed by one surgeon. The surgery was performed either via midline sternotomy or via right thoracotomy with induced ventricular fibrillation. The aorta was not cross clamped and thus heart was not arrested in diastole using cardioplegic solution in any of the patients. Once the heart was fibrillated and the right atrium opened, a pump sucker was left in the coronary sinus and intermittent suction was performed through the atrial septal defect into the left atrium to achieve bloodless field. The various measurements as described before were taken by the single observer using a string of black silk suture which was cut at an appropriate measured point from the margin of the defect. The length of the suture was measured on a ruler and the findings were noted down by the member of the team. Two independent measurements were taken for each dimension in the first six patients. No difference was observed between the two readings and therefore in the later part of the study only one measurement was obtained in the remaining ten patients.

Statistical analysis

The data are expressed as mean values and standard deviations (mean ±SD). A paired t-test was used to compare the maximum to minimum atrial septal defect dimensional change during the cardiac cycle as measured by three-dimensional echocardiography. Least square regression analysis was performed to test the correlation between the horizontal and vertical dimension of an atrial septal defect, the distances from the atrial septal defect rim to inferior vena cava, superior vena cava, coronary sinus and tricuspid valve measured by both ultrasound techniques grey-scale imaging and Doppler myocardial imaging, Magnetic Resonance Imaging

and surgery. Linear regression analysis was performed to assess the correlation between the changes in atrial septal defect size during the cardiac cycle and age. Finally, the Bland and Altman test was used to assess: (1) the bias (systematic error) between the two ultrasound techniques and Magnetic Resonance Imaging or surgery; (2) how the studied techniques relate to each other (under- or overestimation); (3) reproducibility [Altman et al., 1983; Bland et al., 1986]. Statistical analysis was performed using statistical package UNISTAT 4 for Windows. A p value < 0.05 was considered to be significant.

Interobserver and intraobserver variability

In ten randomly selected patients all the measurements acquired from three-dimensional Doppler myocardial and grey-scale reconstructions pertaining to the maximum and minimum (horizontal & vertical) atrial septal defect dimensions, distances to inferior vena cava, superior vena cava, coronary sinus and tricuspid valve were analysed by two independent observers.

Additionally, in six randomly selected patients, three-dimensional echocardiographic study was performed twice within an average period of 28 ±4 days. Analysis of variance was used to assess the differences between the measurements of atrial septal defect morphology obtained by two observers (interobserver variability) and between measurements taken from the same subjects at different times (intraobserver variability). Both intra- and interobserver variability in atrial septal defect morphology are presented as the mean ±SD.

The interobserver variability for three-dimensional echocardiography for grey-scale imaging was at 0.08 ±0.09 cm (systematic error 16%) and for Doppler myocardial

imaging was 0.07 ±0.08 cm (systematic error 13%). The intraobserver variability for grey-scale imaging was at 0.07 ±0.08 cm (systematic error 15%) and for Doppler myocardial imaging 0.06 ±0.08 cm (systematic error 12%).

5.3. Results

Figure 2 shows the maximum atrial septal defect orifice as defined by: three-dimensional echocardiography using both techniques Doppler myocardial imaging and grey-scale imaging, Magnetic Resonance Imaging phase-contrast cine imaging and surgery.

Table 1 presents the measurements of atrial septal defect dimensions and the distances from the atrial septal defect rim to other structures of the right atrium by three-dimensional echocardiography, Magnetic Resonance Imaging and surgery.

A significant difference was found in changes of both horizontal and vertical atrial septal defect dimensions during the cardiac cycle (**Table 1, Figure 3**). The maximum dimension of atrial septal defects was found in late ventricular systole and minimum in late ventricular diastole. Stepwise multivariate regression analysis showed that the changes in atrial septal defect size are not dependent on the defect size but are inversely related to patient age. **Figure 4** presents the linear regression analysis of the relation between the changes in atrial septal defect size and patients age.

Good correlation was obtained between both maximum horizontal and vertical atrial septal defect dimensions by three-dimensional echocardiography and Magnetic Resonance Imaging (grey-scale imaging: $r=0.96$ cm, $y=0.05+0.89x$, $p<0.0001$; Doppler myocardial imaging: $r=0.97$ cm, $y=0.04+0.97x$, $p<0.001$) or surgery (grey-

scale imaging: r=0.92 cm, y=0.06+0.84x, p<0.001; Doppler myocardial imaging: r=0.95, y=0.06+0.97x, p<0.0001). **Figure 5** shows the difference in atrial septal defect size as determined by three-dimensional echocardiography and Magnetic Resonance Imaging or surgery using Bland and Altman analysis.

The systematic error (bias) between three-dimensional echocardiography and Magnetic Resonance Imaging was low at 0.40 cm (27%) for grey-scale imaging and 0.38 cm (25%) for Doppler myocardial imaging. For surgery the systematic error was at 0.50 cm (29%) and 0.37 cm (22%) respectively.

Additionally, good correlation was also obtained between the distances from the defect rim to inferior vena cava, superior vena cava, coronary sinus and tricuspid valve in its maximum opening by three-dimensional echocardiography and surgery. (**Table 2**)

In children (from three to seventeen years of age, nineteen patients) the feasibility of detecting structures and undertaking measurements was similar for both ultrasound techniques Doppler myocardial imaging and grey-scale imaging. In adult atrial septal defect patients (from eighteen to sixty one years of age, fifteen patients), this was higher for Doppler myocardial imaging than for grey-scale imaging (**Table 3**).

5.4. Discussion

Two-dimensional echocardiography and Magnetic Resonance Imaging are the two most commonly used techniques to assess atrial septal defect size and morphology. The accuracy of Magnetic Resonance Imaging is well established [Dinsomore et al., 1985; Sakakibara et al., 1987] and is claimed to have a sensitivity and specificity greater than 90% in the identification of ostium secundum atrial

septal defect and is superior to standard transthoracic and transoesophageal two-dimensional echocardiography in atrial septal defect sizing [Diethelm et al., 1987]. During the last fifteen years dynamic research has been conducted in the development of three-dimensional echocardiography which may become a bed-side diagnostic technique in the assessment of not only atrial septal defect size and morphology but also its spatial relations to other cardiac structures [Sheikh et al., 1991; Pandian et al., 1992; Roelandt et al., 1994a&b]. This seems to be particularly important in selecting patients for percutaneous atrial septal defect closure by transcatheter device placement [Hellenbrand et al., 1990]. Preliminary studies have been carried out by others showing the ability of three-dimensional echocardiography to reconstruct 'en face' the dynamic morphology of atrial septal defects using transthoracic or transoesophageally acquired ultrasound data [Belohlavek et al., 1993b; Marx et al., 1995; Franke et al., 1997]. However, no comparison has been made to define the accuracy of these reconstructions. It was reported that the quality of transthoracic standard ultrasound images was not satisfactory in all cases and the transthoracic three-dimensional 'en face' reconstruction of atrial septal defect was feasible in 81% of a study group of children [Marx et al., 1995]. Therefore, in this study we have looked not only at the potential accuracy of transthoracic three-dimensional grey-scale reconstruction but at the additional value of three-dimensional reconstruction using Doppler myocardial imaging technique. We have shown that the feasibility of detecting right atrial structures and undertaking measurements by the two studied ultrasound techniques was different with age. In children (<17 years of age) all the required anatomical structures were reconstructed in the similar percentage of patients. However, in

patients over 18 years old, the feasibility of detecting anatomical structures was higher in the case of Doppler myocardial imaging. For both age groups, superior vena cava and coronary sinus were the most difficult to be reconstructed by both ultrasound techniques. We have also shown, that all the atrial septal defects studied changed significantly in dimension during the cardiac cycle with its maximum size in late left ventricular systole and minimum in late left ventricular diastole. Although, this difference was present in all patients, it was inversely correlated with age. A similar finding of a significant difference in atrial septal defect area during the cardiac cycle has been reported by others [Franke et al., 1997]. This may give us potentially new information about the natural history of secundum atrial septal defect which may be taken into account when assessing a patient for percutaneous atrial septal defect occlusion using a device placement. The comparison of measurements by three-dimensional echocardiography and Magnetic Resonance Imaging or surgery was good and within the acceptable limits for a potential clinical application. The maximum atrial septal defect dimension measured by three-dimensional echocardiography correlated well with both Magnetic Resonance Imaging and surgery. The systematic error, for the group as a whole, was slightly lower for Doppler myocardial imaging than for grey-scale imaging when compared to both Magnetic Resonance Imaging (25% versus 27%, respectively) and surgery (22% versus 29%, respectively). This was not verified for the two age subgroups (**Table 2**) because of the relatively small sample size. The comparison between the distances from the atrial septal defect rim to inferior vena cava, superior vena cava, tricuspid valve and coronary sinus, in late ventricular diastole, by three-dimensional

echocardiography and surgery was also good with again slight favour of Doppler myocardial imaging over grey-scale imaging technique.

5.5. Limitations

Technical limitations

(1) Despite growing interest and extensive research in developing real-time three-dimensional echocardiography, current three-dimensional reconstructions are available off-line only. In this particular study time was of minor importance as the information on atrial septal defect morphology was needed as a baseline to plan the treatment strategy. The average acquisition time of a single data-set is approximately three minutes. The time required for the off-line processing of the ultrasound data may take up to twenty minutes. Finally, the time required to reconstruct the data in three-dimensions differs according to the quality of the acquired ultrasound images and may take from two minutes to twenty minutes and sometimes in a complicated case even longer.

(2) Using this three-dimensional acquisition system, the position of the ultrasound transducer during the data acquisition is calculated according to the mechanical steering logic and not according to the transducer spatial co-ordinates. Therefore, the three-dimensional system does not record unexpected change in the transducer position which may create a rotational artefact.

(3) Care also needs to be taken during the adjustment of image gain settings. The three-dimensional system is sensitive enough to reconstruct the ultrasound 'noise' if

such is left on the image. This will result in insufficiently clear three-dimensional reconstruction.

Methodological limitations

In this study the information on atrial septal defect sizing was compared to that obtained from Magnetic Resonance Imaging or surgery. Taking measurement from Magnetic Resonance phase-contrast images one has to make sure that the shunt flow is orthogonal to the cine imaging plane. This is because the technique depends on flow-related enhancement and phase-contrast effects. In most cases the shunt orifice is best seen at end-systole or early-diastole only. It is difficult to assess the dynamic change in atrial septal defect size during the cardiac cycle reliably. Therefore, in this study only the maximum atrial septal defect dimensions (horizontal and vertical) were measured from Magnetic Resonance images.

Surgical closure of an atrial septal defect is usually performed using a cardioplegic solution achieving diastolic arrest of the heart. This, unfortunately, does not reflect the in vivo situation of the beating heart. The relaxed state of the heart tends to overestimate the size of the defect and the various distances measured. In this study, we elected to perform the surgical closure in a fibrillating heart thus maintaining the cardiac tone. The measurements taken at surgery were therefore a more accurate reflection of the in vivo situation.

5.6. Conclusions

Transthoracic three-dimensional grey-scale imaging and Doppler myocardial imaging both accurately displayed the varying morphology, dimensions and spatial

relationships of atrial septal defects. For the group as a whole there was no difference between the two ultrasound techniques in the accuracy of reconstructed three-dimensional images. However, in adult atrial septal defect patients, Doppler myocardial imaging had a greater efficacy than grey-scale imaging technique in reconstructing a surgical view of atrial septal defects. This study shows that a dynamic 'en face' three-dimensional image of an atrial septal defect is no longer restricted to the one seen only by a surgeon during an atrial septal defect repair, but may be reconstructed through the closed chest prior to closure of the defect. This should help to plan the surgical strategy or, where applicable, facilitate the selection of patients for percutaneous device closure.

Table 1. The measurements of ASD dimensions and the distances from the ASD rim to the other structures of the right atrium.

Mean±SD (cm)	Dimension				Distance to			
	Maximum		Minimum					
	H	V	H	V	IVC	SVC	CS	TV
GSI	1.9±0.8*	1.6±0.6*	1.2±0.7	0.9±0.5	1.4±0.5	1.1±0.5	0.9±0.5	2.1±0.6
DMI	1.8±0.7*	1.6±0.6*	1.2±0.7	0.9±0.6	1.5±0.8	1.0±0.4	1.0±0.5	2.3±0.7
MRI	1.7±0.8	1.4±0.6	n/a	n/a	n/a	n/a	n/a	n/a
Surgery	1.9±0.6	1.7±0.5	n/a	n/a	1.3±0.6	0.8±0.3	0.9±0.4	1.9±0.7
Mean±SD	1.8±0.8*	1.6±0.6*	1.2±0.7	0.9±0.5	1.4±0.7	1.0±0.4	0.9±0.5	2.2±0.6

ASD, atrioseptal defect; CS, coronary sinus; DMI, Doppler myocardial imaging; GSI, grey-scale imaging; H, horizontal; IVS, vena cava inferior; MRI, magnetic resonance imaging; SVC, vena cava superior; TV, tricuspid valve; V, vertical. *, $p<0.001$ compared to minimum.

Table 2. Correlation between the measurements obtained by three-dimensional echocardiography and surgery. (for abbreviations see Table 1.)

	Dimension				DMI			
	r	coefficient	SE (cm)	P value	r	coefficient	SE (cm)	P value
IVC	0.84	0.82	0.19	0.0025	0.92	0.96	0.12	0.0001
SVC	0.64	0.57	0.21	0.0198	0.73	1.03	0.27	0.0023
CS	0.68	1.39	0.50	0.0223	0.96	0.98	0.08	0.0001
TV	0.82	0.75	0.15	0.0004	0.86	0.94	0.15	0.0001
Mean±SD	0.75±0.08	0.88±0.31	0.26±0.14	0.0113±0.001	0.87±0.09	0.98±0.03	0.16±0.07	0.0007±0.001

Table 3. Feasibility of detecting structures and undertaking measurements from three-dimensional ASD reconstructions by both imaging techniques GSI and DMI.

	Group 1 (mean age 8±5 yrs) [n=19]				Group 2 (mean age 35±15 yrs) [n=15]			
	GSI		DMI		GSI		DMI	
	n	%	n	%	n	%	n	%
max. D	19	100	19	100	12	80	15	100
min.D	16	84	18	95	11	73	14	93
SVC	13	68	15	79	10	67	12	80
IVC	14	74	16	84	11	73	12	80
CS	12	63	16	84	8	53	12	80
TV	19	100	19	100	12	80	15	100
Mean±SD	15±3	82±15	17±2	90±8	11±1	71±9	13±1	89±9

For abbreviations see Table 1.

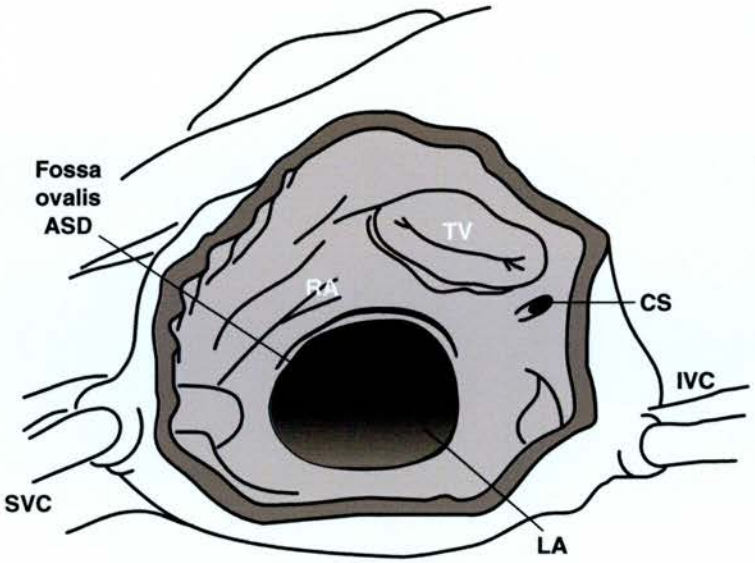

Figure 1. The schematic presentation of the secundum atrial-septal defect (ASD) as seen by the surgeon. CS, coronary sinus; IVC, vena cava inferior; LA, left atrium; RA, right atrium; SVC, vena cava superior; TV, tricuspid valve.

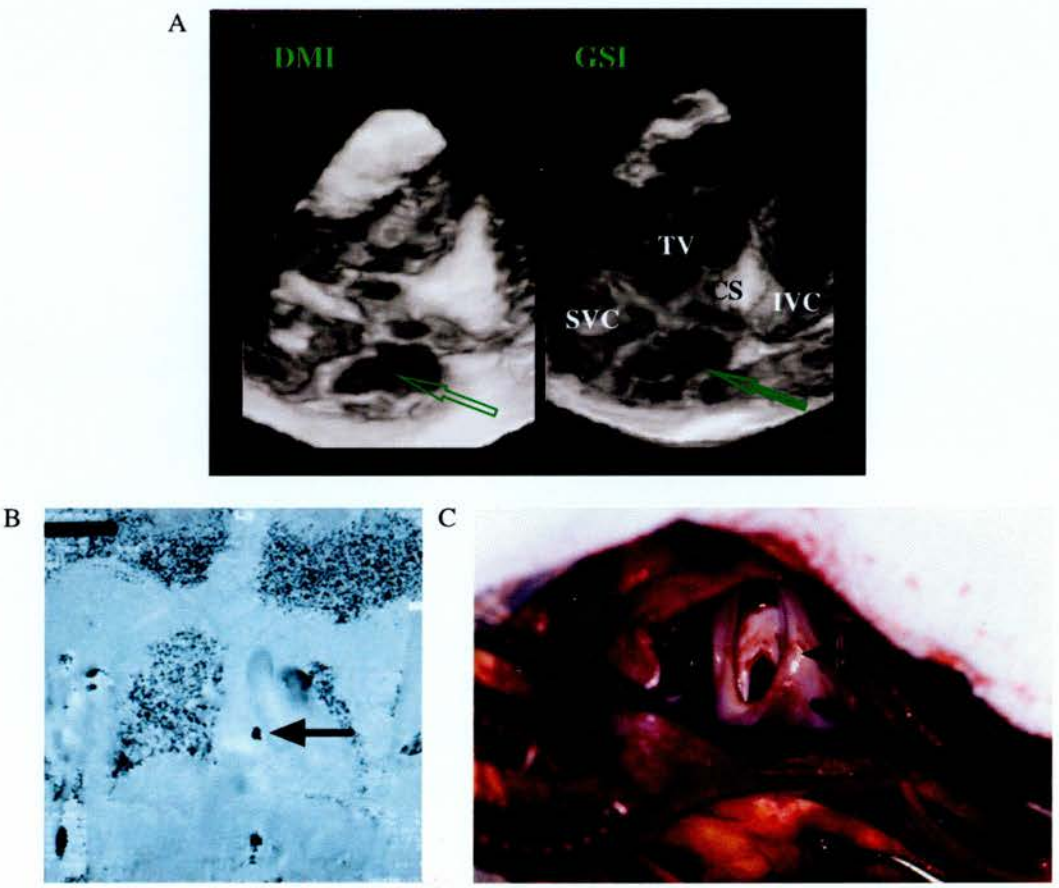

Figure 2. This shows the maximum orifice of an atrial-septal defect as defined by three-dimensional echocardiography (**A**); phase-contrast cine MRI (**B**); and surgery (**C**); For abbreviations see Figure 1. DMI, Doppler myocardial imaging; GSI, grey-scale imaging

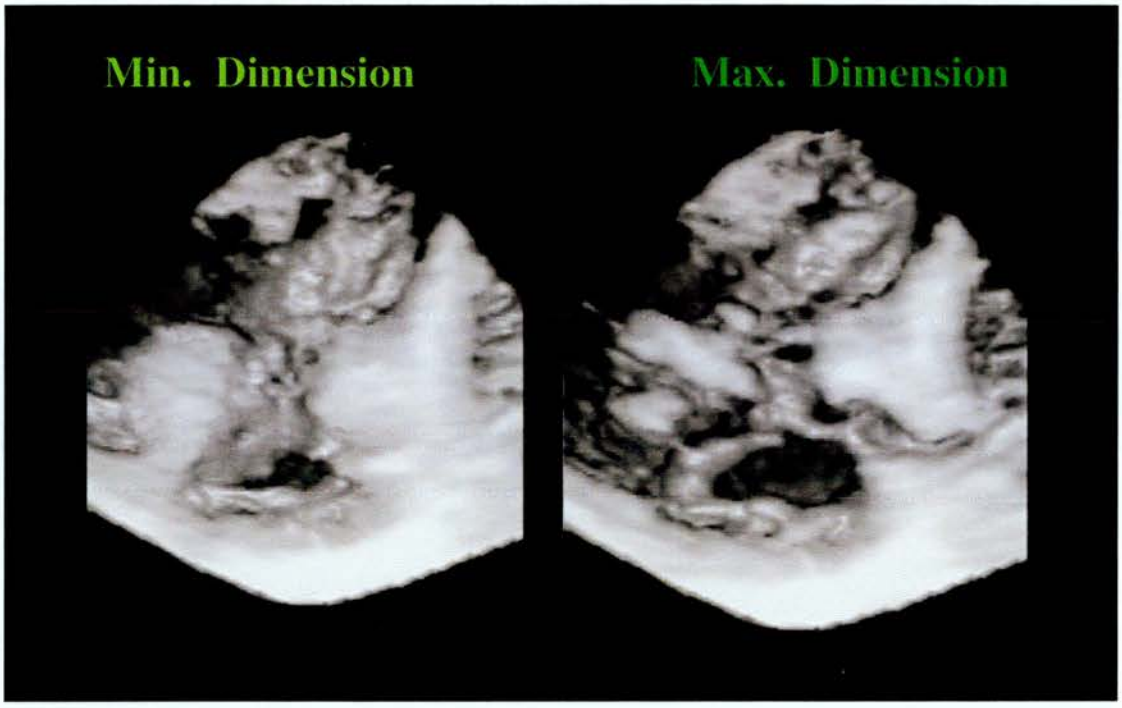

Figure 3. Changes in atrial septal defect dimension during a cardiac cycle as seen by three-dimensional Doppler myocardial imaging echocardiography.

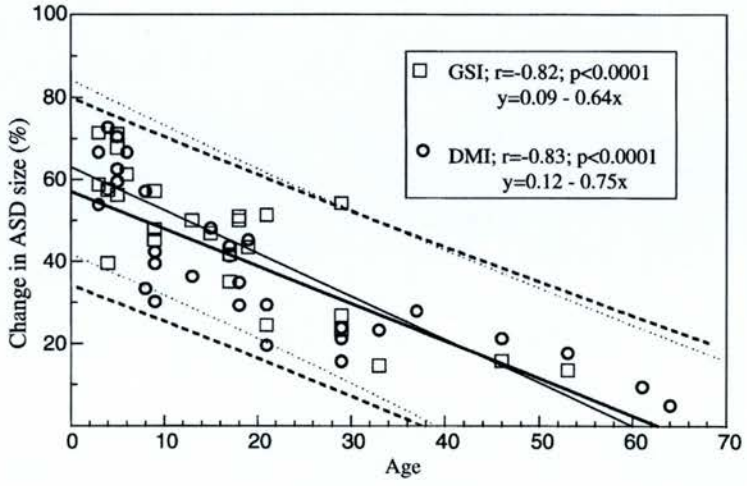

Figure 4. Linear regression analysis of the correlation between the patients age and the dynamic changes in atrial septal defect dimension during the cardiac cycle.

The differences in secundum atrial septal defect dimension changes were calculated as follows: [(HED - HES) + (VED - VES) / (HED + VED)] x 100%. **Bold lines** show the results obtained from the Doppler myocardial imaging technique. The **dotted lines** indicate the 95% predictive interval. HED, horizontal end-diastolic dimension; HES, horizontal end-systolic dimension; VED, vertical end-diastolic dimension; VES, vertical end-systolic dimension.

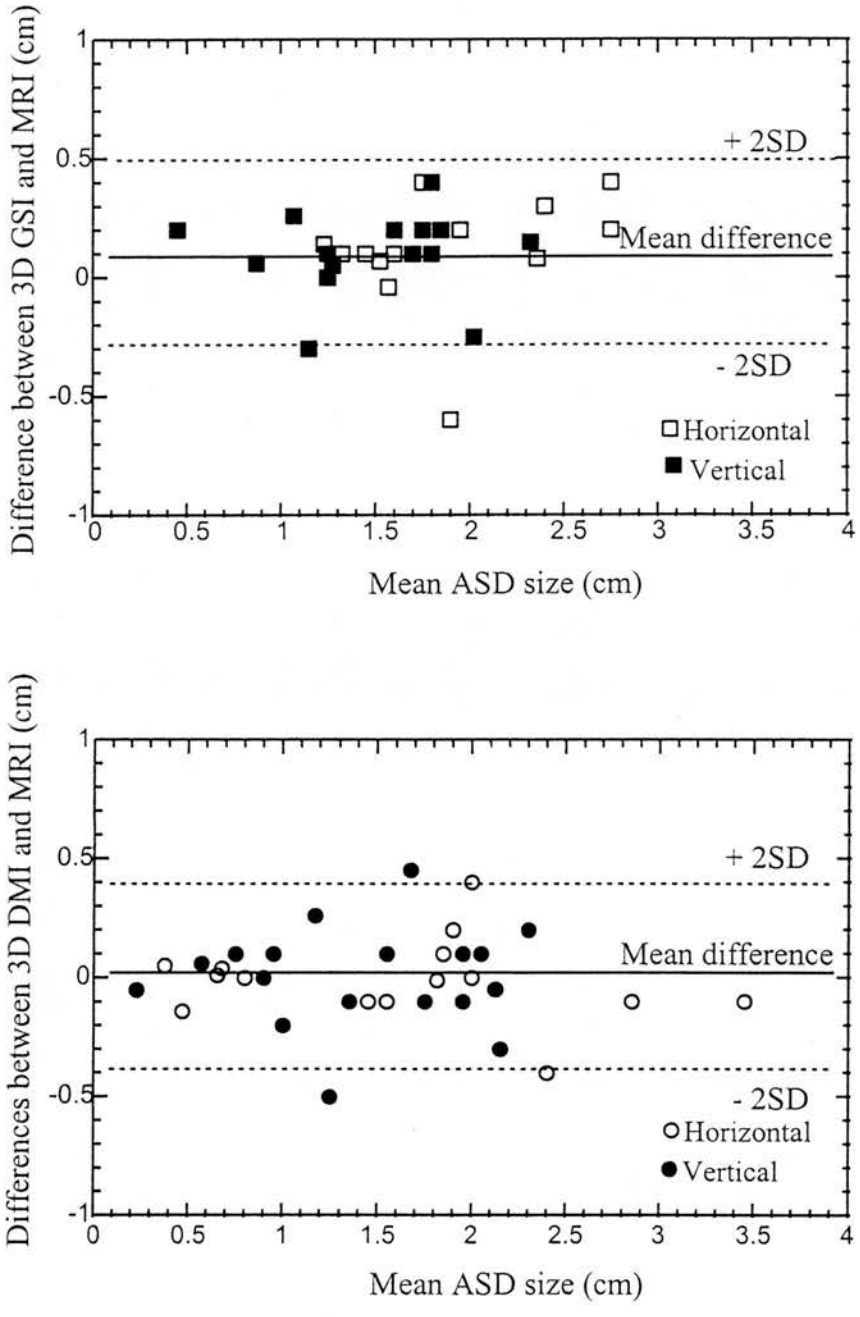

Figure 5a. Bland and Altman's analysis of the accuracy of ASD dimension measurements by three-dimensional echocardiography using grey-scale imaging (GSI) (**top**) and Doppler myocardial imaging (DMI) (**bottom**) technique against phase-contrast cine Magnetic Resonance Imaging (MRI). The solid line shows the mean difference between the techniques used; the dotted lines show the 95% limit of agreement.

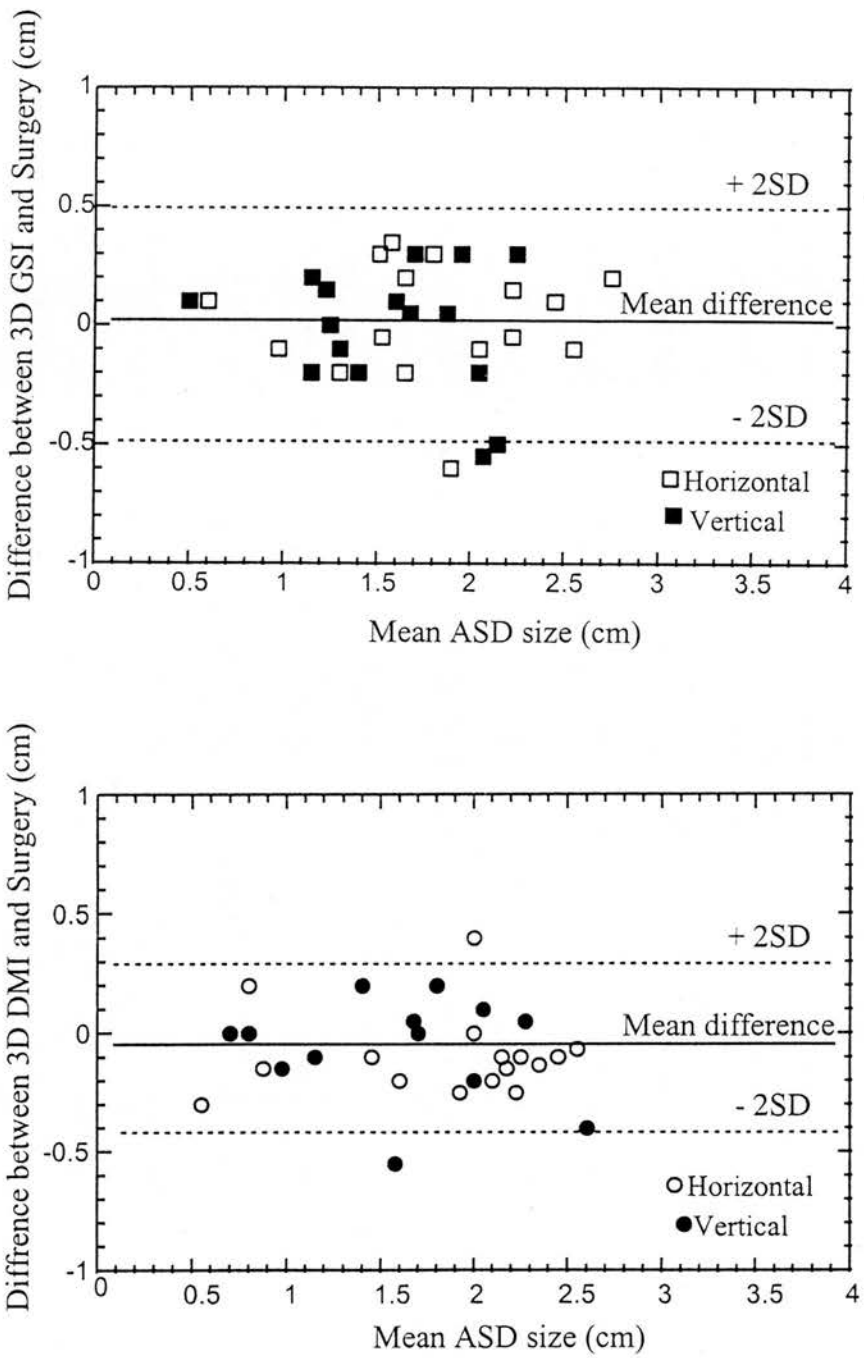

Figure 5b. Bland and Altman's analysis of the accuracy of ASD dimension measurements by three-dimensional echocardiography using grey-scale imaging (GSI) (**top**) and Doppler myocardial imaging (DMI) (**bottom**) technique against surgery.

The solid line shows the mean difference between the techniques used; the dotted lines show the 95% limit of agreement.

CHAPTER 6

The Role of Transthoracic Three-Dimensional Echocardiography in the Diagnosis of Sinus Venosus Atrial Septal Defect

6.1. Background

Sinus venosus atrial septal defect is an uncommon congenital cardiac anomaly and accounts for 5 to 10% of all atrial septal defects [Dickenson et al., 1981]. In most cases it is associated with an abnormal connection of the right pulmonary veins to either the right atrium or to the superior vena cava [Lewis et al., 1955]. Sinus venosus atrial septal defect was first described by Wagstaffe in 1868 [Wagstaffe, 1868]. He described the deficiency of the superior auricular septum adjacent to the orifice of the superior vena cava, along with anomalous entry of the right pulmonary vein. The first two-dimensional echocardiographic report of sinus venosus atrial septal defect was published in 1981 by Nasser et al. [Nasser et al., 1981]. The anatomic classification, and the embryology of this condition, still remains a controversial issue. This has been addressed recently by Zaghal et al. and by Ettedguiet et al., who have suggested that the 'key anatomical criteria for the diagnosis of sinus venosus defects is an overriding of the mouth of the superior caval vein across the intact muscular border of the oval fossa. The interatrial communication is then formed within the mouth of the overriding vein, but is outside the confines of the oval fossa' [Al Zaghal et al., 1997; Ettedgui et al., 1990]. In children most cases of sinus venous atrial septal defect can be diagnosed by transthoracic two-dimensional echocardiography using a subcostal four chamber view [Muhler et al., 1992; Shub et al., 1983]. In adolescents or adult patients transoesophageal rather than transthoracic approach is used to acquire diagnostic two-dimensional images [Kronzon et al., 1991]. However, although the transoesophageal approach allows imaging of the superior part of the septum, where sinus venosus defects are located, this technique is semi-invasive and not always sufficient to delineate precisely the exact spatial relations between the defect and abnormal drainage of the pulmonary veins [Pascoe et al., 1996].

In this study transthoracic three-dimensional echocardiography was used to evaluate its usefulness and potential superiority over currently used ultrasound techniques (standard transthoracic and transoesophageal two-dimensional echocardiography) in the detailed assessment of sinus venosus atrial septal defect.

6.2. Methods

Study population

Between 1993 and 1997, nine patients (age range from 5 to 84 years, 6 male, the median age at the time of transoesophageal echocardiogram 8 years) diagnosed as having sinus venosus atrial septal defect were studied at our institution. Five patients presented with dyspnoea or palpitations, and one had unexplained presyncope. Three patients had no cardiovascular symptoms and were seen for routine medical examination. Auscultation revealed an abnormally split second heart sound in seven patients (78%), which was fixed in four. All patients had systolic murmur, seven patients had a predominantly pulmonary or left sternal border murmur, and six patients had a diastolic murmur.

The diagnosis of sinus venosus septal defect was based on both echocardiography and cardiac catheterisation. The presence of the overriding of the superior vena cava, and the extraseptal location of an interatrial communication were accepted as diagnostic criteria of sinus venosus atrial septal defect [Al Zaghal et al., 1997; Ettedgui et al., 1990]. Prior to cardiac catheterisation, all patients underwent standard transthoracic and transoesophageal two-dimensional ultrasound examination. After the diagnosis had been made, but prior to the surgical repair of the defect, all patients underwent transthoracic three-dimensional examination by an experienced cardiologist who was blinded to the outcome of other tests.

In four patients, the diagnostic interpretation was correlated with the surgical findings and in the remaining five with the outcome of cardiac catheterisation.

Transthoracic two-dimensional echocardiography

Each patient underwent routine transthoracic echocardiography that included M-mode and two-dimensional imaging, pulsed and continuous wave Doppler ultrasound and colour flow mapping. The interatrial septum was explored in the short-axis, apical four- chamber and subxiphoid views. Toshiba PowerVision ultrasound scanner and 5 MHz phased array transducer was used to acquire diagnostic information in all patients. The diagnosis of atrial septal defect was considered certain when the characteristic flow velocity pattern across the septum was identified. Attempts to identify anomalous pulmonary veins drainage were made in each patient.

Transoesophageal two-dimensional echocardiography

Transoesophageal echocardiography was performed in a standard manner. All studies, except for two adult patients, were carried out under general anaesthesia. Both cardiac catheterisation and transoesophageal echocardiography (5 MHz biplane transducer) were accomplished during the same anaesthesia.

The interatrial septum was imaged using the longitudinal view and the basal short axis view. These views were obtained from the mid oesophagus. The defect appeared as an absence of the atrial septum just beneath the orifice of the superior vena cava. This was visualised both by two-dimensional imaging and colour Doppler flow. The longitudinal view was used to identify the anatomy of venous connection to the left atrium, while typical anomalous connection of the right sided pulmonary veins was best visualised by the use of the transverse plane. Colour Doppler flow complemented the appreciation of the anomalous venous connection.

Transthoracic three-dimensional echocardiography

The instrumentation used for three-dimensional images consisted of an ultrasound scanner (Acuson Sequoia Mountain View, California, USA) and a three-dimensional acquisition system (TomTec Echo-Scan, TomTec Imaging systems, Munich,

Germany). The protocol for data acquisition has been described in detail in Chapter 2. The ultrasound images were obtained with a 5.0 MHz phase array transducer, fixed in a cylindrical mechanical rotational device. After positioning it on the chest in a standard apical position (four chamber view), the transducer was rotated by mechanical device at 2° steps over 180° by an external stepper motor, controlled by the Echo-Scan and according to echocardiographic and respiratory gating. None of the patients required any sedation and the procedure was tolerated well by all patients.

In each patient, three-dimensional reconstructions were carried out from three different perspectives. (1) Superiorly angulated apical four chamber view which allowed visualisation of the right sided pulmonary veins, the entrance of the superior vena cava, and the outline of the sinus venosus septal defect. (2) The four chamber reconstruction was then cut (a) vertically, along a longitudinal plane through the right atrial free wall; and (b) horizontally, parallel to the line of atrio-ventricular valves at the inferior edge of the defect to visualize the defect *en face*.

Cardiac catheterisation

Except for two adult patients, the procedure was carried out under general anaesthesia. Haemodynamic measurements and oxygen saturations were recorded according to standard catheterisation protocol for our laboratory. Pulmonary artery angiograms were carried out and anteroposterior and lateral four chamber views were obtained. Pulmonary venous drainage was noted on recirculation. Selective pulmonary venous angiograms in right upper pulmonary vein were also performed in all cases considered to be inconclusive. Cine images were recorded 25 frames/second (Lateral ARC 2/poly DIAGNOST C2, Philips Medical Systems Netherlands B.V).

Surgical data

Four out of nine patients have undergone corrective surgery, during the study period. All operations were performed by a single surgeon. The surgery was carried out through a midline sternotomy. Sinus venosus atrial septal defects were closed using autologous pericardial patch and anomalous pulmonary veins were diverted the to left atrium. The superior vena cava/right atrial junction were enlarged by autologous pericardial patch in all four patients.

Surgery was performed on cardiopulmonary bypass, under moderate hypothermia. Information acquired during surgery included, exact location of defect, the number of anomalous pulmonary venous connections, and the presence of any associated additional defect. The observations were documented at the end of the operation, by the surgeon in charge, for each patient.

6.3. Results

Table 1 shows the clinical data of the study group and the diagnostic information obtained from standard transthoracic two-dimensional echocardiograms from all nine patients.

Transthoracic two-dimensional echocardiograms

Although in all nine patients typical echocardiographic features of right ventricular volume overloading were detected, and seven patients (78 %) had a paradoxical interventricular septal motion, a clear shunt that suggested an interatrial connection above the foramen ovale was detected by transthoracic two-dimensional echocardiogram only in two patients (22 %). Standard transthoracic echocardiograms were also less accurate than both transoesophageal and transthoracic three-dimensional ultrasound techniques in detecting the abnormal drainage of pulmonary veins. Only in two patients (22 %) were these findings noted by transthoracic two-dimensional echocardiogram. In these two patients, transthoracic two-dimensional

images detected an abnormal drainage of the right upper pulmonary vein to the right atrium confirmed later by cardiac catheterisation and/or surgery. In addition to the detected anomalous drainage of the right upper pulmonary vein, one of these two patients also had an abnormal drainage of the right mid pulmonary vein which was not detected by the transthoracic two-dimensional echocardiogram.

Information obtained from two-dimensional transoesophageal echocardiograms, transthoracic three-dimensional echocardiograms, cardiac catheterisation and surgical findings are shown in **Table 2**.

Two-dimensional transesophageal echocardiography

In all nine patients the presence of sinus venosus defect was correctly diagnosed by transoesophageal echocardiogram. The abnormal drainage of nine right sided pulmonary veins (seven right upper pulmonary veins and two right mid pulmonary veins) was detected by transoesophageal two-dimensional imaging.

Transthoracic three-dimensional echocardiography

Good quality transthoracic three-dimensional data was acquired in six of the nine patients studied. In the remaining three patients: the quality of the three-dimensional data-set was still sufficient in two patients to obtain the required information and in one patient a small rotation artefact was present. Three-dimensional reconstruction of the images took between 11 and 22 minutes (mean 15 ±4 min.) depending on the quality of data-set and the complexity of the defect's anatomy.

In all nine patients (including both adults) transthoracic three-dimensional echocardiograms allowed identification of the presence of a sinus venosus atrial septal defect. The assessment of the abnormal drainage of pulmonary veins by transthoracic three-dimensional echocardiography was superior to that by two-dimensional both transthoracic and transoesophageal echocardiography. In all nine patients abnormal drainage of the pulmonary veins was visualised. In two cases (8 year old boy and 10 year old boy) it was assessed that the mid upper pulmonary vein

drained to the right atrium rather than to the junction of the right atrium and the superior vena cava. Also, in one patient (nine year old girl) an additional anomalous drainage of the right mid pulmonary vein was not detected.

Comparison between two-dimensional transoesophageal echocardiography and three-dimensional transthoracic echocardiography

Both techniques correctly recognised the presence of the sinus venosus defect in all nine patients studied. Transthoracic three-dimensional echocardiography was more accurate in the identification of the anomalous drainage of right sided pulmonary veins. In our study group of nine patients, thirteen right sided pulmonary veins (nine right upper pulmonary veins and four right mid pulmonary veins) drained on the right side of the septum. Transoesophageal two-dimensional imaging confirmed the abnormal drainage of nine right sided pulmonary veins (seven right upper pulmonary veins and two right mid pulmonary veins). In contrast, three-dimensional transthoracic imaging detected the abnormal drainage of twelve right sided pulmonary veins (nine right upper pulmonary veins and three right mid pulmonary veins). The anomalous drainage of four pulmonary veins (two right upper and two right mid pulmonary veins) was not detected by transoesophageal imaging compared with only one right mid pulmonary vein that was missed by transthoracic three-dimensional imaging. It appears that the abnormal drainage of the right mid pulmonary vein was most difficult for visualisation by transoesophageal two-dimensional echocardiography (two out of four detected). This was improved by transthoracic three-dimensional echocardiography (three out of four detected).

6.4. Discussion

In this study the completeness of diagnostic information on sinus venosus septal defect including the description of the anomalous connections of right sided pulmonary veins was compared between transthoracic two-dimensional

echocardiography, transoesophageal two-dimensional echocardiography and transthoracic three-dimensional echocardiography. Although transthoracic two-dimensional echocardiography is an effective technique in diagnosing ostium primum and ostium secundum atrial septal defects, it has been reported to be less sensitive in the demonstration of sinus venosus atrial septal defects [Shub et al., 1983; Kronzon et al., 1991; Pascoe et al., 1996]. The sensitivity of detecting both sinus venosus defects and the anomalous drainage of the right sided pulmonary veins improves significantly with the use of the transoesophageal echocardiography [Kronzon et al., 1991; Pascoe et al., 1996]. However, transoesophageal imaging remains a semi-invasive technique which in children is mostly carried out under a general anaesthesia. With increasing interest in three-dimensional echocardiography, in this study the completeness of diagnostic information obtained from two-dimensional imaging (both transthoracic and transoesophageal) was compared to that obtained from transthoracic three-dimensional imaging.

Transthoracic two-dimensional echocardiography

The presence of sinus venosus defect was detected by transthoracic two-dimensional imaging in only two (22%) of the nine patients studied (eight year old male and eighty four year old male). Additionally, in these two patients, right upper pulmonary veins were found to drain into the right atrium. This diagnostic yield obtained from transthoracic two-dimensional imaging was similar to that described by Pascoe et al. and lower than that described by Shub et al. [Pascoe et al., 1996; Shub et al., 1983]. It is unlikely that this reflects poor imaging technique or lack of awareness of the condition, but rather it is a consequence of the far-field location of sinus venosus defects. Apart from the clinical spectrum of symptoms referable to the cardiovascular system, the important features observed from transthoracic two-dimensional images that led to further investigation by transoesophageal echocardiography and cardiac catheterisation were the dilatation of the right side of the heart (all nine patients) and

paradoxical septal motion (in seven of the nine patients, 78%). Again, similar findings were reported by Pascoe et al. where 96% of studied group of patients presented with a dilated right heart [Pascoe et al., 1996].

Transoesophageal two-dimensional echocardiography

In contrast to transthoracic two-dimensional echocardiography, transoesophageal two-dimensional imaging proved to be an accurate way of diagnosing sinus venosus defect. It was more accurate in diagnosing not only the presence of the defect but also in detecting the anomalous pulmonary venous connection. Transoesophageal imaging correctly identified the presence of the sinus venosus defect in all nine patients. The longitudinal imaging plane in the mid-oesophagus provided the most reliable visualization of sinus venosus defect (**Figure 1**). This plane allows the best view of the fossa ovalis region with the superior limbus of the atrial septum and the superior vena cava in long-axis. Anomalous pulmonary venous connections were appreciated consistently with the use of the colour Doppler flow at the level of the superior vena cava near the junction with the right atrium and more superiorly at the level of the right pulmonary artery. The anomalous pulmonary drainage of the right upper pulmonary vein was correctly identified in seven of the nine patients studied. In two of these seven patients an additional mid upper pulmonary vein was found to drain into the right atrium at cardiac catheterisation and surgery. In one patient the right mid pulmonary vein was thought to described to drain into the right atrium was found at surgery to drain rather into the junction of the right atrium and the superior vena cava. In the remaining two patients in whom no clear information on the pulmonary venous connection was obtained by transoesophageal imaging, right upper pulmonary veins drained to the superior vena cava.

Transthoracic three-dimensional echocardiography

Transthoracic three-dimensional imaging was as accurate in the diagnosis of sinus venosus defect as transoesophageal two-dimensional imaging and allowed identification of the presence of the sinus venosus defect in all nine patients (**Figure 2**). The assessment of the exact mechanism of the anomalous pulmonary venous drainage by transthoracic three-dimensional echocardiography was superior to that by transoesophageal two-dimensional imaging. It was basically correct in all nine patients with the minor qualification that in two of these nine patients the right mid pulmonary vein was described as draining to the right atrium rather than to the junction of the right atrium and the superior vena cava and in one other patient the presence of an abnormal drainage of the mid upper pulmonary vein was not observed by transthoracic three-dimensional reconstruction.

6.5. Limitations

Technical limitations

In our previous *in vitro* work described in Chapter 3 it appears that the recognition of spatial details from three-dimensional reconstruction is satisfactory and that a minimum size of a relatively strong reflector of 1 mm dimension and two reflectors distant from each other by 2 mm can be correctly identified from a three-dimensional image. *In vivo,* this spatial resolution will vary according to several parameters e.g. imaging frequency, depth settings, image quality and the position of the structure-of-interest within the ultrasound sector. This therefore may create a potential problem when looking for pulmonary vein entrance in poorly echogenic patients. As described in previous chapters the inability of the three-dimensional system used to change interactively the settings selected (cut-planes, threshold and opacity) for three-dimensional reconstruction extends the time required to obtain

diagnostic images. Future development in real-time three-dimensional scanning should shorten the time needed to acquire and to reconstruct the data and also would enhance the diagnostic confidence of the examiner.

Clinical limitations

A relatively small number of patients was studied. No attempt has been made to analyse other often concomitant valvular abnormalities i.e. pulmonary or tricuspid regurgitation, in this group of patients. To the best of our knowledge, no validation of three-dimensional echocardiographic definition of this abnormality has been so far undertaken. Therefore our efforts were focused on the detection of septal defects and anomalous pulmonary drainage.

6.5. Conclusions

Based on our patient population it appears that transthoracic three-dimensional echocardiography is highly accurate in the description of the presence of sinus venosus atrial septal defects and provides a precise description of the anomalous drainage of right sided pulmonary veins. Transthoracic three-dimensional imaging was superior to transthoracic two-dimensional echocardiography in the diagnosis of sinus venosus defects. As the size of our study group was small, it is difficult to state emphatically whether transthoracic three-dimensional imaging was also superior to transoesophageal imaging, although, such a trend was observed in our results. If this is the case than there is a clear advantage of transthoracic imaging over transoesophageal imaging which is an invasive test with well-described although rare complications [Daniel et al., 1991].

Table 1. Clinical and standard transthoracic ultrasound two-dimensional data.

Nr	Age (months)	Gender (F/M)	Rhythm	TRANSTHORACIC 2D ECHO			
				Size	Right Ventricle Overloading	Paradoxical Septal Motion	Pulmory Vein Abnormal Drainage
1	8	F	SR	no shunt	++	yes	no
2	8	M	SR	++	+++	no	RUPV→RA
3	10	M	SR	no shunt	++	yes	no
4	7	F	SR	no shunt	++	yes	no
5	8	M	SR	no shunt	++	yes	no
6	9	F	SR	no shunt	+	no	no
7	5	M	SR	no shunt	++	yes	no
8	84	M	AF	++	++	yes	RUPV→RA
9	76	M	AF	no shunt	++	yes	no

F, female; M, male; 2D, two-dimensional;SR, sinus rhythm; AF, atrial fibrillation; RUPV, right upper pulmonary vein; RA, right atrium

+, mild ; ++, moderate, +++, severe; →, draining to.

Table 2. Comparison between transoesophageal two-dimensional (2D) echocardiogram, transthoracic three-dimensional (3D) echocardiogram, cardiac catheterisation and surgical findings.

Nr	Transoesophageal 2D echo	Transthoracic 3D echo	Cardiac Catheterisation	Surgical findings
1	RUPV→RA	RUPV→RA	RUPV→RA	RUPV→RA
	-	RMPV→RA	RMPV→RA	RMPV→RA
2	RUPV→SVC/RA	RUPV→SVC/RA	RUPV→SVC/RA	n/a
	-	RMPV→RA	RMPV→SVC/RA	
3	RUPV→SVC/RA	RUPV→SVC/RA	RUPV→SVC/RA	RUPV→SVC/RA
	RMPV→RA	RMPV→RA	RMPV→SVC/RA	RMPV→SVC/RA
4	-	RUPV→SVC	RUPV→SVC	RUPV→SVC
5	-	RUPV→SVC	RUPV→SVC	RUPV→SVC
6	RUPV→SVC/RA	RUPV→SVC/RA	RUPV→SVC/RA	n/a
	RMPV→RA	-	RMPV→SVC/RA	
7	RUPV→RA	RUPV→RA	RUPV→RA	n/a
8	RUPV→SVC	RUPV→SVC	RUPV→SVC	n/a
9	RUPV→SVC/RA	RUPV→SVC	RUPV→SVC	n/a

RUPV, right upper pulmonary vein; RA, right atrium; RMPV, right middle pulmonary vein; SVC, superior vena cava; SVC/RA, junction of superior vena cava and right atrium; →, draining to; -, not seen; n/a, not performed

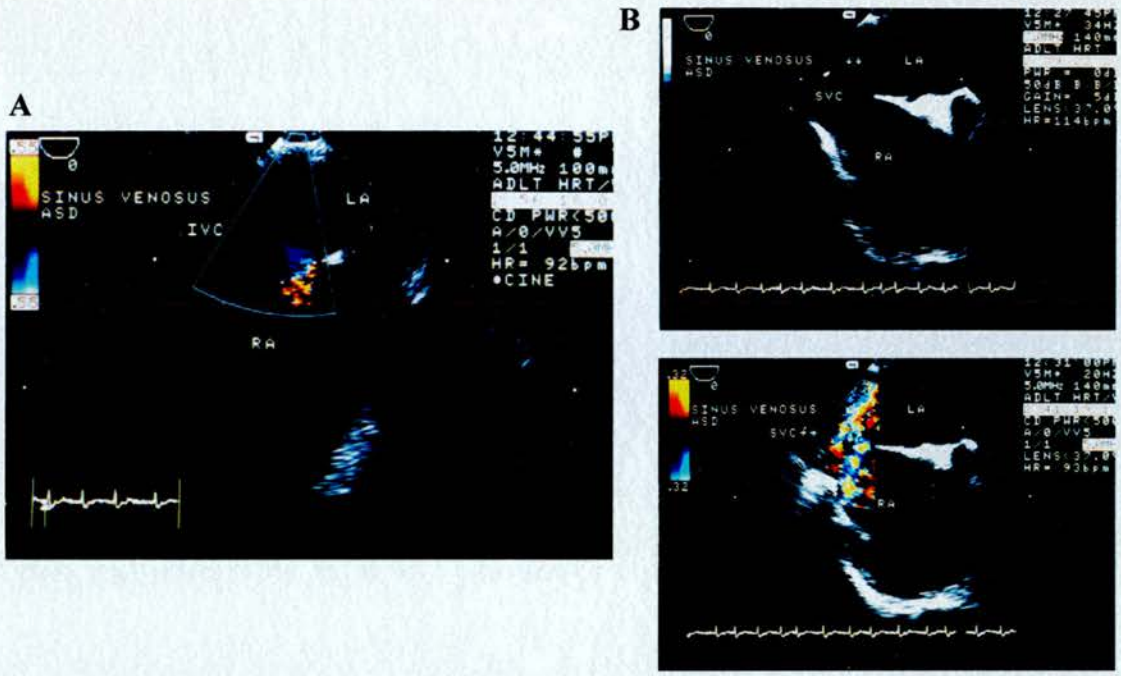

Figure 1. A seventy six year old male with sinus venosus atrial-septal defect; **A**, longitudial view of the atrial septum, which highlights sinus venosus atrial-septal defect (colour Doppler flow) located in the superior fatty limbus of the atrial septum; **B**, transverse view of the atrial septum with the sinus venosus defect displaying in B-mode (**upper panel**) and visualised shunt by colour Doppler flow (**lower panel**). ASD, atrial-septal defect; LA, left atrium; RA, right atrium; SVC, superior vena cava; IVC, inferior vena cava

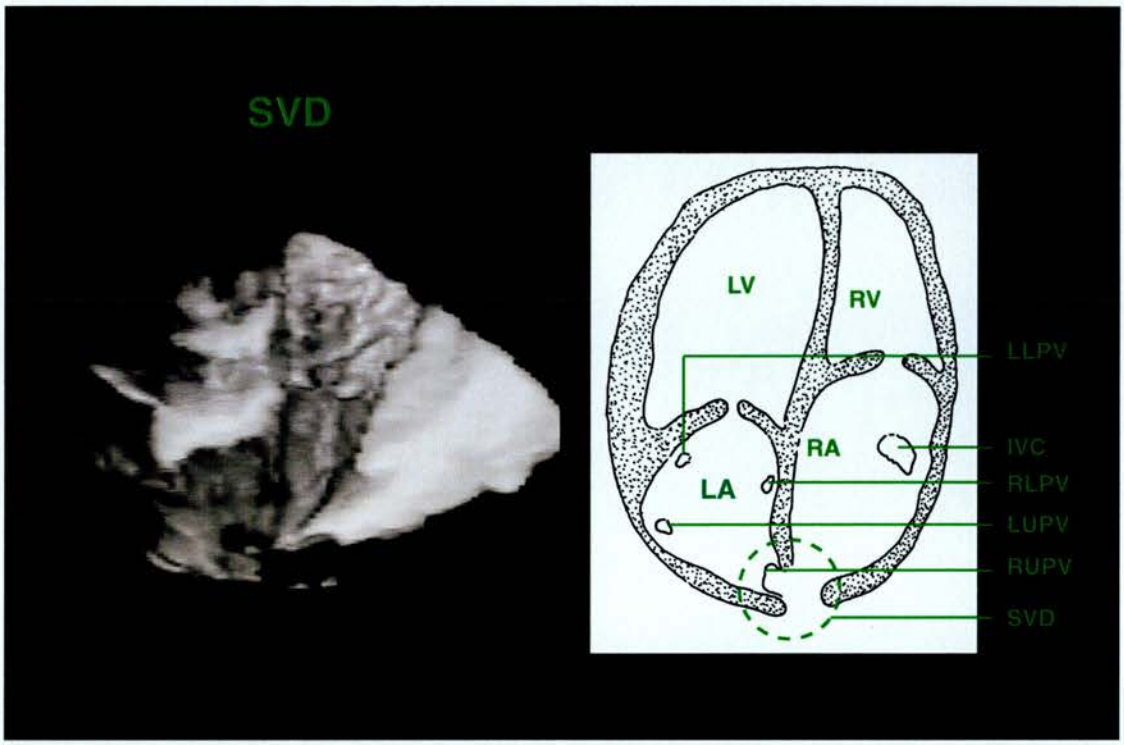

Figure 2. Three-dimensional transthoracic reconstruction delineating sinus venosus atrial septal defect and an abnormal drainage of the right upper pulmonary vein (**left side**) with a corresponding schematic diagram (**right side**).

LA, left atrium; LLPV, left lower pulmonary vein; LUPV, left upper pulmonary vein; LV, left ventricle; RA, right atrium; RLPV, right lower pulmonary vein; RUPV, right upper pulmonary vein; RV, right ventricle; SVD, sinus venosus atrial-septal defect.

CHAPTER 7

Transthoracic Three-Dimensional Echocardiography in the Pre-Operative Assessment of Atrio-Ventricular Septal Defect Morphology

7.1. Background

The characteristic morphology of an atrio-ventricular septal defect has been outlined by many authors using either post-mortem hearts [Rastelli et al., 1966; Piccoli et al., 1979a&b; Bharati et al., 1980; Anderson et al., 1998; Suzuki et al., 1998], angiography [Macartney et al., 1979], or echocardiography [Williams et al., 1974; Sahn et al., 1974; Hagler et al., 1979; Smallhorn et al., 1982a&b; Cohen et al., 1996]. Transthoracic echocardiography has been shown to be the technique of choice in the definition of morphologic abnormalities of the atrio-ventricular junction [Godman et al., 1974; Sahn et al., 1974; Hagler et al., 1979; Sutherland et al., 1981; Smallhorn et al., 1982a; Sutherland et al., 1983].

From the anatomic point of view, atrio-ventricular septal defects can be diagnosed by the presence of several characteristic features i.e. a common atrio-ventricular junction, an unwedged aorta with an often narrowed left ventricular outflow tract and disproportion in the left ventricular aspect of the septum (inlet/outlet disproportion). However, the most characteristic anatomic feature is the arrangement of the five atrio-ventricular valve leaflets that guard the common atrio-ventricular junction. The right-side of the junction consists of two leaflets (inferior and antero-superior), one is exclusive to the left ventricle (the mural leaflet), and the other two leaflets bridge the ventricular septum in the superior and inferior position [Piccoli et al., 1979a&b; Bharati et al., 1980; Anderson et al., 1998]. Two potential inter-chamber shunting spaces are often concomitant with the abnormal atrio-ventricular valve, through the interatrial or interventricular septum. In cases when the two bridging leaflets are joined together by a tongue of tissue running along the ventricular septal crest, only atrial shunting is present. These cases are diagnosed as partial atrio-ventricular septal defects. However, cases can be found where separate valvar orifices exist together with an extensive communication between the valve leaflets and the ventricular septum. These are sometimes called 'intermediate' or 'transitional' [Wakai et al.,

1958; Bharati et al., 1980]. All patients however have a common atrio-ventricular junction with the three- leaflet left component of the valve which guards this part of the junction even when there is a separate valvar orifice for the left ventricle [Anderson et al., 1998]. This is independent of all the above described features.

Because of the complexity of the atrio-ventricular septal defect, echocardiography seems to be the most accurate technique to provide a clinical diagnosis and describe the extent and the character of the malformation [Hagler et al., 1979; Smallhorn et al., 1982a&b]. In the late 1970s first reports were published on the role of M-mode echocardiography in identifying abnormalities of the atrio-ventricular junction and differentiation between partial and complete atrio-ventricular septal defects [Williams et al., 1974; Godman et al., 1974; Pieroni et al., 1975; Hagler et al., 1976]. Two-dimensional imaging allows a complete diagnosis of the defect with the demonstration of the sites and the severity of intracardiac shunting by colour Doppler flow [Hagler et al., 1979; Smallhorn et al., 1982a&b; Cohen et al., 1996]. Despite the diagnostic accuracy of two-dimensional echocardiography, the information on valve morphology and the mechanism of valve reflux is obtained from several two-dimensional cross-sections using different acoustic windows which then have to be mentally reconstructed into a three-dimensional image. More detailed pre-operative description of the valve malformation would prove beneficial in planning the surgical approach to correction of the defect [Han et al., 1995; Studer et al., 1982; McGrath et al., 1987]. Volume-rendered three-dimensional echocardiography creates such a possibility [Belohlavek et al., 1993a; Pandian et al., 1994; Vogel et al., 1994]. Dynamic volume-rendered three-dimensional echocardiography enables the reconstruction of heart structures from views unavailable by standard two-dimensional echocardiography [Rivera et al., 1994; Belohlavek et al., 1993b; Ludomirsky et al., 1994; Schwartz et al., 1994; Roelandt et al., 1995]. It has been shown by Salustri and co-workers that the additional data

provided by three-dimensional echocardiography is particularly useful in imaging the mitral valve, aortoseptal continuity and atrial septum [Salustri et al., 1995]. Vogel et al. have studied successfully a group of various forms of congenital heart disease that included also seven cases of atrio-ventricular septal defects [Vogel et al., 1994].

The aim of this study was to assess whether transthoracic three-dimensional echocardiography enhances the assessment of the complex morphology of atrio-ventricular septal defects and, in particular, the dynamic mechanism of valve reflux compared to that available from standard two-dimensional echocardiography.

7.2. Methods

A prospective study of the transthoracic three-dimensional echocardiographic definition of atrio-ventricular septal defect morphology and its dynamic changes during the cardiac cycle was performed. The information obtained from two-dimensional and three-dimensional echocardiography was compared with intraoperative findings.

Patient population

Fifteen patients (median age 22 months, age range from 7 to 96 months, 11 female) with a common atrio-ventricular junction were studied. According to the criteria described in the introductory section, nine patients had a complete atrio-ventricular septal defect and six had a partial atrio-ventricular septal defect. Two-dimensional and three-dimensional echocardiography was performed by two independent cardiologists blinded to each other's results. The average time between the three-dimensional echocardiogram and surgery was 10 ± 35 days. All patients were informed about the purpose of the study and gave informed consent to be enrolled in the study.

Two-dimensional echocardiography

All studies were performed at 4 MHz using an Acuson Sequoia ultrasound scanner and were recorded on both the system's hard disk and SVHS videotape. In each patient several two-dimensional cross-sections were acquired including the precordial four-chamber view; subcostal four-chamber, long- and short-axis views. The information obtained from two-dimensional imaging was complemented by that obtained from colour Doppler flow. The following was noted for each patient: the morphology and the degree of valve insufficiency and the size of the atrial and the ventricular septal defect (patients were categorised as having a large unrestrictive defect or a small restrictive or no defect by two-dimensional and Doppler colour flow echocardiography).

Three-dimensional echocardiography

A detailed protocol of the method of three-dimensional image acquisition has been outlined in Chapter 2. In brief, the instrumentation used for the three-dimensional imaging protocol consisted of an ultrasound scanner (Acuson Sequoia, California) and a three-dimensional acquisition system (TomTec Echo-Scan, TomTec Imaging Systems; Munich, Germany). The ultrasound images were obtained at 4.0 MHz using transthoracic apical transducer position. During the acquisition, the Echo-Scan was connected to the ultrasound video output of the Acuson scanner via a black/white video cable. ECG and respiratory gated two-dimensional images were acquired at 2^{o} steps over 180^{o}. A total of 90 cardiac cycles were stored during one acquisition. Most of the patients required a mild sedation using Triclofos Elixir BP.

After acquisition, the data-sets were stored on the system hard drive and then analysed off-line. In each patient, several different three-dimensional reconstructions were carried out. Firstly, an apical four chamber view was reconstructed. Secondly, the unroofed view from the left atrium orientated towards the atrio-ventricular

junction was reconstructed to display the common valve *en face*. Thirdly, to reconstruct the atrial and/or ventricular septal defect *en face*, the acquired data-set was cut vertically by a longitudinal plane through the right atrial free wall, tricuspid valve and anterior right ventricular free wall and then orientated anterior to posterior.

Surgical data

All operations were performed by one surgeon.

The repair was performed on cardiopulmonary bypass, under moderate hypothermia. After the usual preparations, a median sternotomy incision was made and a large piece of pericardium was removed and set aside. The right atrium was opened widely. The internal anatomy was inspected. Cold saline was injected twice through the valve(s), and the closure pattern and any regurgitant leaks were studied. The functional anatomy of the valve(s) was re-stated with the use of sutures and/or Dacron patches. After the closure of the interventricular septal defect with the Dacron patch, the pericardial interatrial patch was trimmed to the appropriate shape and size and the first part of its insertion was then accomplished. Saline solution was then injected in order to study the valve(s) closure pattern and competence. If a central leak persisted, an annuloplasty stitch was placed. The repair was completed by suturing of the rest of the pericardial interatrial patch in place.

7.3. Results

In all fifteen patients with an atrio-ventricular septal defect three-dimensional echocardiography was feasible using the standard transthoracic apical window. The time needed to acquire a three-dimensional data-set ranged from three to fifteen minutes. The average time of data analysis was from fifteen to ninety minutes.

All fifteen patients had a common atrio-ventricular junction with nine cases diagnosed as complete and six as partial atrio-ventricular septal defects. In all cases the clinical diagnosis was based on standard two-dimensional echocardiography and

was confirmed later by both three-dimensional echocardiography and intraoperative findings.

Standard Echocardiography

Combined information from two-dimensional echocardiography and colour Doppler flow allowed the morphological diagnosis in all patients. Two-dimensional images were acquired from different acoustic windows: the common atrio-ventricular junction was best visualised using the subcostal short-axis view, and to assess both bridging leaflets the subcostal four-chamber view (inferior bridging leaflet) and/or the apical or the parasternal four-chamber view (superior bridging leaflet) was used.

Three-dimensional Echocardiography

Four-chamber view reconstruction was possible in all study patients (**Figure 1**). Short-axis views that visualised the atrio-ventricular valve(s) *en face* from above (**Figure 2 & 3**) or from below (**Figure 4**) were most useful for the comprehensive assessment of dynamic valve morphology, leaflet morphology and motion, orifice area, and the mechanism of valve reflux.

In all but two patients, anatomic dynamic reconstructions of the common atrio-ventricular valve clearly displayed valve leaflets and their morphology and function. In two patients, the quality of the data-set was suboptimal but still allowed for data reconstruction.

In the analysis of septa (both interatrial and interventricular), the saggital view orientated antero-posterior allowed *en face* reconstruction of atrial and ventricular septal defects with a clear description of their dynamic morphology, size and their spatial relations to other cardiac structures (**Figure 5**).

The comparison between two-dimensional echocardiography, three-dimensional echocardiography and surgery is presented in **Table 1**.

Left-sided valve reflux

Left-sided valve reflux was assessed conventionally by colour Doppler flow imaging and three-dimensional echocardiography. Both results were compared with intraoperative findings. The assessment of valve reflux from volume-rendered three-dimensional images was similar to that performed during surgery. In this study, the unroofed cut plane of the left atrium was most informative and enabled the reconstruction of the atrio-ventricular valve(s) from above displaying the anatomic valve abnormality together with leaflet insufficiency and the completeness of leaflet closure line during diastole.

The assessment of the severity of valve reflux by two-dimensional echocardiography was confirmed at surgery in eleven patients. In the remaining four, there was a one step difference between the echocardiographic and the surgical assessment. In two of these four patients, the reflux was assessed as moderate by colour Doppler flow but severe at surgery. In the remaining two, the left sided reflux was assessed as mild by colour Doppler flow and as moderate and severe at surgery.

For three-dimensional echocardiography, in only one of the fifteen patients a one step difference was found when compared with surgical data. In this one patient, left sided valve insufficiency was assessed as mild by three-dimensional echocardiography but moderate by the surgeon.

Right-sided valve reflux

The method of assessment of right-sided valve reflux was similar to that of the left-sided valve. The results of colour Doppler flow (standard echocardiography) and three-dimensional echocardiography were compared with intraoperative findings. For the assessment of right-sided valve reflux, three-dimensional reconstruction was performed using the unroofed cut plane of the left atrium orientated towards the common atrio-ventricular junction.

In seven of the fifteen patients, the severity of valve reflux described by two-dimensional echocardiography was confirmed at surgery. In the remaining eight patients, a one step difference was found. In three of these eight patients, the reflux was noted as mild by colour Doppler flow but moderate at surgery. In three patients, right-sided reflux was assessed as moderate by Doppler flow but severe by the surgeon. In the remaining patient, no significant reflux was found by Doppler flow but during the valve repair, right-sided valve insufficiency was assessed as mild. For three-dimensional echocardiography, in three of the fifteen patients, a one step difference was found when compared to the surgical data. In one patient, right-sided valve insufficiency was assessed as mild by three-dimensional echocardiography but as moderate by the surgeon, in one patient it was assessed as severe and as moderate and in the third patient as moderate and as severe, respectively.

Primum atrial septal defect

Primum atrial septal defect was found in all fifteen patients by both echocardiographic techniques. Although in all patients the diagnosis made by two- and three-dimensional echocardiography was confirmed during surgery, in three patients a difference was present in the description of the defect size between two-dimensional echocardiography and surgery. Two-dimensional echocardiography underestimated the size of defect in two patients and overestimated the size of defect in one patient. The results obtained from three-dimensional echocardiography agreed with those taken during surgery.

Secundum atrial septal defect

Secundum atrial septal defect was found in ten of the fifteen patients by both echocardiographic techniques. In all ten patients the diagnosis was then confirmed at surgery. Disagreement regarding the size of the defect was present only for two-dimensional echocardiography. In two of the ten patients, there were small differences in the assessment of the defect size by two-dimensional

echocardiography. In one the defect was overestimated (moderate as opposed to small at surgery) and in the second case it was underestimated (moderate as opposed to large at surgery). In all ten patients three-dimensional echocardiography precisely assessed the size of the defect. Additionally, in two cases, defects were correctly described by three-dimensional echocardiography as fenestrated (multiple fenestrations in both of them).

Ventricular septal defect

Ventricular septal defect was observed in eight patients by two-dimensional echocardiography and in nine patients by three-dimensional echocardiography. At surgery ventricular septal defect was found in nine patients. The ventricular septal defect that was missed by two-dimensional echocardiography was very small and positioned in the aneurysmal muscular ventricular septum. Additionally, in four of the eight patients diagnosed by two-dimensional echocardiography defect size was slightly underestimated. No differences in the description of the defect size was found between three-dimensional echocardiography and surgery.

7.4. Discussion

In the present study, we investigated the three-dimensional echocardiographic definition of the common atrio-ventricular junction and analysed the relation of this variable to two-dimensional echocardiographic definition and surgical findings.

The technique of rotational image acquisition that has been used in this study was relatively easy to perform but like all new techniques requires a training period. Three-dimensional image acquisition was performed in a routine clinical setting, with acceptable prolongation of the standard echocardiographic assessment. Good quality three-dimensional reconstructions of the four-chamber view were achieved in all fifteen patients studied (unselected study group). Good quality *en face*

reconstructions of the common valve were obtained in thirteen of the fifteen patients studied.

It needs to be emphasised that a clear anatomic reconstruction of either the atrio-ventricular valve or atrial/ventricular septal defect is more difficult than reconstruction using an apical view alone and requires a longer learning curve. To reconstruct a surgical view of the defect a greater experience is needed in both image acquisition and image reconstruction. During image acquisition it is important to select the highest transducer frequency available for optimum detail definition with appropriate angulation of acquired two-dimensional cut-planes and elimination of potential rotational artefacts. During image reconstruction the selection of optimum two-dimensional cut-plane for three-dimensional reconstruction and also threshold/opacity settings are experience related and using the current three-dimensional system require a learning curve.

In all fifteen patients, diagnostic information by transthoracic three-dimensional echocardiography concurred with the diagnosis by two-dimensional echocardiography and findings at surgery. The unroofed view of the left atrium was most useful in displaying the morphology of the atrio-ventricular valve(s) and closely resembled the actual anatomy of the heart. In each patient three-dimensionally reconstructed images of the valve were compared to the drawings and observations taken at surgery. As illustrated in Table 1. good agreement was found between standard echocardiography and surgical findings in the assessment of both valve insufficiency and the sizing of atrial/ventricular septal defects. Apart from a few small differences when two-dimensional echocardiography under- or over-estimated the severity of the anomaly the difference has never been bigger than one step i.e. from mild to moderate but not from mild to severe. Dynamic three-dimensional surgical reconstruction of the atrio-ventricular valve(s) was available with only some minutes delay in the standard echocardiographic procedure. The

advantage of the latter technique was that no mental reconstruction was required to have a full and detailed insight into the three-dimensional morphology of the valve and atrial/ventricular septal defects. Therefore the assessment of valve insufficiency by three-dimensional echocardiography was closer to surgical findings than for two-dimensional echocardiography. Also, the process of describing valve morphology to fellow cardiologist was much easier using the three-dimensional display rather than using complex two-dimensional information.

The *en face* reconstruction of both primum and secundum atrial septal defect was feasible in all patients. Full agreement was found in the description of defect size between three-dimensional echocardiography and surgery. Additionally in two cases the secundum atrial septal defect had multiple fenestrations observed by three-dimensional echocardiography but not by standard echocardiography. These results are in agreement with previous studies, including our own, on patients with secundum atrial septal defects [Belohlavek et al., 1993b; Franke et al., 1997; Chapter 5]. Three-dimensional reconstructions of ventricular septal defects were feasible in all patients but the *en face* view of the defect was achieved in only six of the nine patients. In the remaining three patients, the assessment of defect size was performed from the reconstructed four-chamber view. Full agreement was found between three-dimensional echocardiography and surgical findings in the assessment of defect size. Additionally one small defect which was missed by two-dimensional echocardiography was correctly identified and sized by three-dimensional echocardiography. The reconstruction of the surgical view of the defect was more difficult than reconstruction of the atrial septal defect. The process was affected by the often complex anatomy of the crest of the septum, which differed according to the attachment of the bridging leaflets and multiple cords that often run between abnormal papillary muscles via the septal crest to the bridging leaflets [Rastelli et al., 1966; Piccoli et al., 1979a&b; Anderson et al., 1998]. It was not always straight

forward to find the best angulation of three-dimensional reconstruction to identify these structures. Using the current three-dimensional system, interactive changes of the selected parameters for three-dimensional reconstruction are not possible and in some cases finding the right angle for three-dimensional reconstruction required some perseverance. Our experience from this study in reconstructing ventricular septal defects slightly differs from that of others but their reconstructions of ventricular septal defects were performed in otherwise normal hearts [Rivera et al., 1994; Vogel et al., 1994&1995b; Salustri et al., 1995].

7.5. Limitations

Technical limitations

In Chapter 3 it was shown that *in vitro* the recognition of spatial details from three-dimensional reconstruction is satisfactory and that a minimum size of a relatively strong reflector of 1 mm dimension and two reflectors distant from each other by 2 mm can be correctly identified from a three-dimensional image. *In vivo,* this spatial resolution will vary according to several parameters e.g. imaging frequency, depth settings, image quality and the position of the structure-of-interest within the ultrasound sector. Also, the current sampling rate of 25 frames/sec for three-dimensional echocardiography is lower than that available in two-dimensional echocardiography and may not be sufficient to follow rapid events. The inability of the three-dimensional system used to change interactively the settings selected (cut-planes, threshold and opacity) for three-dimensional reconstruction extends the time required to obtain diagnostic images.

Clinical limitations

Because of the complexity of the study, only the anatomy of the atrio-ventricular junction and septal defects was analysed. No attempt has been made to analyse the subvalvular apparatus and papillary muscles or search for other potentially co-existing abnormalities such as left- and/or right-ventricular tract obstruction. To the best of our knowledge, except for one short report of Vogel et al. in which three-dimensional echocardiography was used to reconstruct seven cases of atrio-ventricular septal defect, no validation of three-dimensional echocardiographic definition of this abnormality has been so far undertaken [Vogel et al., 1995b]. Therefore our efforts were focused on the atrio-ventricular valve and septal defects as the accuracy of the information obtained on these structures could easily be confirmed at surgery. Additionally, others experience of reconstructing the subvalvular apparatus indicate that it is not an easy task [Salustri et al., 1996]. The spatial resolution of the current three-dimensional acquisition system does not allow a detailed reconstruction of both the atrio-ventricular junction and the subvalvular apparatus in one image. To take advantage of the best spatial resolution settings in three-dimensional reconstruction, the 'structure-of-interest' needs to be located in the centre of the ultrasound scan sector. All structures located in the far field of the ultrasound sector will have an inferior spatial resolution compared to that in the centre of the image. This would not be detrimental for reconstructing the left ventricular cavity but is an important limiting factor in the reconstruction of such fine structures as subvalvular chordeae. Therefore, in order to analyse the subvalvular apparatus, an additional data-set would need to be acquired which would extend both the study protocol and the time required to complete three-dimensional reconstructions.

7.6. Conclusions

Two-dimensional echocardiography provided a very good description of the morphology of atrio-ventricular septal defects and the severity of valve insufficiency. The disadvantage of two-dimensional echocardiography is its lack of complete spatial information, which has to be mentally reconstructed from multiple individual tomographic planes obtained from different acoustic windows. The completeness and accuracy of this technique is therefore dependent on the experience and good spatial imagination of the examiner. Dynamic volume-rendered three-dimensional reconstruction of echocardiographic images allows an enhancement of the anatomic diagnostic capability of standard echocardiography. Transthoracic three-dimensional echocardiography was feasible in the whole unselected study group. It provided excellent and accurate surgical reconstructions of the common atrio-ventricular junction and septal defects. A maximum of ninety minutes was required for detailed and easy to comprehend information on valve morphology and the severity and mechanism of valve insufficiency. This period of time can hopefully be shortened with the future development of real-time three-dimensional scanners.

Table 1. Assessment of atrio-ventricular septal defects by echocardiography (two-dimensional and three-dimensional) and surgery.

Nr	Age (months)	Gender (F/M)	Left-sided Valve Reflux			Right-sided Valve Reflux			Primum ASD			Secundum ASD			VSD		
			2D	3D	S	2D	3D	S	2D	3D	S	2D	3D	S	2D	3D	S
1	48	F*	++	+++	+++	+	+	+	+	+	+	++	+	+	++	++	++
2	15	F*	+	+	+	++	+++	+++	++	++	++	+	+	+	+++	+++	+++
3	22	F*	++	++	++	+	+	+	++	++	++	+	+	+	-	-	-
4	32	M*	-	-	-	+	+	++	+	+	+	-	-	-	-	+	+
5	48	F*	++	++	++	+	+++	++	++	+	+	-	-	-	+	+	+
6	96	F	+	+	+	+	+	+	++	++	++	-	-	-	-	-	-
7	54	F	+	++	++	-	+	+	+	+	+	-	-	-	-	-	-
8	17	M*	++	+++	+++	++	++	++	++	++	++	+	+	+	+	+	+
9	7	M	+++	+++	+++	++	+++	+++	++	+++	+++	++	++	++	+	++	++
10	9	F*	+++	+++	+++	+	+	+	++	++	++	-	-	-	+	++	++
11	10	F	+	+	+	++	+	+	++	+++	+++	+	+#	+#	-	-	-
12	49	F	++	++	++	++	+++	+++	+++	+++	+++	++	++#	++#	-	-	-
13	67	F	++	++	++	+	++	++	++	++	++	+	++	++	-	-	-
14	7	F*	++	++	++	++	++	++	+++	+++	+++	++	++	++	+	+	++
15	8	M	+	+	++	++	++	+++	++	++	++	+	+	+	+	++	++

F, female; M, male; 2D, two-dimensional; 3D, three-dimensional; S, surgery; ASD, atrial-septal defect; VSD, ventricular-septal defect.

+, mild or small; ++, moderate, +++, severe or large

*, Down syndrome; #, multiple fenestration.

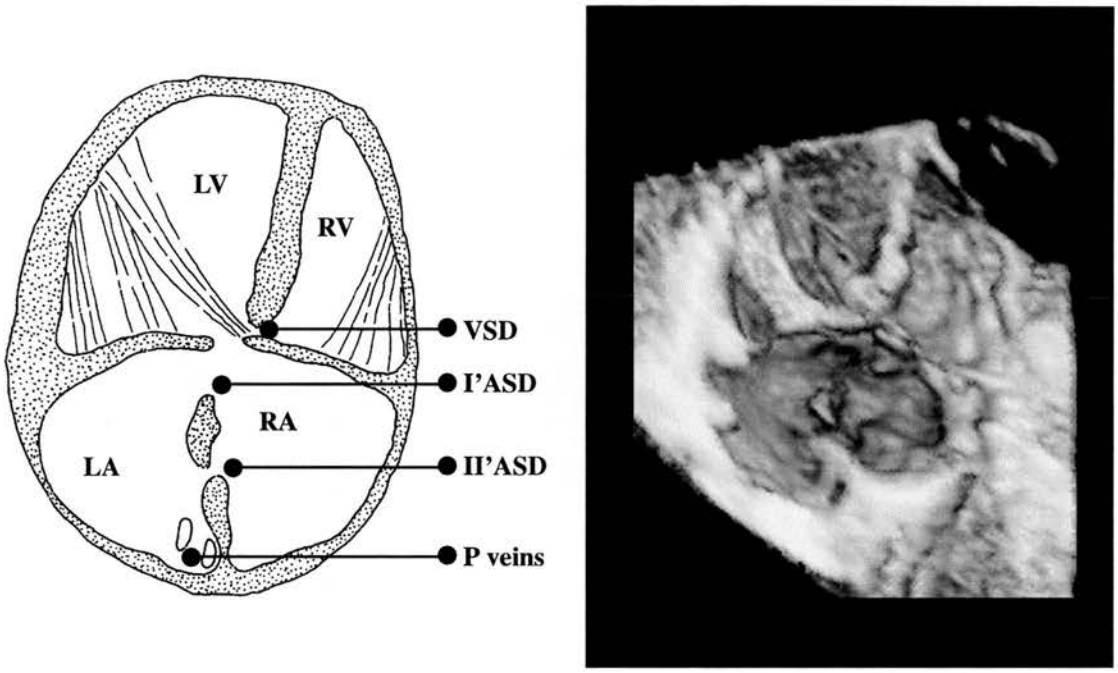

Figure 1. Three-dimensional four-chamber view of a complete atrio-ventricular septal defect (**right**) with a corresponding schematic diagram (**left**)

LV, left ventricle; LA, left atrium; RV, right ventricle; RA, right atrium; VSD, ventriculo-septal defect; I'ASD, primum atrial-septal defect; II'ASD, secundum atrial-septal defect; Pveins, pulmonary veins

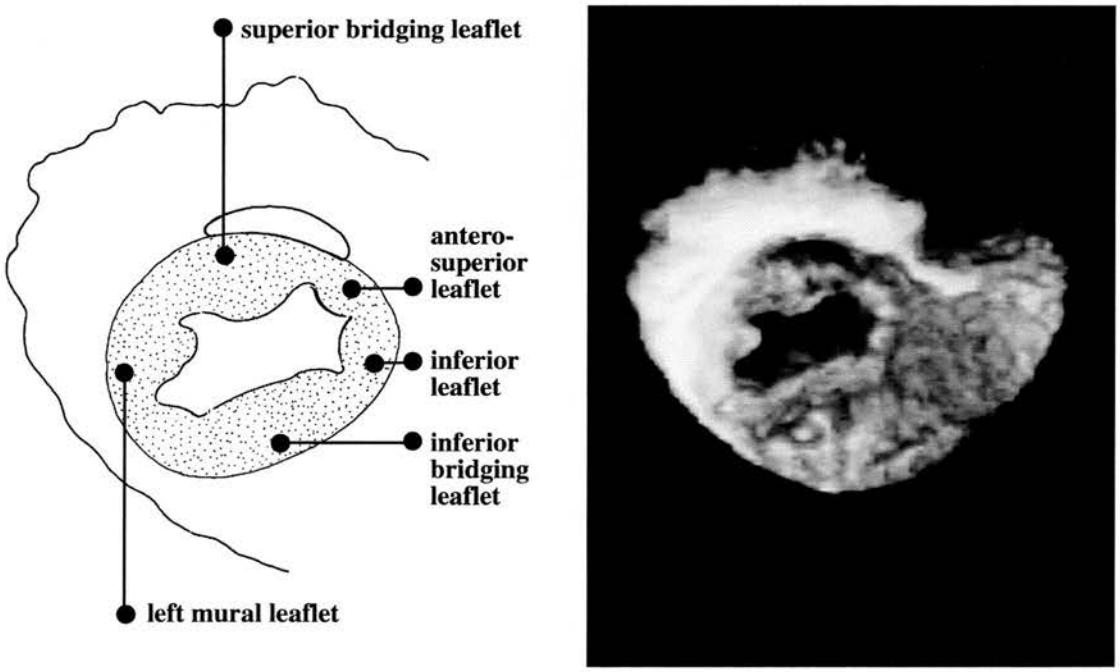

Figure 2. Three-dimensional reconstruction of a common atrio-ventricular valve *en face* directed from the left atrium (**right**) with a corresponding schematic diagram (**left**)

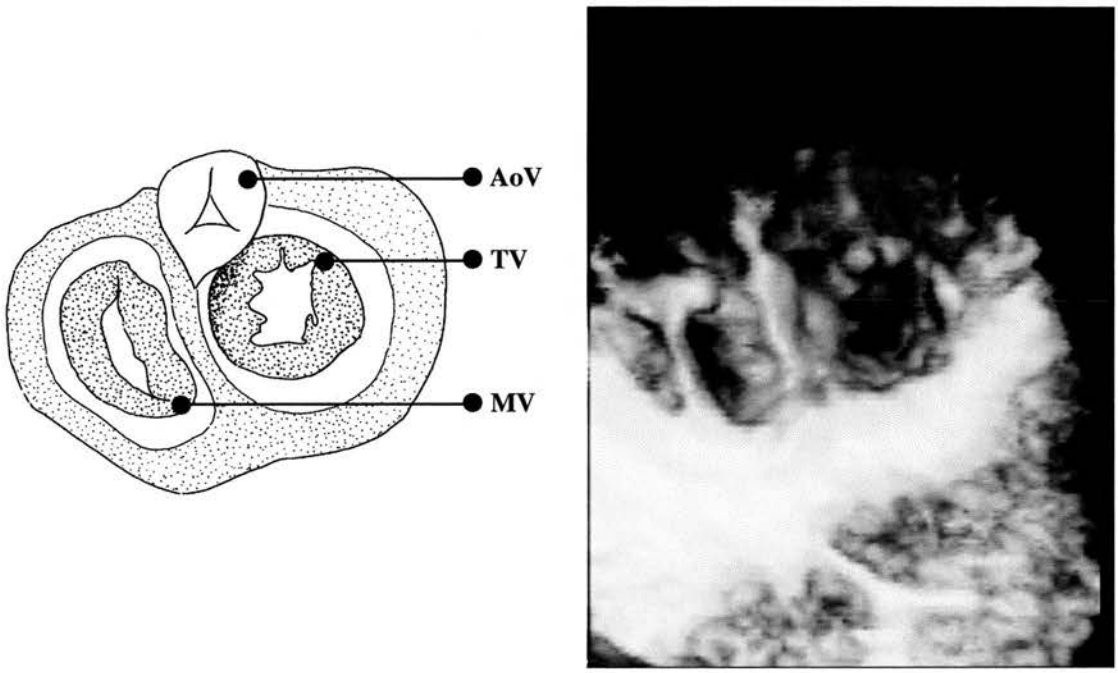

Figure 3. Three-dimensional reconstruction of a partial atrio-ventricular septal defect with *en face* view of the atrio-ventricular junction directed from the atrial perspective (**right**) with corresponding schematic diagram (**left**).

AoV, aortic valve; MV, mitral valve; TV, tricuspid valve.

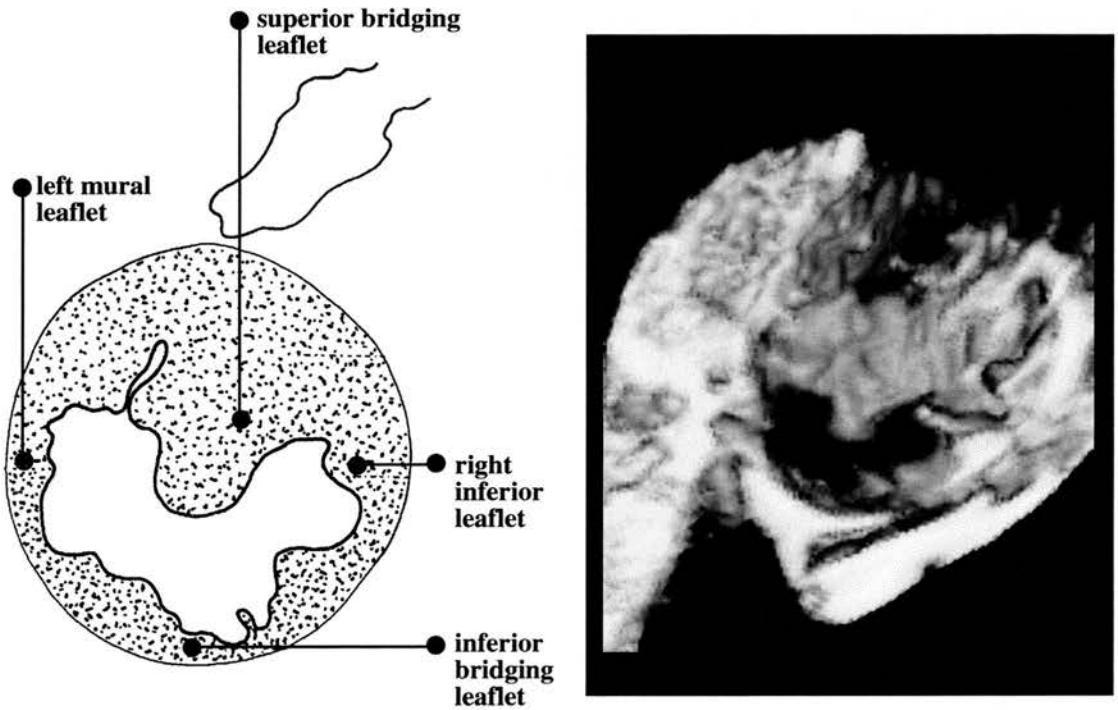

Figure 4. Three-dimensional reconstruction of a common atrio-ventricular valve *en face* from left ventricular perspective (**right**) with a corresponding schematic diagram (**left**).

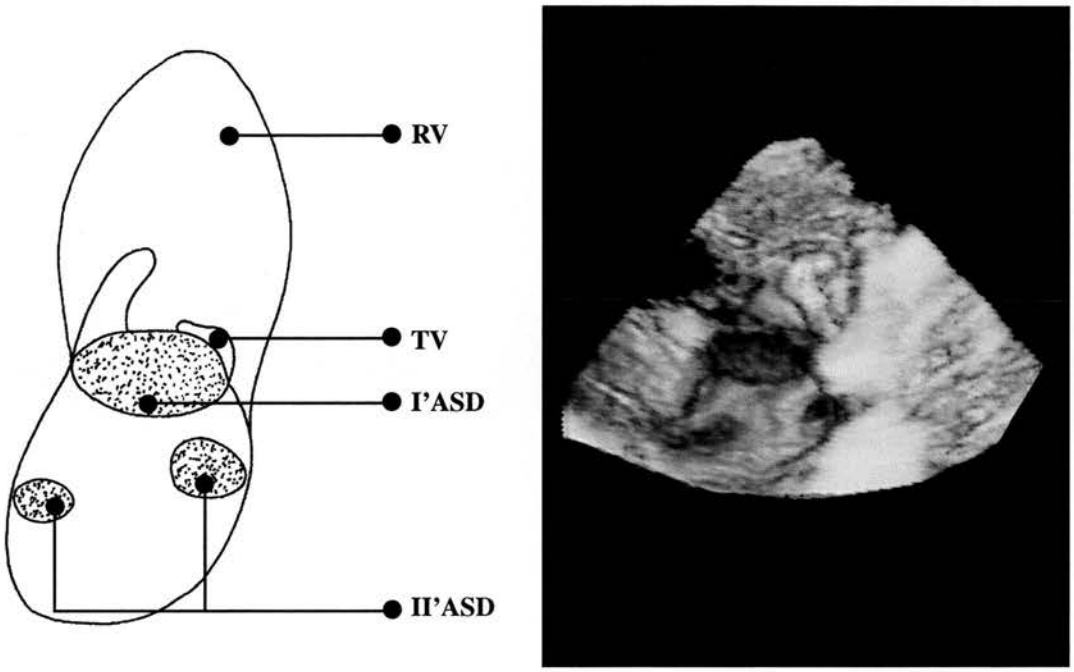

Figure 5. Three-dimensional reconstruction of a primum and a secundum atrial-septal defect *en face* (**right**) with a corresponding schematic diagram (**left**).

I'ASD, primum artial-septal defect; II'ASD, secundum atrial-septal defect; RV, right ventricle; TV, tricuspid valve.

CHAPTER 8

Summary and Conclusions

At present, two-dimensional echocardiography is the most commonly used imaging technique for diagnosing congenital and acquired heart malformations. The interpretation of two-dimensional ultrasound images requires the mental assembly of a series of cross-sectional cut-planes of the heart and their spatial co-ordinates into a three-dimensional image. The introduction of three-dimensional echocardiography eliminates the need for mental reconstruction of two-dimensional images and potentially facilitates image interpretation. Anatomic region-orientated views, including those similar to ones encountered during cardiac surgery, have the potential to enhance our understanding of the anatomy of cardiac malformations and to facilitate the transfer of this understanding to fellow cardiologists and cardiac surgeons. Furthermore, quantitative applications of three-dimensional echocardiography for estimation of cardiac volumes, mass, and function do not rely on geometric assumptions inherent in two-dimensional techniques and should be more accurate and reproducible.

The prospective study presented in this thesis consisted of an *in vitro* and a clinical part. Previous *in vitro* studies to analyse the accuracy of three-dimensional echocardiography were based either on static phantoms (strings and nails) or ventricular casts and therefore not valid for simulating a dynamic clinical setting. In this thesis, to validate *in vitro* the accuracy of measurements taken from three-dimensional ultrasound images, both a computer-generated virtual phantom and a dynamic tissue mimicking phantom were designed and tested. The dynamic phantom was exclusively designed to simulate the *in vivo* conditions of a contracting left ventricle. The clinical part involved seventy four patients from different age groups and with varied cardiac malformations.

The findings obtained from three-dimensional volume-rendered reconstructed images were correlated with either other established diagnostic techniques or intraoperative findings.

Except for the first two chapters, introductory and methods, each chapter reported in this thesis was designed to address (1) the feasibility, (2) the accuracy, and (3) the additional diagnostic value of three-dimensional echocardiography in the assessment of heart disease. The selection of study groups of patients and the order in which these were studied was made according to the complexity of cardiac anomaly (from the simple assessment of the left ventricle to the complex analysis of the atrio-ventricular junction) and the potential clinical applications of this technique perceived.

After the introductory and methodology chapters, Chapter 3 describes the *in vitro* spatial resolution of dynamic volume-rendered three-dimensional tissue-mimicking images acquired using two different imaging techniques: standard grey-scale and Doppler myocardial imaging. As explained earlier in the thesis, Doppler myocardial imaging is a new modality which acquires colour Doppler tissue data-sets from cardiac structures. As the Doppler technique is less subject to chest wall attenuation it should produce more complete data-sets than grey-scale imaging for three-dimensional reconstruction. To measure this, a computer-generated virtual phantom and a dynamic tissue mimicking phantom were tested. Analysis of three-dimensional images of the virtual phantom showed that it is possible to reconstruct a detail of 1 mm dimension and two details separated from each other by a distance of 1 mm. Analysis of three-dimensional images of the dynamic phantom showed that both imaging techniques (grey-scale and Doppler myocardial imaging) underestimated the

true volume of the phantom but the bias (standard error) was more than three times greater for grey-scale imaging than for Doppler myocardial imaging technique. Finally, it has been shown that 1 mm isolated crystal may be correctly identified and measured in a three-dimensional grey-scale and Doppler myocardial imaging dynamic reconstructions. These results served as a baseline for the clinical studies indicating the potential accuracy of three-dimensional image assessment.

The clinical study described in Chapter 4 was designed to compare the accuracy of standard grey-scale imaging and Doppler myocardial imaging three-dimensional left ventricular volume measurements by comparing them to the clinically accepted method of left ventricular volume measurement, cineventriculography. Although there was a good correlation between both three-dimensional ultrasonic techniques and cineventriculography in left ventricular volume measurements, the magnitude of the mean difference between the three-dimensional echocardiography and the cineventriculography was significantly smaller for Doppler myocardial imaging than for grey-scale imaging for both end-diastole and end-systole. Additionally, Doppler myocardial imaging proved to be significantly more efficient than the standard grey-scale imaging in endocardial boundary detection at both end-diastole and end-systole. On the basis of these results it appears that if three-dimensional echocardiography is to be used to estimate left ventricular volume, Doppler myocardial imaging is the ultrasound technique of choice.

In Chapter 5 the accuracy of transthoracic three-dimensional echocardiography in reconstructing secundum atrial septal defects using both standard grey-scale and Doppler myocardial imaging was assessed against Magnetic Resonance Imaging or intraoperative findings. It has been shown that visualization of a dynamic *'en face'*

three-dimensional image of an atrial septal defect is no longer the preserve of only the surgeon during an atrial septal defect repair, but may be reconstructed through the closed chest prior to closure of the defect. Transthoracic three-dimensional imaging using both grey-scale and Doppler myocardial imaging accurately displayed the varying morphology, dimensions and spatial relationships of atrial septal defect. However, Doppler myocardial imaging was a more effective technique than grey-scale imaging in describing atrial septal defect morphology in adults. We have also shown, that all the atrial septal defects studied changed significantly in dimension during the cardiac cycle with a maximum size in late left ventricular systole and minimum in late left ventricular diastole. Although, this difference was present in all patients, it was inversely correlated with age. This may give us potentially new information about the natural history of secundum atrial septal defect which may be taken into account when assessing a patient for percutaneous atrial septal defect occlusion using a device placement. Based on these results it appears that the use of three-dimensional echocardiography in this group of patients should help to plan the surgical strategy or, where applicable, facilitate the selection of patients for percutaneous device closure.

In Chapter 6 the completeness of diagnostic information on sinus venosus septal defect including the description of the anomalous connections of right sided pulmonary veins was compared between transthoracic two-dimensional echocardiography, transoesophageal two-dimensional echocardiography and transthoracic three-dimensional echocardiography. Based on our results it appears that transthoracic three-dimensional echocardiography is highly accurate in the description of the presence of sinus venosus atrial septal defects and provides precise

description of the anomalous drainage of right sided pulmonary veins. Transthoracic three-dimensional imaging was superior to transthoracic two-dimensional echocardiography in the diagnosis of sinus venosus defects. As the size of our study group was small, it is difficult to state conclusively whether transthoracic three-dimensional imaging was also superior to transoesophageal imaging, however, such a trend was observed in our results. If this is the case than there is a clear advantage of transthoracic imaging over transoesophageal imaging which is an invasive test with well-described although rare complications.

In Chapter 7 the three-dimensional echocardiographic definition of the common atrio-ventricular junction and the relation of this variable to two-dimensional echocardiographic definition and surgical findings was investigated. In all patients, diagnostic information by transthoracic three-dimensional echocardiography concurred with the diagnosis by two-dimensional echocardiography and findings at surgery. The unroofed view of the left atrium was most useful in displaying the morphology of the atrio-ventricular junction and closely resembled the actual anatomy of the heart. Good agreement was found between standard echocardiography and surgical findings in the assessment of both valve insufficiency and the sizing of atrial/ventricular septal defect. Apart from a few small differences when two-dimensional echocardiography under- or over-estimated the severity of the anomaly the difference has never been bigger than one step i.e. from mild to moderate but not from mild to severe. Dynamic three-dimensional reconstruction of the atrio-ventricular junction was available with only a couple of minutes delay in the standard echocardiographic procedure. The advantage of the latter technique was that no mental reconstruction was required to have a full and detailed insight into the

three-dimensional morphology of the valve and atrial/ventricular septal defects. Therefore the assessment of valve insufficiency by three-dimensional echocardiography was closer to the surgical findings than for two-dimensional echocardiography. Also, the process of describing valve morphology to fellow cardiologist promises to be much easier using a three-dimensional display rather than using complex two-dimensional information.

On the basis of the studies reported in this thesis it appears that volume-rendered three-dimensional echocardiography is an accurate and a feasible technique which provides additional diagnostic information on cardiac anatomy and function to that available from currently used imaging techniques. Throughout the studies an apical four chamber view was the easiest to reconstruct in three-dimensions and this view proved reliable in the assessment of left ventricular volume and in identifying both atrial septal defects and atrio-ventricular valve malformations. The ability of reconstructing 'surgical views' of atrial septal defects and atrio-ventricular valves enhanced the information on defects morphology and function to that available from two-dimensional cross-sectional ultrasound images. Based on our results the technique appears feasible in a clinical setting including small children. The accuracy of measurements obtained from three-dimensional reconstructions was acceptable and the repeatability was consistent throughout the studies. We believe that in the future three-dimensional echocardiography will be incorporated into a routine echocardiographic examination. Future development of a real-time volume-rendered three-dimensional echocardiography including colour Doppler echocardiography, which it is believed will make the technique more user-friendly and will also provide the solutions to many of the limitations described in this work.

Echocardiography is an accurate, repeatable and safe clinical diagnostic tool. Recent development of dynamic three-dimensional ultrasound imaging of the heart has the potential to further our understanding of the dynamic anatomy of complex heart malformations. The main advantage of three-dimensional echocardiography is that one can better define the morphology and the spatial location of cardiac structures. Within the last two decades considerable effort has been spent in facilitating this new imaging modality into routine clinical settings. There have been many landmark advances in the transformation of this technique from the research bench to clinical practice: the ability to acquire dynamic three-dimensional data from a beating heart, the use of volume-rendered rather than surface-rendered data to reconstruct three-dimensional images, shortening the time of data acquisition and reconstruction from several hours to only a few minutes; last but not least is the ability to reconstruct colour Doppler data in three-dimensions. Despite this, the technique requires further transformation to achieve the ultimate goal of becoming a real-time imaging tool. Although it has clear potential clinical applications, its feasibility should be tested in large clinical trials. I hope that the work presented in this thesis has cast some new information into the understanding of the importance of dynamic three-dimensional echocardiography in every-day cardiology.

REFERENCES

Altman DG, Bland JM. Measurement in medicine: the analysis of method comparison studies. The Statistician 1983;32:307-17.

Altmann K, Shen Z, Boxt LM, King DL, Gersony WM, Alan LD, Apfel HD. Comparison of three-dimensional echocardiographic assessment of volume, mass, and function in children with functionally single left ventricles with two-dimensional echocardiography and magnetic resonance imaging. Am J Cardiol 1997;80:1060-65.

Al Zaghal AM, Li J, Anderson RH, Lincoln C, Shore D, Rigby ML. Anatomical criteria for the diagnosis of sinus venosus defects. Heart 1997;78:298-304.

Anderson RH, Ho SY, Falcao S, Daliento L, Rigby ML. The diagnostic features of atrioventricular septal defect with common atrioventricular junction. Cardiol Young 1998;8:33-49.

Ariet M, Geiser EA, Lupkiewicz SM, Conetta DA, Conti CR. Evaluation of a three-dimensional reconstruction to compute left ventricular volume and mass. Am J Cardiol 1984;54:415-20.

Azevedo J, Garcia-Fernandez M, Puerta P, Moreno M, SanRoman D, Torrecilla E, Lopez de Sa E, Vallejo J, Delcan JL. Dynamic 3-Dimensional echocardiographic reconstruction of the left ventricle using color Doppler myocardial tissue imaging technique. In vivo experimental and clinical study. [Abstract] J Am Coll Cardiol 1996;27(Suppl A): 21A.

Baker DW. Pulsed ultrasonic Doppler blood flow sensing. IEEE Trans Sonics Ultrason 1969;17:170-85.

Belohlavek M, Foley DA, Gerber TC, Kinter TM, Greenleaf JF, Seward JB. Three- and four-dimensional cardiovascular ultrasound imaging: a new era for echocardiography. Mayo Clin Proc 1993;68:221-40 (a).

Belohlavek M, Foley DA, Gerber TC, Greenleaf JF, Seward JB. Three-dimensional ultrasound imaging of the atrial septum: Normal and pathologic anatomy. J Am Coll Cardiol 1993;22:1673-78 (b).

Bharati S, Lev M, McAllister HA, Kirklin JW. Surgical anatomy of the atrioventricular valve in the intermediate type of common atrioventricular orifice. J Thorac Cardiovasc Surg 1980;79:884-9.

Bishop YMM, Fienberg SE, Holland PW. Discrete multivariate analysis. Theory and practice. In: The MIT Press, Cambridge, Massachusett, and London, England, eds. Analysis of square tables: symmetry and marginal homogeneity. 1975:281-310.

Bland JM, Altman DG. Statistical methods for assessing agreement between two methods of clinical measurement. Lancet 1986;I:307-10.

Bom N. New concepts in echocardiography. Stenfert Kroese, Leiden 1972.

Boutin C, Musewe NN, Smallhorn JF, Dyck JD, Kobayashi T, Benson LN. Echocardiographic follow-up of atrial septal defect after catheter closure by double-umbrella device. Circulation 1993;88:621-7.

Brinkley JF, Muramatsu SK, McCallum WD, Popp RL. In vitro evaluation of an ultrasonic three-dimensional imaging and volume system. Ultrasonic Imag 1982;4:126-39.

Burke RP, Michielon G, Wernovsky G. Video-assisted cardioscopy in congenital heart operations. Annals Thoracic Surgery 1994;58:864-8.

Chan KC, Godman MJ. Morphological variations of fossa ovalis atrial septal defects (secundum): feasibility for transcutaneous closure with the clam-shell device. Br Heart J 1993;69:52-5.

Chen Q, Nosir YFM, Vletter WB, Kint PP, Salustri A, Roelandt JRTC. Accurate assessment of mitral valve area in patients with mitral stenosis by three-dimensional echocardiography. J Am Soc Echocardiogr 1997;10:133-40.

Cohen MS, Jacobs ML, Weinberg PM, Rychik J. Morphometric analysis of unbalanced common atrioventricular canal using two-dimensional echocardiography. J Am Coll Cardiol 1996;28:1017-23.

Coisne D, Blouin CP, Allal J, Barraine R. Total digital three-dimensional colour Doppler imaging reconstruction of proximal isovelocity surface area: volume flow rate calculation in different experimental conditions. [Abstract] Eur Heart J 1998;19:481.

Cook LT, Cook PN, Lee KR, Batnitzky S, Wong BYS, Fritz SL, Ophir J, Dwyer III SJ, Bigongiari LR, Templeton AW. An algorithm for volume estimation based on polyhedral approximation. IEEE Trans Biomed Eng 1980;BME-27:493-500.

Daniel WG, Erbel R, Kasper W, Visser CA, Engberding R, Sutherland GR, Grube E, Hanrath P, Maish B, Dennig K, Schartt M, Kremer P, Angermann C, Iliceto S, Curtis JM, Mugge A. Safety of transesophageal echocardiography. A multicentre survey of 10,419 examinations. Circulation 1991;83:817-21.

Dekker DL, Piziali R, Dong E Jr. A system for ultrasonically imaging the human heart in three-dimensions. Comput Biomed Res 1974;7:544-53.

Delabays A, Sugeng L, Pandian NG, Hsu T-L, Ho S-J, Chen C-H, Marx G, Schwartz SL, Cao Q-L. Dynamic three-dimensional echocardiographic assessment of intracardiac blood flow jets. Am J Cardiol 1995;76:1053-8.

De Simone R, Glombitza G, Vahl CF, Albers J, Nakamura G, Mayer A, Makabe M, Meinzer HP, Hagl S. Quantitative assessment and visualization of mitral regurgitant jets by three-dimensional colour Doppler. [Abstract] Eur Heart J 1998;19:480.

Dickenson DF, Arnold R, Wilkinson JL. Congenital heart disease among 160 480 live born children in Liverpool 1960 to 1969. Implication for surgical treatment. Br Heart J 1981;46:55-62.

Diethelm L, Dery R, Lipton MJ, Higgins CB. Atrial level shunts: sensitivity and specificity of MR diagnosis. Radiology 1987;162:181-6.

Dinsomore RE, Wismer GL, Guyer D, Thompson R, Liu P, Stratemeier E, Miller S, Okada R, Brady T. Magnetic resonance imaging of the interatrial septum and atrial septal defects. Am J Roentgenol 1985;145:697-703.

Dodge HT, Sandler H, Ballew DW, Lord JD Jr. The use of biplane angiocardiography for the measurement of left ventricular volume in man. Am Heart J 1960;60:762-76.

Donovan CL, Armstrong WF, Bach DS. Quantitative Doppler tissue imaging of the left ventricular myocardium: Validation in normal subjects. Am Heart J 1995;130:100-04.

Edler I, Hertz CH. The use of the ultrasonic reflectoscope for the continuous recording of the movements of the heart walls. Kungl. Fysiografiska Sällskapets i Lund Förhanlingar 1954;24:40-58.

Erbel R, Schweizer P, Lambertz H, Henn G, Meyer J, Krebs W, Effert S. Echoventriculography - A simultaneous analysis of two-dimensional echocardiography and cineventriculography. Circulation 1983;67:205-15.

Ettedgui JA, Siewers RD, Anderson RH, Park SC, Pahl E, Zuberbuhler JR. Diagnostic ehocardiographic features of the sinus venosus defect. Br Heart J 1990;64:329-31.

Eyer MK, Brandestini MA, Phillips DJ, Baker DW. Color digital echo/Doppler image presentation. Ultrasound Med Biol 1981;7:21-31.

Fazzalari NL, Davidson JA, Mazumdar J, Mahar LJ, DeNardi E. Three dimensional reconstruction of the left ventricle from four anatomically defined apical two-dimensional echocardiographic views. Acta Cardiol 1984;39:409-36.

Fleishman CE, Ota T, Ohazama CJ, Stetten G, Lewis CW, Li J, von Ramm OT, Kisslo J. Real-time, three-dimensional echocardiography: measurement of left ventricular mass in dogs. [Abstract] Circulation 1996;94 (Suppl I):I-688 (a).

Fleishman CE, Li J, Ota T, Ohazama CJ, Stetten, Adams D, von Ramm OT, Kisslo J. Identification of congenital heart defects using real-time three-dimensional echo in pediatric patients. [Abstract] Circulation 1996;94 (Suppl I):I-416 (b).

Fleming AD, McDicken WN, Sutherland GR, Hoskins PR. Assessment of colour Doppler tissue imaging using test-phantoms. Ultrasound Med Biol 1994;20:937-57.

Fleming AD, Palka P, McDicken WN, Fenn LN, Sutherland GR. Verification of cardiac Doppler tissue images using grey-scale M-mode images. Ultrasound Med Biol 1996;22:573-81.

Franke A, Kuhl HP, Rulands D, Jansen C, Erena C, Grabitz RG, Dabritz S, Messmer BJ, Flachskampf FA, Hanrath P. Quantitative analysis of the morphology of secundum-type atrial septal defects and their dynamic change using transoesophageal three-dimensional echocardiography. Circulation 1997;96 (Suppl II):II-323-II-327.

Geiser EA, Ariet M, Conetta DA, Lupiewicz SM, Chrisite LG Jr, Conti CR. Dynamic three-dimensional reconstruction of the intact human left ventricle: technique and initial observations in patients. Am Heart J 1982;103:1056-65.

Ghosh A, Nanda NC, Maurer G. Three-dimensional reconstruction of echocardiographic images using the rotation method. Ultrasound Med Biol 1982;8:655-61.

Godman MJ, Tham P, Kidd BSL. Echocardiography in the evaluation of the cyanotic newborn infant. Br Heart J 1974;36:154-66.

Gopal AS, Keller AM, Rigling R, King DL Jr, King DL. Left ventricular volume and endocardial surface area by three-dimensional echocardiography: comparison to two-dimensional echocardiography and magnetic resonance imaging in normal subjects. J Am Coll Cardiol 1993;22:258-70.

Gopal AS, Keller AM, Shen Z, Sapin PM, Schroeder KM, King DL Jr, King DL. Three-dimensional echocardiography: in vitro and in vivo validation of left ventricular mass and comparison with conventional echocardiographic methods. J Am Coll Cardiol 1994;24:504-13.

Gorcsan J III, Gulati VK, Mandarino WA, Katz WE. Color-coded measures of myocardial velocity throughout the cardiac cycle by tissue Doppler imaging to quantify regional left ventricular function. Am Heart J 1996;131:1203-13.

Gorcsan J III, Strum DP, Mandarino WA, Gulati VK, Pinsky MR. Quantitative assessment of alterations in regional left ventricular contractility with color-coded tissue Doppler echocardiography. Comparison with sonomicrometry and pressure-volume relations. Circulation 1997;95:2423-33.

Hagler DJ. Echocardiographic findings in atrioventricular canal defects, edited by Feldt RH. Philadelphia, WB Saunders Company 1976, pp 87-109.

Hagler DJ, Tajik AJ, Seward JB, Mair DD, Ritter DG. Real-time wide-angle sector echocardiography: atrioventricular canal defects. Circulation 1979;59:140-50.

Han L, Ung Kang S, Park SC, Ettedgui JA, Neches WH. long-term left atrioventricular valvular function following surgical repair of atrioventricular septal defect. Cardiol Young 1995;5:230-7.

Hellenbrand WE, Fahey JT, McGowan FX, Weltin GG, Kleinman CS. Transesophageal echocardiographic guidance of transcatheter closure of atrial septal defect. Am J Cardiol 1990;66:207-13.

Holmvang G, Palacios IF, Vlahakes GJ, Dinsmore RE, Miller SW, Liberthson RR, Block PC, Ballen B, Brady TJ, Kantor HL. Imaging and sizing of atrial septal defects by magnetic resonance. Circulation 1995;92:3473-80.

Jiang L, Siu SC, Handschuhmacher MD, Guerrerro JL, Vasquez de Prada JA, King ME, Picard MH, Weyman AE, Levine RA. Three-dimensional echocardiography. In vivo validation for right ventricular volume and function. Circulation 1994;89:2342-50.

Kasai K, Namekawa K, Koyano A, Omoto R. Real-time two-dimensional blood flow imaging using an autocorrelation technique. IEEE Trans Sonics Ultrason 1985;32:458-64.

Kasprzak JD, Salustri A, Roelandt JRTC, Ten Cate FJ. Three-dimensional echocardiography of the aortic valve: feasibility, clinical utility and limitations. Echocardiography 1998;15:127-38 (a).

Kasprzak JD, Nosir YFM, Dall'Agata A, Elhendy A, Taams M, Ten Cate FJ, Roelandt JRTC. Quantification of the aortic valve area in three-dimensional echocardiographic data sets: Analysis of orifice overestimation resulting from suboptimal cut-plane selection. Am Heart J 1998;135:995-1003(b).

King DL, Al-Banna SJ, Larach DL. A new three-dimensional random scanner for ultrasonic/computer graphic imaging of the heart. In: White DN, Barnes R (ed): Ultrasound in Medicine, Vol 2. New York, Plenum Press, 1976;2:363-72.

King DL, King DL Jr, Shao M Yi-Ci. Evaluation of in vitro measurement accuracy of a three-dimensional ultrasound scanner. J Ultrasound Med 1991;10:77-82.

King DL, Harrison MR, King DL Jr, Gopal AS, Martin RP, DeMaria AN. Improved reproducibility of left atrial and left ventricular measurements by guided three-dimensional echocardiography. J Am Coll Cardiol 1992;20:1238-45.

King DL, Gopal AS, King DL Jr, Shao MYC. Three-dimensional echocardiography: in vitro validation for quantitative measurement of total and 'infarct' surface area. J Am Soc Echocardiogr 1993;6:69-76.

Kronzon I, Tunick PA, Freedberg RS, Trehan N, Rosenzweig, BP, Schwinger ME. Transesophageal echocardiography is superior to transthoracic echocardiography in the diagnosis of sinus venosus atrial septal defect. J Am Coll Cardiol 1991;17:537-42.

Kupferwasser I, Mohr-Kahaly S, Erbel R, Makowski T, Wittlich N, Kearney P, Mumm B, Meyer J. Three-dimensional imaging of cardiac mass lesions by transoesophageal echocardiographic computed tomography. J Am Soc Echocardiogr 1994;7:561-70.

Kuroda J, Kinter TM, Seward JB, Yanagi H, Greenleaf JF. Accuracy of three-dimensional volume measurement using biplane transoesophageal echocardiographic probe: in vitro experiment. J Am Soc Echocardiogr 1991;4:475-84.

Lange A, Bouki K, Fenn LN, Palka P, McDicken NW, Sutherland GR. A comparative study of grey scale versus Doppler tissue imaging left ventricular volume measurements using three dimensional reconstruction. [Abstract] Eur Heart J. 1995;16(Suppl):P266.

Lange A, Wright RA, Al-Nafusi A, Sang C, Palka P, Sutherland GR. Doppler myocardial imaging: a new method of data acquisition for three-dimensional echocardiography. J Am Soc Echocardiogr 1996;9:918-21.

Lange A, Palka P, Caso P, Fenn LN, Olszewski R, Ramo MP, Shaw TRD, Nowicki A, Fox KAA, Sutherland GR. Doppler myocardial imaging vs. B-mode grey-scale imaging: a comparative in vitro study into their relative efficacy in endocardial boundary detection. Ultrasound Med Biol 1997;23:69-75.

Levine RA, Triulzi MO, Harrigan P, Weyman AE. The relationship of mitral annular shape to the diagnosis of mitral valve prolapse. Circulation 1987;75:756-67.

Levine RA, Handschumacher MD, Sanfilippo AJ, Hagege AA, Harrigan P, Marshall JE, Weyman AE. Three-dimensional echocardiographic reconstruction of the mitral valve, with implications for the diagnosis of mitral valve prolapse. Circulation 1989;80:589-98.

Levy WC, Cerqueira MD, Matsuoka DT, Harp GD, Sheehan FH, Stratton JR. Four radionuclide methods for left ventricular volume determination: Comparison of manual and an automated technique. J Nucl Med 1992;33:763-70.

Lewis FJ, Taufic M, Varco ML, Niazi S. The surgical anatomy of atrial septal defect; experience with repair under direct vision. Ann Surg 1955; 142;401-17.

Linker DT, Moritz WE, Pearlman AS. A new three-dimensional echocardiographic method of right ventricular volume measurement: in vitro validation. J Am Coll Cardiol 1986;8:101-6.

Lloyd TR, Rao S, Beekman RH III, Mendelsohn AM, Sideris EB. Atrial septal defect occlusion with the buttoned device (a multinstitutional U.S. trial). Am J Cardiol 1994;73:286-91.

Ludomirsky A, Vermilion R, Nesser J, Marx G, Vogel M, Derman R, Pandian N. Transthoracic real-time three-dimensional echocardiography using the rotational scanning approach for data acquisition. Echocardiography 1994;11:599-606.

Macartney FJ, Rees PG, Kieran D, Piccoli GP, Taylor JFN, De Lewal MR, Stark J, Anderson RH. Angiocardiographic appearances of atrioventricular defects with particular reference to distinction of ostium primum atrial septal defect from common atrioventricular orifice. Br Heart J 1979;42:640-56.

Magni G, Hijazi ZM, Marx G, Das G, Delabays A, Levine J, Fulton D, Pandian N. Utility of 3-D echocardiography in patient selection and guidance for atrial septal defect (ASD) closure by the new Das-angel wings occluder device. [Abstract] J Am Coll Cardiol 1996;27(Suppl A):190A.

Martin RW, Bashein G. Measurement of stroke volume with three-dimensional transesophageal ultrasonic scanning. Anaesthesiology 1989;70:470-6.

Marx GR, Fulton DR, Pandian NG, Vogel M, Cao Q-L, Ludomirsky A, Delabays A, Sugeng L, Klas B. Delineation of site, relative size and dynamic geometry of atrial septal defects by real-time three-dimensional echocardiography. J Am Coll Cardiol 1995;25:482-90.

McDicken WN, Sutherland GR, Moran CM, Gordon L. Colour Doppler velocity imaging of the myocardium. Ultrasound Med Biol 1992;18:651-4.

McGrath LB, Gonzalez-Lavin L. Actuarial survival, freedom from reoperation, and other events after repair of atrioventricular septal defects. J Thorac Cardiovasc Surg 1987;94:582-90.

McPherson DD, Skorton DJ, Kodiyalam S, Petree L, Noel MP, Kieso R, Kerber RE, Collins SM, Chandran KB. Finite element analysis of myocardial diastolic function using three-dimensional echocardiographic reconstruction: application of a new method for the study of acute ischaemia in dogs. Circ Res 1987;60:674-82

Mehta RH, Helmcke F, Nanda NC, Pinheiro L, Samdarshi TE, Vinod KS. Uses and limitations of transthoracic echocardiography in the assessment of atrial septal defect in the adult. Am J Cardiol 1991; 67:288-94.

Miyatake K, Yamagishi M, Tanaka N, Uematsu M, Yamazaki N, Mine Y, Sano A, Hirama M. New method for evaluating left ventricular wall motion by color coded tissue Doppler imaging: in vitro and in vivo studies. J Am Coll Cardiol 1995;25:717-24.

Morimoto K, Matsuzaki M, Tohma Y, Shiro O, Tanaka N, Michishige H, Murata K, Anno Y, Kusukawa R. Diagnosis and quantitative evaluation of secundum-type atrial septal defect by transoesophageal Doppler echocardiography. Am J Cardiol 1990;66:85-91.

Mortitz WE, Pearlman AS, McCabe DH, Medema DK, Ainsworth ME, Boles MS. An ultrasonic technique for imaging the ventricle in three dimensions and calculating its volume. IEEE Trans Biomed Eng 1983;30:482-91.

Muhler EG, Engelhardt W, Von Bernuth G. Detection of sinus venosus atrial septal defect by two-dimensional echocardiography. Eur Heart J 1992;13:453-456.

Nanda NC, Roychoudhury D, Chung SM, Kim KS, Ostlund V, Klas B. Quantitative assessment of normal and stenotic aortic valve using transoesophageal three-dimensional echocardiography. Echocardiography 1994;11:617-25.

Nasser FN, Tajik AJ, Seward JB, Haggler DJ. Diagnosis sinus venosus atrial septal defect by two dimensional echocardiography. Mayo Clinic Procc 1981;56:568-72.

Nixon JV, Saffer SI, Lipscomb K, Blomqvist CG. Three-dimensional echoventriculography. Am Heart J 1983;106:435-43.

Nowicki A, Olszewski R, Etienne J, Karlowicz P, Adamus J. Assessment of wall velocity gradient imaging using a test phantom. Ultrasound Med Biol 1996;22:1255-60.

Palka P, Lange A, Fleming AD, Sutherland GR, Fenn LN, McDicken WN. Doppler tissue iamging: myocardial wall motion velocities in normal subjects. J Am Soc Echocardiogr 1995;8:659-8.

Palka P, Lange A, Fleming AD, Fenn LN, Bouki KP, Shaw TRD, Fox KAA, McDicken WN, Sutherland GR. Age-related transmural peak mean velocities and peak velocity gradients by Doppler myocardial imaging in normal subjects. Eur Heart J 1996; 17:940-50.

Palka P, Lange A, Fleming AD, Donnelley JE, Dutka DP, Starkey IR, Shaw TRD, Sutherland GR, Fox KAA. Differences in myocardial velocity gradient measured throughout the cardiac cycle in patients with hypertrophic cardiomyopathy, athletes and patients with left ventricular hypertrophy due to hypertension. J Am Coll Cardiol 1997;30:760-8.

Pandian NG, Nanda NC, Schwartz SL, Fan P, Cao Q-L, Sanyal R, Hsu T-L, Mumm B, Wollschlager H, Weintraub A. Three-dimensional and four-dimensional transoesophageal echocardiographic imaging of the heart and aorta in humans using a computed tomographic imaging probe. Echocardiography 1992;9:677-87.

Pandian NG, Roelandt J, Nanda NC. Dynamic three-dimensional echocardiography: methods and clinical potential. Echocardiography 1994;11:237-59.

Pascoe RD, Oh JK, Warnes CA, Danielson GK, Tajik AJ, Seward BJ. Diagnosis sinus venosus atrial septal defect with transesophageal echocardiography. Circulation 1996;94:1049-55

Pearlman AS. Measurement of left ventricular volume by three-dimensional echocardiography - present promise and potential problems. [Editorial] J Am Coll Cardiol 1993;22:1538-40.

Peronneau PA, Hinglais J, Pellet M, Leger F. Vélocimètre sanguin par effet Doppler á émission ultra-sonore pulsée. L'Onde Électrique 1969;50:369-89.

Phillips DJ, Power JE, Eyer MK, Blackshear WM, Bodily KC, Strandness DE, Baker DW. Detection of peripheral vascular disease using duplex scanner III. Ultrasound Med Biol 1980;6:205-18.

Piccoli GP, Wilkinson JL, Macartney FJ, Gerlis LM, Anderson RH. Morphology and classification of complete atrioventricular defects. Br Heart J 1979;42:633-99 (a).

Piccoli GP, Gerlis LM, Wilkinson JL, Lozsadi K, Macartney FJ, Anderson RH. Morphology and classification of atrioventricular defect. Br Heart J 1979;42:62-32 (b).

Pieroni DR, Homey E, Freedom RM. Echocardiography in atrioventricular canal defects: a clinical spectrum. Am J Cardiol 1975;35:54-8.

Pini R, Costi M, Mensah GA, Masotti L, Novis KL, Greenberg DP. Computed tomography of the heart by ultrasound. Comput Cardiol 1991, 17-20.

Pini R, Giannazzo G, Bari MD, Innocenti F, Rega L, Casolo G, Devereux RB. Transthoracic three-dimensional echocardiographic reconstruction of left and right ventricles: In vitro validation and comparison with magnetic resonance imaging. Am Heart J 1997;133:221-9.

Rastelli GC, Kirklin JW, Titus JL. Anatomic observations on complete form of persistent common atrioventricular canal with special reference to atrioventricular valves. Mayo Clin Proc 1966;41:296-308.

Reeder GS, Hagler DJ, Tajik AJ. Sensitivity of two-dimensional echocardiography in direct visualization of atrial septal defect utilizing the subcostal approach: experience with 154 patients. J Am Coll Cardiol 1983;2:127-35.

Rivera JM, Siu SC, Handschumacher MD, Lethor J-P, Guerrero L, Vlahakes GJ, Mitchell JD, Weyman AE, King MEE, Levine RA. Three-dimensional reconstruction of ventricular septal defects: validation studies and in vivo feasibility. J Am Coll Cardiol 1994;23:201-8.

Rodriguez L, Garcia M, Ares M, Griffin BP, Nakatani S, Thomas JD. Assessment of mitral annular dynamics during diastole by Doppler tissue imaging: Comparison with mitral Doppler inflow in subjects without heart disease and in patients with left ventricular hypertrophy. Am Hear J 1996;131:982-7.

Roelandt JRTC, Ten Cate FJ, Bruining N, Salustri A, Vletter WB. Transoesophageal rotoplane echo-CT. A novel approach to dynamic three-dimensional echocardiography. Thoraxcentre J. 1994;6:4-8 (a).

Roelandt JRTC, Ten Cate FJ, Vletter WB, Taams MA, Bekkering L, Glastra H, Djoa KK, Weber F. Ultrasonic dynamic three-dimensional visualization of the heart with a multiplane transesophageal imaging transducer. J Am Soc Echocardiogr 1994;7:217-29 (b).

Roelandt JRTC, Salustri A, Bekkering L, Bruining N, Vletter WB. Precordial three dimensional echocardiography with a rotational imaging probe: methods and initial clinical experience. Echocardiography 1995;12:243-52.

Rome JJ, Keane JF, Perry SB, Spevak PJ, Lock JE. Double-umbrella closure of atrial defects. Initial clinical applications. Circulation 1990;82:751-8.

Sahn DJ, Terry RW, O'Rourke R, Leopold G, Friedman WF. Multiple crystal echocardiographic evaluation of endocardial cushion defect. Circulation 1974;50:25-32.

Sakakibara M, Kobayashi S, Imai H, Watanabe S, Masuda Y, Inagaki Y. Diagnosis of atrial septal defect using magnetic resonance imaging. J Cardiol 1987;17:817-29.

Salustri A, Spitaels S, McGhie J, Vletter W, Roelandt JRTC. Transthoracic three-dimensional echocardiography in adult patients with congenital heart disease. J Am Coll Cardiol 1995;26:759-76.

Salustri A, Becker AE, van Herwerden L, Vletter WB, Ten Cate FJ, Roelandt JRTC. Three-dimensional echocardiography of normal and pathologic mitral valve: a comparison with two-dimensional transoesophageal echocardiography. J Am Coll Cardiol 1996;27:1502-10.

Sapin PM, Schroeder KD, Smith MD, DeMaria AN, King DL. Three-dimensional echocardiographic measurement of left ventricular volume in vitro: comparison with two-dimensional echocardiography and cineventriculography. J Am Coll Cardiol 1993;22:1530-7.

Sapin PM, Schroeder KM, Gopal AS, Smith MD, DeMaria AN, King DL. Comparison of two- and three-dimensional echocardiography with cineventriculography for measurement of left ventricular volume in patients. J Am Coll Cardiol 1994;24:1054-63.

Sapin PM, Clarke GB, Gopal AS, Smith MD, King DL. Validation of three-dimensional echocardiography for quantifying the extent of dyssynergy in canine acute myocardial infarction: comparison with two-dimensional echocardiography. J Am Coll Cardiol 1996;27:1761-70

Satomura S. Ultrasonic Doppler method for the inspection of cardiac functions. J Acoust Soc Am 1957;29:1181-5.

Sawada H, Fujii J, Kato K, Onoe M, Kuno Y. Three dimensional reconstruction of the left ventricle from multiple cross sectional echocardiograms. Value for measuring left ventricular volume. Br Heart J 1983;50:438-42.

Schapira JN, Martin RP, Fowles RE, Popp RL. Single and two-dimensional echocardiographic features of the interatrial septum in normal subjects and patients with an atrial septal defect. Am J Cardiol 1979;43:816-19.

Schnittger I, Fitzgerald PJ, Daughters GT, Ingels NB, Kantrowitz NE, Schwarzkopf A, Mead CW, Popp RL. Limitations of comparing left ventricular volumes by two-dimensional echocardiography, myocardial markers and cineangiography. Am J Cardiol 1982;50:512-9.

Schroeder KM, Sapin PM, King DL, Smith MD, DeMaria AN. Three-dimensional echocardiographic volume computation: in vitro comparison to standard two-dimensional echocardiography. J Am Soc Echocardiogr 1993;6:467-75.

Schwartz SL, Cao Q, Azevedo J, Pandian NG. Simulation of intraoperative visualization of cardiac structures and study of dynamic surgical anatomy with real time three-dimensional echocardiography. Am J Cardiol 1994;73:501-7.

Schwartz DS, Ribakove GH, Grossi EA, Stevens JH, Siegel LC, St Goar FG. Minimally invasive cardiopulmonary bypass with cardioplegic arrest: a closed chest technique with equivalent myocardial protection. J Thorac Cardiovasc Surg 1996;111:556-66.

Scott PJ, Blackburn ME, Wharton GA, Wilson N, Dickinson DF, Gibbs JL. Transoesophageal echocardiography in neonates, infants and children: applicability and diagnostic value in everyday practice of a cardiothoracic unit. Br Heart J 1992;68:488-92.

Sheikh KH, Smith SW, von Ramm OT, Kisslo J. Real-time, three-dimensional echocardiography: feasibility an initial use. Echocardiography 1991;8:119-25.

Shiota T, Jones M, Chikada M, Fleishman CE, Castellucci JB, Cotter B, DeMaria AN, von Ramm OT, Kisslo J, Ryan T. Real-time three-dimensional echocardiography for determining right ventricular stroke volume in an animal model of chronic right ventricular volume overload. Circulation 1998;97:1897-1900.

Shiota T, Jones M, Delabays A, Li X, Yamada I, Ishii M, Acar P, Holcomb S, Pandian NG, Sahn DJ. Direct measurement of three-dimensionally reconstructed flow convergence surface area and regurgitant flow in aortic regurgitation. In vitro and chronic animal model studies. Circulation 1997;96:3687-95.

Shub C, Dimopoulos IN, Seward JB, Tancredi RG, Schattenberg TT, Reeder GS, Haggler DJ, Tajik AJ. Sensitivity of two dimensional echocardiography in the direct visualisation of atrial septal defect utilizing the subcostal approach: experience in 154 patients. J Am Coll Cardiol 1983;2:127-135.

Smallhorn JF, Tommasini G, Anderson RH, Macartney FJ. Assessment of atrioventricular septal defects by two dimensional echocardiography. Br Heart J 1982;47:109-21 (a).

Smallhorn JF, De Leval M, Stark J, Somerville J, Taylor JFN, Anderson RH, Macartney FJ. Isolated anterior mitral cleft. Two dimensional echocardiographic assessment and differentiation from 'clefts' associated with atrioventricular septal defect. Br Heart J 1982;48:109-16 (b).

Snyder JE, Kisslo J, von Ramm OT. Real-time orthogonal mode scanning of the heart. I. System design. J Am Coll Cardiol 1986;7:1279-83.

Starling MR, Crawford MH, Sorensen SG, Levi B, Richards KL, O'Rourke RA. Comparative accuracy of apical biplane cross-sectional echocardiography and gated equilibrium radionuclide angiography for estimating left ventricular size and performance. Circulation 1981;63:1075-84.

Stickels KR, Wann LS. An analysis of three-dimensional reconstructive echocardiography. Ultrasound Med Biol 1984;10:575-80.

Studer M, Blackstone EH, Kirklin JW, Pacifico AD, Soto B, Chung GK, Kirklin JK, Bargeron LM Jr. Determinants of early an late results of repair of atrioventricular septal (canal) defects. J Thorac Cardiovasc Surg 1982;84:523-42.

Sugeng L, Cao Q-L, Delabays A, Esakof D, Marx G, Vannan M, Washburn D, Pandian NG. Three-dimensional echocardiographic evaluation of aortic disorders with rotational multiplanar imaging: experimental and clinical studies. J Am Soc Echocardiogr 1997;10:120-32.

Sutherland GR, Godman MJ, Anderson RH, Hunter S. The spectrum of atrioventricular valve atresia: a two-dimensional echocardiographic-pathologic correlation. In: Rijsterborgh H, ed. Echocardiography 1981. The Hague: Martinus Nijhoff, 1981:345-53.

Sutherland GR, Smallhorn JF, Anderson RH, Rigby ML, Hunter S. Atrioventricular discordance: cross-sectional echocardiographic-morphological correlative study. Br Heart J 1983;50:8-20.

Sutherland GR, Steward MJ, Grounstroem KWE, Moran CM, Fleming A, Guell-Peris FJ, Riemersma RA, Fenn LN, Fox KAA, McDicken WN. Color Doppler myocardial imaging: a new technique for the assessment of myocardial function. J Am Soc Echocardiogr 1994;7:441-58.

Suzuki K, Ho SY, Anderson RH, Becker AE, Neches WH, Devine WA, Tatsuno K, Mimori S. Morphometric analysis of atrioventricular septal defect with common valve orifice. J Am Coll Cardiol 1998;31:217-23.

Tortoledo FA, Quinones MA, Fernandez GC, Waggoner AD, Winters WL. Quantification of left ventricular volumes by two-dimensional echocardiography: a simplified and accurate approach. Circulation 1982;67:579-84.

Uematsu M, Miyatake K, Tanaka N, Matsuda H, Sano A, Yamazaki N, Hirama M, Yamagishi M. Myocardial velocity gradient as a new indicator of regional left ventricular contraction: detection by two-dimensional tissue Doppler imaging technique. J Am Coll Cardiol 1996;26:217-23.

Utsunomiya T, Ogawa T, Doshi R, Patel D, Quan M, Gardin JM. Doppler color flow from 'proximal isovelocity surface area' method for estimating volume flow rate: effects of orifice, shape and machine factors. J Am Coll Cardiol 1991; 17:1103-11.

Vas R, Diamond GA, Forrester JS, Whiting JS, Swan HJC. Computer enhancement of direct and venous-injected left ventricular contrast angiography. Am Heart J 1981; 102:719-28.

Vogel M, Losch S. Dynamic three-dimensional echocardiography with a computed tomography imaging probe: initial clinical experience with transthoracic application in infants and children with congenital heart defects. Br Heart J 1994;71:462-67.

Vogel M, White PA, Redington AN. In vitro validation of right ventricular volume measurement by three dimensional echocardiography. Br Heart J 1995;74:460-63 (a).

Vogel M, Ho SY, Anderson RH. Comparison three dimensional echocardiography findings with anatomical specimens of various congenitally malformed heart. Br Heart J 1995;73:566-70 (b).

von Ramm OT, Smith SW. Real-time volumetric ultrasound imaging system. J Digit Imaging 1990;3:261-6.

Wagstaffe WW. Two cases of free communication between the auricles, by deficiency of upper part of the septum auricularum. Trans Pathol Soc Lond 1868;19:96-8.

Wakai CS, Edwards JE. Pathologic study of persistent common atrioventricular canal. Am Heart J 1958;56:779-94.

Wells PNT. A range-gated ultrasonic Doppler system. Med Biol Engng 1969;7:641-52.

Williams RG, Rudd M. Echocardiographic features of endocardial cushion defects. Circulation 1974;49;418-22.

Wyatt HL, Heng MK, Meerbaum S, Gueret P, Hestenes J, Dula E, Corday E. Cross-sectional echocardiography. II. Analysis of mathematic models for quantifying volume of the formalin-fixed left ventricle. Circulation 1980;61:1119-25.

Wyme J, Green LH, Mann T, Levin D, Grossman W. Estimation of left ventricular volumes in man from biplane cineangiograms filmed in oblique projections. Am J Cardiol 1978;41:726-32.

Yao J, Cao Q-L, Masani N, Delabays A, Magni G, Acar P, Laskari C, Pandian NG. Three-dimensional echocardiographic estimation of infarct mass based on quantification of dysfunctional left ventricular mass. Circulation 1997;96:1660-6.

APPENDIX

PUBLISHED WORK ARISING FROM OR RELEVANT TO THIS THESIS

Doppler Myocardial Imaging: A New Method of Data Acquisition for Three-Dimensional Echocardiography

Aleksandra Lange, MD,[a] Robert A. Wright, MRCP, A. Al-Nafusi, MD, Christopher Sang, FRCS, Przemyslaw Palka, MD, and George R. Sutherland, FRCP, FESC,
Edinburgh, United Kingdom

The precise morphologic characteristics of any intracardiac tumor have important implications regarding surgical planning and operative repair. Three-dimensional echocardiography has proved to be a valuable clinical technique in this field. Current methods of three-dimensional reconstruction of two-dimensional images are based on the standard gray-scale imaging technique. However, precordial gray-scale data-set information is frequently of suboptimal quality because of data degradation caused by ultrasound attenuation by chest wall structures. This has limited the use of the transthoracic three-dimensional technique to "echogenic" patients. Doppler myocardial imaging (DMI), a new ultrasound technique based on the Doppler principle, is influenced less by chest wall attenuation and in addition offers a better boundary detection algorithm for the cardiac structures. To determine if there may be a potential benefit of DMI to acquire data for three-dimensional reconstruction, a 33-year-old woman with a large intracardiac mass was studied. In this case three-dimensional gray-scale and DMI data sets were compared and contrasted with pathologic information. DMI allowed both the quantification of mass volume and the correct definition of the morphology of the mass. It was also possible to identify the precise site of attachment of the mass to the mitral valve leaflets. The information thus obtained was correlated with both operative and pathologic findings. (J Am Soc Echocardiogr 1996;9:918-21.)

Three-dimensional (3D) echocardiography has already proved to be clinically effective in the assessment of cardiac structures.[1] At present, standard two-dimensional (2D) gray-scale images are used to reconstruct 3D data sets. However, the precordial 2D gray-scale imaging technique is frequently impaired because of data degradation caused by ultrasound attenuation by chest wall structures. For the first time 3D was performed with Doppler myocardial imaging (DMI). DMI is based on the Doppler principle whereby the special algorithms are applied to visualize cardiac structures.[2] An important feature of DMI is that it is relatively independent of the amplitude of the returning ultrasonic signal and is not directly affected by the attenuating effect of the chest wall.[3] Thus DMI has the potential to provide better-quality images than standard 2D gray-scale echocardiography in poorly echogenic patients.

We present the precordial 3D appearance of a large intracardiac mass attached to both leaflets of the mitral valve causing mitral valve obstruction. We describe the role of DMI in 3D echocardiography and its usefulness in the surgical management of patients.

CASE REPORT

A 33-year-old woman was admitted to the hospital with a 6-month history of increasing shortness of breath, paroxysmal nocturnal dyspnea, and two-pillow orthopnea. She had a 10-year history of systemic lupus erythematosus (SLE). On clinical examination she had sinus tachycardia with a loud first heart sound and both a 3/6 apical pansystolic and a 2/6 mid-diastolic murmur. An electrocardiogram showed sinus tachycardia, biatrial enlargement, and right ventricular hypertrophy. Standard transthoracic 2D gray-scale ultrasonic images were obtained and were of moderate quality (Figure 1). A large echogenic mobile mass was visualized adherent to the posterior leaflet of what appeared to be a normal mitral valve. This mass was approximately 2 cm in circumference. During diastole, the mass prolapsed freely into the left ventricle. Color flow Doppler imaging demonstrated a mitral inflow pattern with multiple aliasing, suggesting high-velocity turbulent flow and valve obstruction. A continuous-wave Doppler

From the Department of Cardiology, Western General Hospital, the Department of Pathology, University of Edinburgh, and the Department of Cardiothoracic Surgery, Royal Infirmary, University of Edinburgh.

[a]Scottish Office Home and Health Department Research Fellow.

Reprint requests: A. Lange, MD, Department of Cardiology, Western General Hospital, Crewe Rd., Edinburgh EH4 2XU, Scotland, UK.

0894-7317/96 $5.00 + 0 27/4/70904

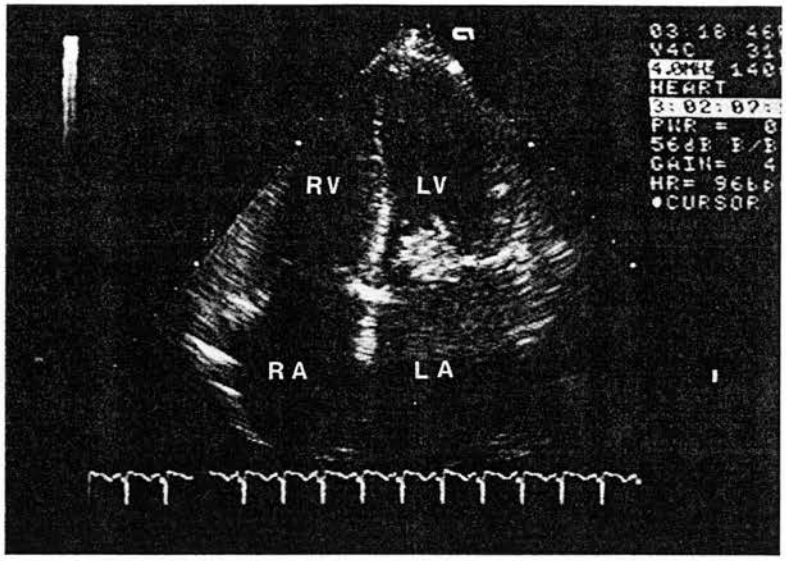

Figure 1 Transthoracic 2D gray-scale image of apical four-chamber view presenting SLE mass obstructing mitral valve orifice. (*LA,* Left atrium; *RA,* right atrium; *LV,* left ventricle; *RV,* right ventricle.)

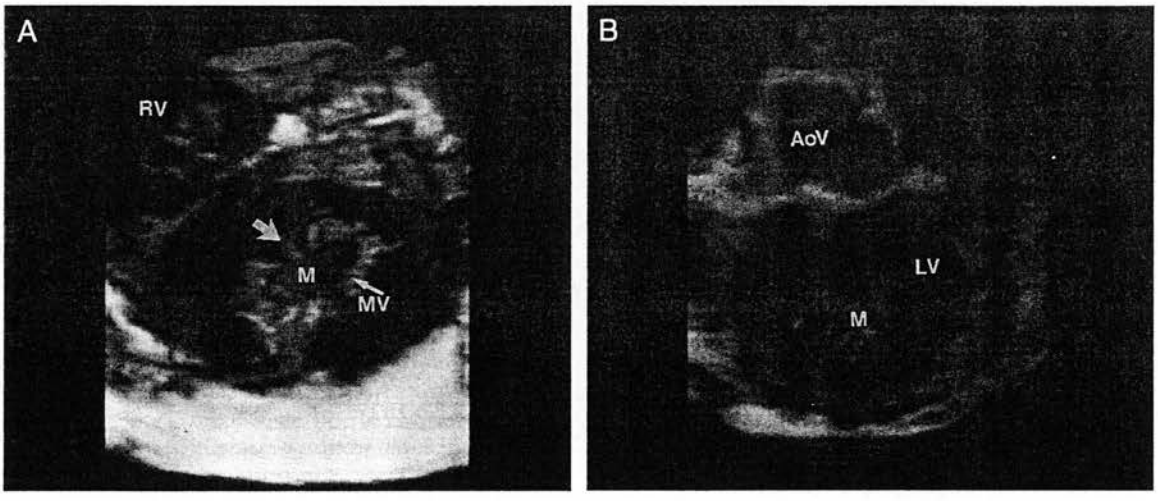

Figure 2 DMI 3D reconstructions of SLE mass obstructing mitral valve orifice. Apical short-axis view is selected as a reference cut plane beyond which by choosing appropriate treshhold and opacity the 3D system displays all structures in three dimensions. **A,** Mitral valve is in closed position. **B,** Mitral valve is in open position, as seen from left ventricular apex. (*AoV,* Aortic valve; *LV,* left ventricle; *M,* SLE mass; *MV,* mitral valve; *RV,* right ventricle.)

study demonstrated a peak diastolic transmitral velocity of 2.5 m/sec and a mean gradient of 14 mm Hg. An effective mitral valve area of 0.7 cm^2 was calculated by the measurement of pressure half-time. There was minimal associated mitral regurgitation. The findings were consistent with predominant stenosis but were presumed to be due to tumor obstruction of the valve orifice. She had no previous ultrasonic study with which to make a comparison.

Transthoracic 3D echocardiography was performed with an Acuson XP 10 scanner (Acuson Inc., Mountain View, Calif.) with DMI software and a 3D acquisition system (Echo-Scan; TomTec Imaging Systems GmbH, Munich, Germany). During the acquisition, all images were transferred from the scanner to the 3D system as a black/white video signal. Images were obtained with a 2.5 MHz phased-array transducer steered by the transducer

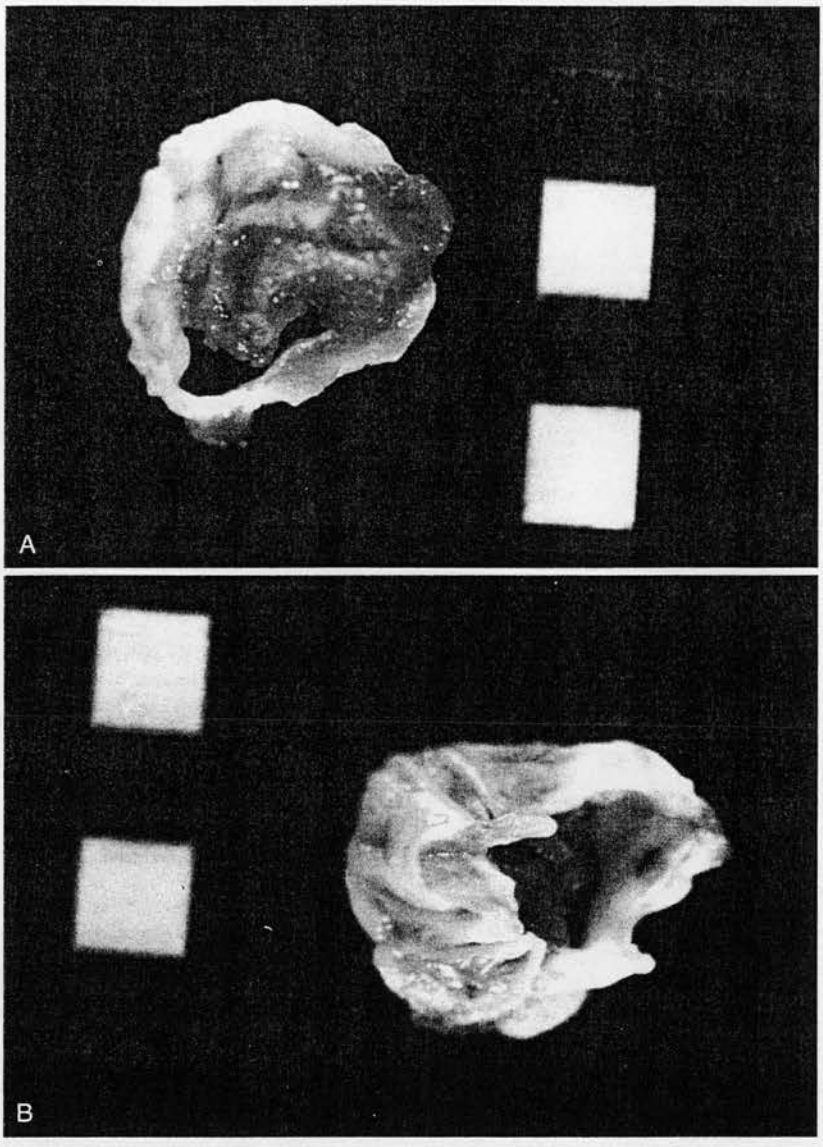

Figure 3 Corresponding pathologic specimens of SLE mass. **A,** Mass visualized from the atrial aspect. **B,** Mass visualized from ventricular aspect. Mitral leaflets have been fixed in open position with mass retracted.

mechanical rotational device at 2 degrees over 180 degrees. Two sets of images were acquired by different 2D imaging techniques, standard gray scale, and DMI velocity map. The scanner modifications for DMI have been described previously in our work.[4] Velocity range settings were used to encode myocardial velocities (0 to 16 cm/sec) that are lower than those typically used for blood flow. The display of Doppler information was therefore enabled for tissue instead of blood, the distinction being made on overall signal strength. Image persistence was turned off to eliminate blurring of the moving cardiac structures. Doppler receive gain was also set to achieve maximum color Doppler information of the mitral valve while limiting color information within the blood pool. For gray-scale imaging, the gain was adjusted to optimize the clarity of the acquired images.

With the gray-scale imaging technique, the acquired data set allowed for a volume measurement of 5.8 ml but did not provide sufficient definition to allow a satisfactory 3D reconstruction. Thus the definition of the shape of the mass was not clear. With DMI, a high-quality data set was acquired and a mass of inhomogeneous texture of 6.4 ml volume obstructing the mitral orifice was reconstructed (Figure 2). In addition, the superior quality of the 3D DMI data set allowed a better definition of the morphology of the mass and detection of the site of its attachment to the mitral valve leaflets.

At surgery, a brown pigmented mass of 7.3 ml volume was found attached to both valve leaflets and the chordae tendineae (Figure 3). The mitral valve and chordae were excised and replaced with a 27 mm Carpentier-Edwards xenograft. The site of attachment to the leaflets and volume measurements had been assessed accurately from the 3D DMI data set. The patient made an uneventful postoperative recovery and was discharged home.

Microscopically, the mass had the typical appearance of a Libman-Sacks fibrinous vegetation with entrapped macrophages. Six blood cultures have not been reported as showing any organism and two blood cultures taken after surgery were also negative.

DISCUSSION

We present a unique case of 3D DMI reconstruction of an SLE mass causing acute mitral valve obstruction that mimicked mitral stenosis. There are reported cases of mitral stenosis in the literature attributed to Libman-Sacks lesions, but few of these were hemodynamically significant.[5-8] It has been shown previously that dynamic 3D reconstruction may provide a unique opportunity to define and present cardiac lesions and their relationship to intracardiac structures.[1,9,10] Because of the relatively good spatial resolution of the 2D gray-scale modality, relatively small abnormalities such as interventricular or interatrial septal defects can be visualized. However, at present the main limitation of 3D echocardiography from the transthoracic approach is the poor quality of acquired images available for reconstruction. The quality of standard gray-scale images is dependent on the amplitude of the ultrasound signal returning from the cardiac structure, which is often significantly attenuated by the chest wall. DMI has slightly poorer spatial resolution than the 2D gray scale but is less subject to attenuation and has a better boundary detection algorithm.[11] Thus from the precordial approach, DMI offers higher image quality than the gray-scale imaging technique. In this patient in whom gray-scale imaging was suboptimal, 3D DMI information proved to be superior to that obtained from the 3D gray-scale data set. Standard 2D transesophageal images proved unnecessary because the DMI images obtained noninvasively from the precordial approach were of excellent quality, thus emphasizing the advantage of this technique. It allowed both quantification of mass volume and the correct determination of the morphology of the mass.

REFERENCES

1. King DL, Gopal AS, King DL Jr, Yi-Ci Shao M. Three-dimensional echocardiography: in vitro validation for quantitative measurement of total and "infarct" surface area. J Am Soc Echocardiogr 1993;6:69-76.
2. McDicken WN, Sutherland GR, Moran CM, Gordon L. Colour Doppler velocity imaging of the myocardium. Ultrasound Med Biol 1992;18:651-4.
3. Sutherland GR, Stewart MJ, Groundstroem KWE, et al. Color Doppler myocardial imaging: a new technique for the assessment of myocardial function. J Am Soc Echocardiogr 1994;7:441-58.
4. Palka P, Lange A, Fleming AD, Sutherland GR, Fenn LN, McDicken WN. Doppler tissue imaging: myocardial wall motion velocities in normal subjects. J Am Soc Echocardiogr 1995;8:659-68.
5. Nihoyannopoulos P, Gomez PM, Joshi J, Loizou S, Walport MJ, Oakley CM. Cardiac abnormalities in systemic lupus erythematosus: association with raised anticardiolipin antibodies. Circulation 1990;82:369-75.
6. Doherty NE, Siegel RJ. Cardiovascular manifestations of systemic lupus erythematosus. Am Heart J 1985;110:1257-65.
7. Galve E, Candell-Riera J, Pigrau C, Permanyer-Miralda G, Garcia-del-Castillo H, Soler-Soler J. Prevalence, morphologic types and evaluation of cardiac valvular disease in systemic lupus erythematosus. N Engl J Med 1988;319:817-23.
8. Doherty NE, Siegel RJ. Cardiovascular manifestations of systemic lupus erythematosus. Am Heart J 1985;110:1257-65.
9. Belohlavek M, Foley DA, Gerber TC, Greenleaf JF, Seward JB. Three-dimensional ultrasound imaging of the atrial septum: normal and pathologic anatomy. J Am Coll Cardiol 1993;22:1673-8.
10. Gabriel H, Binder T, Globits S, Zangeneh M, Rothy W, Glogar D. Three-dimensional echocardiography in the diagnosis of postinfarction ventricular septal defect. Am Heart J 1995;129:1038-40.
11. Fleming AD, McDicken WN, Sutherland GR, Hoskins PR. Assessment of colour Doppler tissue imaging test-phantoms. Ultrasound Med Biol 1994;20:937-57.

ELSEVIER

Ultrasound in Med. & Biol., Vol. 23, No. 1, pp. 69–75, 1997

0301-5629/97 $17.00 + .00

PII S0301-5629(96)00187-1

●*Original Contribution*

DOPPLER MYOCARDIAL IMAGING VS. B-MODE GREY-SCALE IMAGING: A COMPARATIVE *IN VITRO* AND *IN VIVO* STUDY INTO THEIR RELATIVE EFFICACY IN ENDOCARDIAL BOUNDARY DETECTION

ALEKSANDRA LANGE,* PRZEMYSLAW PALKA,* PIO CASO,† LYNN N. FENN,* ROBERT OLSZEWSKI,‡ M. PAULIINA RAMO,* THOMAS R. D. SHAW,* ANDRZEJ NOWICKI,§ KEITH A. A. FOX‖ and GEORGE R. SUTHERLAND*

*Department of Cardiology, Western General Hospital, Edinburgh, UK; †Divisione di Cardiologia, Ospedale Monaldi, Napoli, Italy; ‡Central Clinical Hospital, Military Medical Academy, Warsaw, Poland; §Polish Academy of Sciences, Warsaw, Poland; and ‖Cardiovascular Research Unit, University of Edinburgh, Edinburgh, UK

(*Received* 30 *May* 1996; *in final form* 3 *June* 1996)

Abstract—Doppler myocardial imaging (DMI) is a new ultrasound imaging modality in which colour Doppler algorithms are adapted to visualise the myocardium. It allows measurement of regional intramyocardial velocities and quantification of intramural left ventricular function. However promising the technique is, to date the accuracy of endocardial boundary detection by DMI has not been validated. As Doppler velocity estimation is based on measurement of phase shift rather than signal strength, the technique is relatively independent of chest wall attenuation. In the current study, a series of *in vitro* and *in vivo* studies was performed to compare standard B-mode grey-scale imaging (GSI) and DMI techniques in endocardial boundary detection. *In vitro*, the minimum and maximum volumes of a single-chamber tissue-mimicking phantom were calculated using both imaging techniques. *In vivo*, left ventricular end-diastolic (ED) volume and end-systolic (ES) volume indices were measured from GSI and DMI images in a group of 40 volunteers. All images were obtained in the freeze-frame mode with the Doppler display turned on and off so that simultaneous DMI and GSI information was obtained. *In vitro*, the limits of agreement between the minimum volume of the phantom and the minimum volume measured by GSI and DMI was 4% and 3%, respectively. For maximum volumes, limits of agreement were 3% for GSI and 2% for DMI. *In vivo*, the limits of agreement between the two imaging techniques in volume measurements were 6 mL (9%) for ED and 4 mL (11%) for ES. The comparison of the endocardial boundary detection by GSI vs. DMI showed DMI to be significantly superior: ED (72 ± 16% vs. 85 ± 8%, respectively; $p < 0.05$) and ES (71 ± 13% vs. 88 ± 7%, respectively; $p < 0.05$). The results of the study show that: (1) *in vitro*, based on two-dimensional algorithms, DMI provides as accurate volume measurements as GSI; and (2) *in vivo*, there is a very good agreement of left ventricular volume measurements between GSI and DMI. However, the endocardial boundary is more reliably displayed and visually easier to detect using DMI than GSI.

Key Words: **Ultrasound, Doppler myocardial imaging, Left ventricular volume.**

INTRODUCTION

Doppler myocardial imaging (DMI) is a new ultrasonic technique based on colour Doppler principles in which modified algorithms are applied to allow the detection of myocardial velocities instead of the velocity of blood flow within the cardiac chambers (McDicken et al. 1992). This algorithm makes the distinction between myocardial tissue and blood based on a combination of differing velocities and reflectivities inherent in these two entities. DMI colour-encodes myocardial motion using red to represent motion toward the transducer and blue to represent motion away from the transducer. Velocity magnitude is represented by the intensity of the displayed colour. Currently, DMI (otherwise Doppler Tissue Imaging (DTI) or Tissue Doppler Imaging (TDI) software is commercially

Address correspondence to: Dr. Aleksandra Lange, Department of Cardiology, Western General Hospital, Crewe Road, Edinburgh EH4 2XU, United Kingdom.

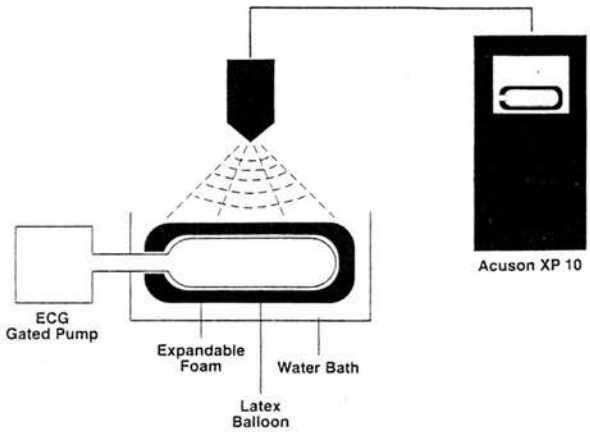

Fig. 1. Schematic of the phantom study.

available in two ultrasound machines, one from Acuson (Mountain View, CA, USA) and the other from Toshiba (Tustin, CA, USA). The potential role of DMI has been evaluated in a series of *in vitro* and *in vivo* studies. *In vitro* studies have confirmed the accuracy of DMI velocity encoding over the range of velocities at which normal and abnormal myocardium would be expected to move (Fleming et al. 1994b). Velocity estimation has been shown to be affected by target velocity, target material, system receive gain and pulse train size, but the inherent error is, at worst, ± 10% of the true mean velocity (Fleming et al. 1994a). The spatial resolution of both the two-dimensional DMI velocity and energy maps was shown to be 1 mm × 1 mm at best and 3 mm × 3 mm at worst (Fleming et al. 1994a; Sutherland et al. 1994). Early *in vivo* studies have assessed the normal range of age-related myocardial velocities and myocardial velocity gradients in healthy hearts (Palka et al. 1995, 1996). A series of initial clinical studies was performed in patients with dilated cardiomyopathies, hypertrophic cardiomyopathies and concentric left ventricular hypertrophy. These studies determined a range of abnormalities in intramural velocities that could not be predicted from standard B-mode grey-scale (GSI) images (Lange et al. 1995; Miyatake et al. 1995; Uematsu et al. 1995). However promising the potential role of DMI technique is in quantifying left ventricular function, the accuracy of endocardial boundary detection by this technique has not been validated. Theoretically, DMI should offer a more robust approach to endocardial boundary detection, as the returning ultrasound signal from the interrogated structures is less dependent on the attenuation caused by overlying tissues and is mainly based on detecting tissue by measurement of the signal frequency shift and rejecting blood pool information. In this study, a series of *in vitro* and *in vivo* studies was performed to compare boundary detection by standard GSI vs. DMI in volume measurements. *In vitro*, DMI volume measurements were validated against a one-chamber-contracting tissue-mimicking test object. *In vivo*, as GSI echocardiography is a clinically accepted tool for quantification of left ventricular volume and function [sensitivity in the assessment of end-diastolic volume (EDV) is 84%, end-systolic volume (ESV) 86%, ejection fraction (EF) 93% (Erbel et al. 1985)], the GSI measurements were compared with DMI volume measurements. As the Doppler technique is not directly affected by the amplitude of the returning signal from the interrogated tissue and the attenuating effect of the chest wall, it should, in theory, provide very accurate boundary definition.

METHODS

To validate volume measurements by transthoracic two-dimensional DMI vs. standard GSI, a series of *in vitro* and *in vivo* studies was performed. In vitro and *in vivo* ultrasound images were obtained using an ultrasound scanner (Acuson XP 10) with DMI software and 2.5-MHz phased array probe. The scanner modifications that allowed for DMI acquisition have been previously described (Palka et al. 1995). Velocity range settings were used to encode myocardial velocities (0–24 cm/s), which are lower than those typically used for blood flow. The display of the Doppler information was enabled for tissue instead of blood, the distinction being made on overall signal strength. Image persistence was turned off to eliminate blurring of the moving myocardium. To analyse pure DMI information, the underlying GSI image was turned off. Doppler receive gain was set to achieve maximum colour Doppler information in the myocardium while limiting any colour information within the blood pool. As shown by Fleming et al. (1994a), the incident angle of the ultrasonic beam does not affect imaging of left ventricular structure, as even very low myocardial velocities of approximate values around 0 m/s are also colour-coded by DMI as a mosaic of red and blue colours. For GSI studies, gain was adjusted to optimise

Table 1. Clinical characteristics of the 40 volunteers.

	Number
Healthy volunteers	9
Ischaemic heart disease	19
Dilated cardiomyopathy	3
Moderate or several mitral regurgitation	2
Moderate or severe mitral stenosis	1
Moderate or severe aortic regurgitation	2
Moderate or severe aortic stenosis	4

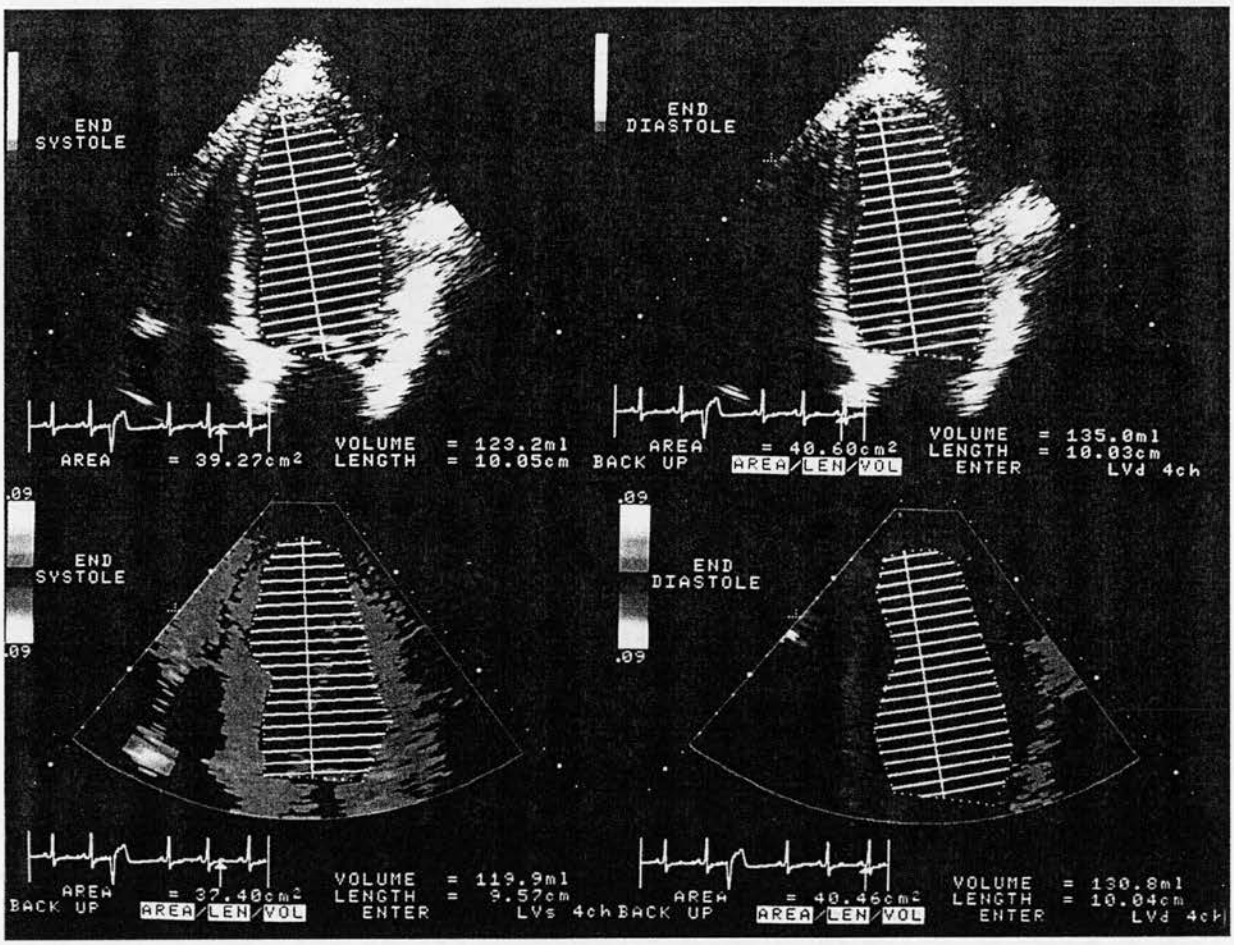

Fig. 2. Four-chamber view obtained from a 55-year-old volunteer using standard GSI (top) and DMI (bottom) techniques. The GSI image was assessed to be of moderate quality and the DMI image of good quality.

the clarity of the endocardial and epicardial boundaries.

In vitro *studies*

The validation of volume measurements was carried out using a tissue-mimicking test object. A one-chamber-contracting phantom of known volumes was placed in a water bath and scanned using both GSI and DMI techniques (Fig. 1). The minimum and maximum volumes of the phantom were calculated using the modified Simpson's method. The mean of three measurements was calculated for all images. To validate the reproducibility of volume measurements, the *in vitro* study was repeated ten times for both GSI and DMI.

In vivo *studies*

To evaluate the accuracy and effectiveness of left ventricular measurements and the derived index of left ventricular function (EF) using GSI vs. DMI techniques, 40 randomly selected volunteers (mean age 36 ± 16 y; mean heart rate 74 ± 14 beats/min, all in sinus rhythm) with either normal or abnormal cardiac function were studied. Table 1 presents the clinical characteristics of the study group of 40 volunteers (30 men and 10 women). Prior to entry into the study,

Table 2. Left ventricular volumes indices and ejection fraction average from all 40 volunteers.

	EDV (mL/M²)	ESV (mL/M²)	EF (%)
GSI	66 ± 19	36 ± 17	46 ± 10
DMI	66 ± 19	36 ± 16	46 ± 10

DMI = Doppler myocardial imaging; EDV = end-diastolic volume; EF = ejection fraction; ESV = end-systolic volume; GSI = grey-scale imaging.

Data are expressed as mean ± SD. The difference between GSI and DMI measurements were not significant (ANOVA test).

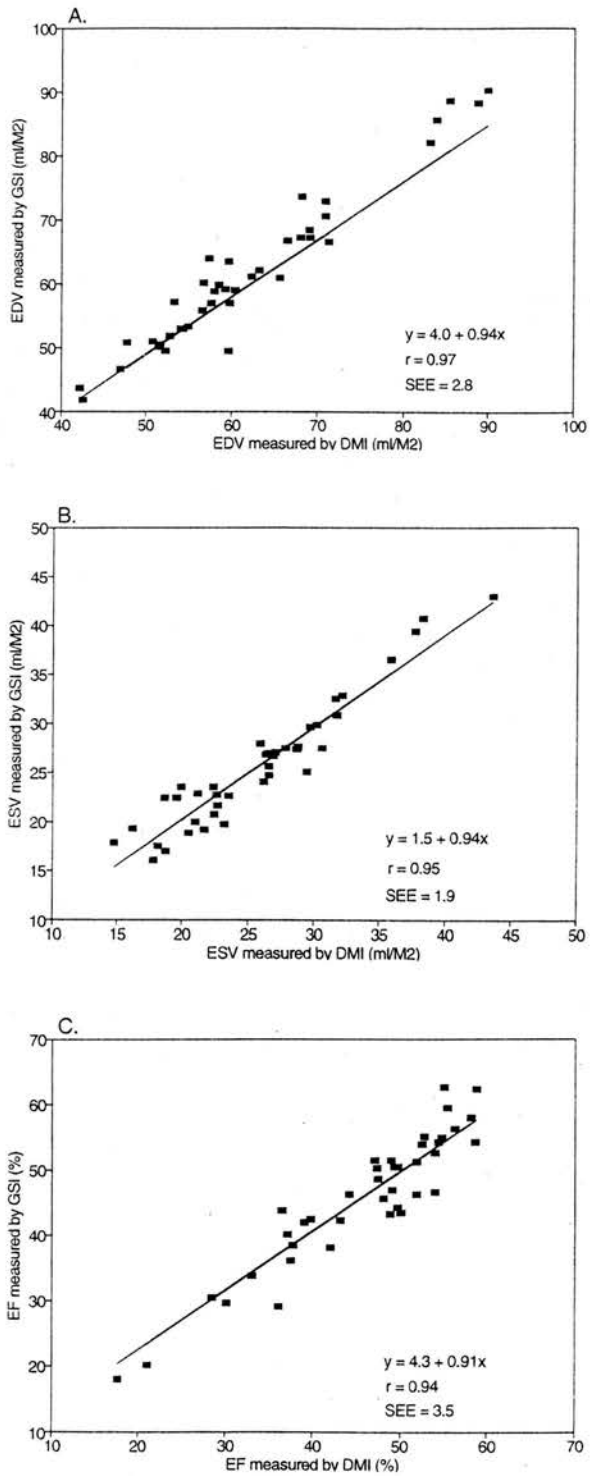

Fig. 3. Assessment of the limits of agreement and a linear correlation between DMI and GSI imaging techniques in left ventricular volume and ejection fraction measurements. (A) End-diastolic volume (EDV); (B) End-systolic volume (ESV); (C) Ejection fraction (EF). DMI = Doppler myocardial imaging; GSI = grey-scale imaging.

informed consent was obtained from all volunteers. Standard GSI and DMI images of the left ventricle were obtained using an apical transducer position to record apical four- and two-chamber views. All the volunteers were scanned while lying in the left lateral position.

From all GSI and DMI images, left ventricular EDV and ESV indices and EF were calculated by two observers using the modified biplane Simpson's method (Fig. 2). The mean of three measurements was calculated for all images. EDV was determined as the frame corresponding to the peak of the R wave of the electrocardiogram, and ESV was defined as the frame corresponding to the smallest left ventricular silhouette. The volumes (in mL) were normalised for body surface area (ml/M^2). Body surface area was calculated from standard tables using the patient's height and weight.

All data were recorded and stored on video tape.

Statistical analysis

The data are expressed as a mean value and a standard deviation (mean ± SD). To assess the level of agreement between the two methods and to test the reproducibility of each of the methods, the test of Bland and Altman (1986) was used. The 95% limits of agreement were calculated as twice the SD. The *in vitro* study assessed the accuracy of minimum and maximum volume measurements by both GSI and DMI techniques vs. true phantom volume during its minimum and maximum contraction. The *in vivo* study was used to define the agreement between GSI and DMI volume measurements. The differences between GSI and DMI measurements were assessed using one-way analysis of variance with subgroup analysis by Fisher's test. The endocardial boundary definition was compared between GSI and DMI images using McNemar's test for marginal homogeneity, which expresses percentage of the clearly defined endocardial

Table 3. Grey-scale and Doppler myocardial images quality obtained from four- and two-chamber views.

		GSI		
Number of subjects		Poor	Moderate	Good
Four-chamber view				
	Poor	0	0	0
DMI	Moderate	2	0	2
	Good	0	17	19
Two-chamber view				
	Poor	2	1	0
DMI	Moderate	11	9	3
	Good	0	8	6

DMI = Doppler tissue imaging; GSI = grey-scale imaging.

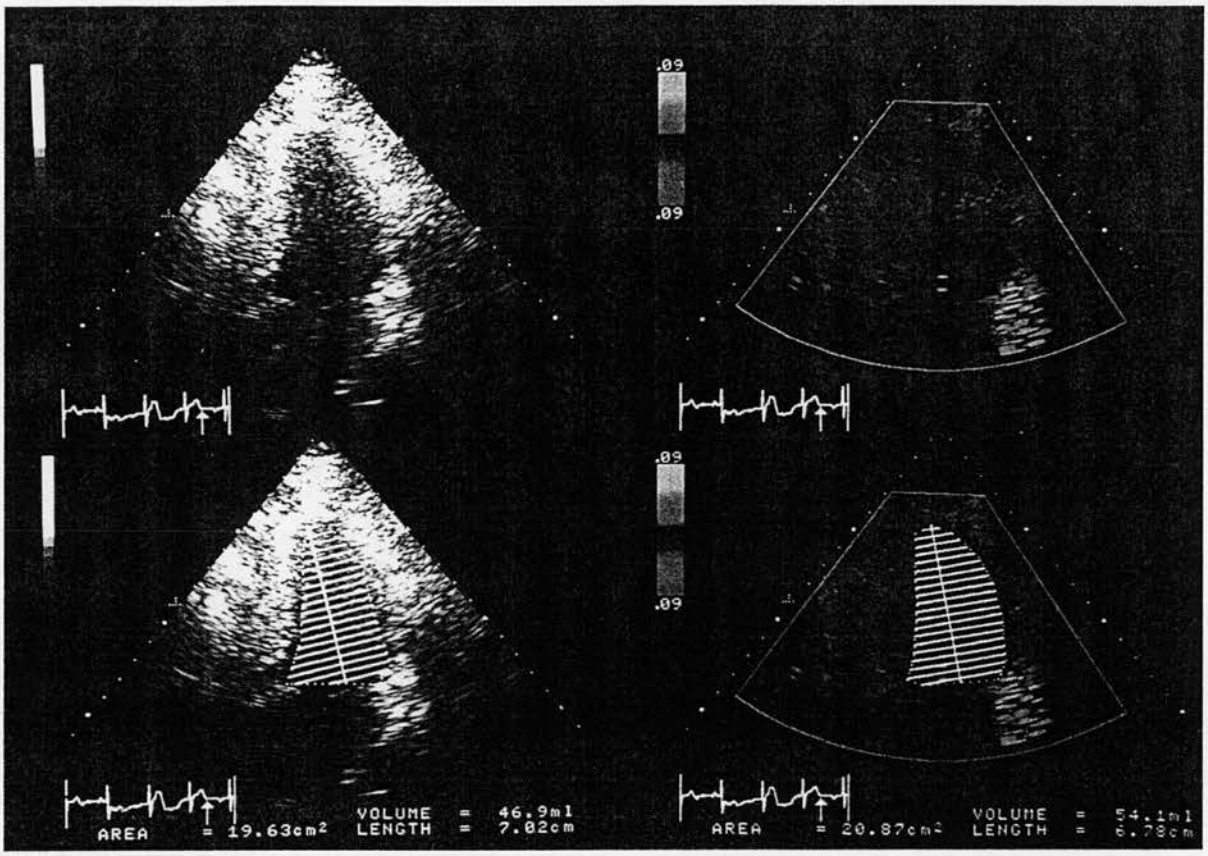

Fig. 4. Two-chamber view obtained from a 48-year-old volunteer using GSI (left) and DMI (right) techniques. The GSI image was assessed to be of poor quality and the DMI image of good quality.

boundary to the circumference of the inner dimension for each measured image of the ventricle (Bishop et al. 1975). $p < 0.05$ was considered significant.

RESULTS

In vitro *studies*

The limits of agreement between the known volume of the phantom and the derived volume measurements were calculated for both techniques at minimum and maximum volumes.

For GSI, the mean value of the minimum volume was 76 ± 2 mL and the limits of agreement 4%; the maximum volume was 140 ± 2 mL and the limits of agreement 3%. For DMI, the mean value of the minimum volume was 75 ± 4 mL and the limits of agreement 3%; the mean maximum volume was 139 ± 2 mL and the limits of agreement 2%.

In vivo *studies*

The average left ventricular volume measurements and EF from all volunteers using GSI and DMI are presented in Table 2.

The mean difference between the two methods was low: 0.1 ± 2.9 mL/M^2 for EDV, 0.05 ± 1.9 mL/M^2 for ESV and 0.01 ± 3.6% for EF. The limits of agreement between GSI and DMI techniques were 6 mL (9%) for ED and 4 mL (11%) for ES (Fig. 3).

The quality of images obtained for left ventricular volume measurements as assessed independently by two observers measured on a scale of 1–3 (where 1 was good, 2 was moderate and 3 was poor image quality) are presented in Table 3. In the four-chamber view, images of good quality were obtained from 21 volunteers using GSI and from 36 volunteers using DMI.

Using the two-chamber view, good quality images were obtained from nine volunteers using GSI and in 14 using DMI (Fig. 4). The assessment of the association between image quality by DMI and GSI scored using a subjective scale showed that, for both apical views, image quality was significantly ($p < 0.01$) better when using DMI (Table 3).

Finally, off-line comparison of the completeness of endocardial boundary detection by both techniques was performed (Bishop et al. 1975).

Table 4. The differences between two observers in left ventricular volumes indices measurement using standard grey-scale images and Doppler myocardial imaging.

Technique	LV volume index	Difference (mL/M^2) mean ± SD	r value	SEE (mL/M^2)
GSI	EDV	0.4 ± 4.2	0.94	4.3
GSI	ESV	0.2 ± 2.7	0.91	2.8
DMI	EDV	0.2 ± 2.7	0.97	2.6
DMI	ESV	0.3 ± 1.9	0.95	2.0

DMI = Doppler tissue imaging; EDV = diastolic volume; ESV = end-systolic volume; GSI = grey-scale imaging; LV = left ventricle; SEE = standard error.

Tracing of endocardial boundaries was performed off-line in each analysed B-mode GSI and DMI image. In GSI, the endocardial boundary was defined as the speckle line near the myocardial borders. The lines often were not continuous: in some instances, they faded and then completely disappeared. In such cases, the trace was terminated. However, when another speckle line was present at a slightly different depth that appeared to be the continuation of the first line, then the trace was continued from the first to the second line across the region of drop-out. In DMI, the endocardial boundary was defined as the line of interface between the myocardial wall and the blood pool. McNemar's test then was used to assess, for both techniques separately, the percentage (X%) of the clearly defined endocardial boundary in analysed two-dimensional cross-section to the circumference of its inner dimension (100%).

DMI proved to be significantly more efficient than standard GSI imaging technique at ED (85 ± 8% vs. 72 ± 16%, respectively; $p < 0.05$) and ES (88 ± 7% vs. 71 ± 13% respectively; $p < 0.05$).

Interobserver variability

Table 4 presents the differences in left ventricular volume measurements between two observers using both GSI and DMI. The differences were low for both techniques.

DISCUSSION

An ultrasonic imaging technique that quantifies regional and global heart function has been an objective of research in two-dimensional echocardiography for more than a decade (Conetta et al. 1985; Geiser et al. 1988; Skorton et al. 1981). Most approaches explored have used off-line computer-assisted analysis of GSI images (Geiser et al. 1990a, 1990b). An on-line technique based on colour-encoded tissue backscatter (color kinesis) has been developed recently to analyse regional wall-motion abnormalities in real time (Schwartz et al. 1966; Tardiff et al. 1994). In clinical practice, conventional GSI echocardiography is used as a standard technique for measuring cardiac chamber dimensions and quantifying left ventricular function (Schiller et al. 1989). Despite its potential, the information on myocardial function is derived indirectly from either parameters measured from endo- and epicardial specular reflections or blood pool Doppler indices. Additionally, the transthoracic GSI image quality is frequently reduced due to the significant attenuation of the ultrasound signal by chest wall structures. DMI has the potential to measure directly indices of myocardial function derived from the myocardial wall itself. Also, since the information for Doppler techniques is contained in the frequency of the transmitted ultrasound rather than the amplitude, it is not strongly affected by the ultrasonic properties of the tissue between the transducer and the myocardial site being studied; thus, it is possible to obtain diagnostic quality DMI images with clear endocardial boundary definition from patients who would be considered poorly echogenic (Palka et al. 1995; Schlief et al. 1993). Therefore, DMI holds promise as a powerful new technique for quantification of left ventricular function and left ventricular endocardial border detection.

In this article, we confirmed the accuracy of the DMI technique for endocardial border detection and compared its merits to standard GSI. Two-dimensional volume reconstruction both *in vitro* and *in vivo* gave essentially the same results using the two techniques. However, the results of the study provide good evidence that, in the clinical situation, endocardial contours could be derived more easily in DMI images. In addition, McNemar's test for marginal homogeneity demonstrated that DMI provided a more complete continuous endocardial boundary when compared to GSI. This accuracy of boundary detection has been assessed in a very simple and indirect way. However, to the best of our knowledge, this is the first report describing the accuracy of DMI volume measurements and the recognition of endocardial borders. In the future, it

would be interesting to compare this technique with other accepted clinical techniques for left ventricular volume measurement *i.e.*, biplane cineventriculography or three-dimensional echocardiography.

Acknowledgements—This work was supported by a grant from the Scottish Office Home and Health Department (Number K/MRS/50/C2357). The authors would like to thank Mr. Bill Adams from the Department of Public Health Sciences, University of Edinburgh, for his advice and support with the statistical analysis. Dr. A. Lange is a Chest Heart and Stroke Association Research Fellow.

REFERENCES

Bishop YMM, Fienberg SE, Holland PW. Discrete multivariate analysis: Theory and practice. In: Analysis of square tables: Symmetry and marginal homogeneity. Cambridge and London: The MIT Press, 1975:281–310.

Bland JM, Altman DG. Statistical methods for assessing agreement between two methods of clinical measurement. Lancet 1986;i:307–310.

Conetta DA, Geiser EA, Oliver LH, Miller AB, Conti CR. Reproducibility of left ventricular area and volume measurements using a computer endocardial edge-detection algorithm in normal subjects. Am J Cardiol 1985;56:947–952.

Erbel R, Schweizer P, Meyer J, Krebs W, Yalkinoglu O, Effert S. Sensitivity of cross-sectional echocardiography in detection of impaired global and regional left ventricular function: Prospective study. Int J Cardiol 1985;7:375–389.

Fleming AD, McDicken WN, Sutherland GR, Hoskins PR. Assessment of colour Doppler tissue imaging using test-phantoms. Ultrasound Med Biol 1994a;20:937–957.

Fleming AD, Xia X, McDicken WN, Sutherland GR, Fenn LN. Myocardial velocity gradient detected by Doppler imaging. Br J Radiol 1994b;67:679–688.

Geiser EA, Oliver LH, Gardin JM. Clinical validation of an edge detection algorithm for two-dimensional echocardiographic short axis images. J Am Soc Echocardiogr 1988;1:410–421.

Geiser EA, Conetta DA, Limacher MC, Ostlund Stockton V, Oliver LH, Jones B. A second generation computer-based edge detection algorithm for short axis, two-dimensional echocardiographic images: Accuracy and improvement in interobserver variability. J Am Soc Echocardiogr 1990a;3:79–90.

Geiser EA, Wilson DC, Gibby GL. Applications of cross correlation techniques to the quantitation of wall motion in short axis two-dimensional echocardiographic images. J Am Soc Echocardiogr 1990b;3:266–275.

Lange A, Palka P, Sutherland GR, et al. Doppler myocardial imaging assessment of systolic and diastolic transmural velocity gradients in dilated cardiomyopathy: A new diagnostic index (abstract). Eur Heart J 1995;16(Suppl):298.

McDicken WN, Sutherland GR, Moran CM, Gordon L. Colour Doppler velocity imaging of the myocardium. Ultrasound Med Biol 1992;18:651–654.

Miyatake K, Yamagishi M, Tanaka N, et al. New method for evaluating left ventricular wall motion by color-coded tissue Doppler imaging: *In vitro* and *in vivo* studies. J Am Coll Cardiol 1995;25:717–724.

Palka P, Lange A, Fleming AD, Sutherland GR, Fenn LN, McDicken WN. Doppler tissue imaging: Myocardial wall motion velocities in normal subjects. J Am Soc Echocardiogr 1995;8:659–668.

Palka P, Lange A, Fleming AD, et al. Age-related transmural peak mean velocities and peak velocity gradients by Doppler myocardial imaging in normal subjects. Eur Heart J 1996;17:940–950.

Schiller NB, Shah PM, Crawford M, et al. Recommendation for quantitation of the left ventricle by two-dimensional echocardiography. J Am Soc Echocardiogr 1989;2:358–367.

Schlief R, Schurmann R, Balzer T, et al. Diagnostic value of contrast enhancement in vascular Doppler ultrasound. In: Nanda NC, Schlief R, eds. Advances in echo imaging using contrast enhancement. Norwell, MA: Kluwer Academic Publishers, 1993:309–323.

Schwartz SL, Cao QL, Vannan MA, Pandian NG. Automatic backscatter analysis of regional left ventricular left ventricular systolic function using color kinesis. Am J Cardiol 1996;77:1345–1350.

Skorton DJ, McNary CA, Child JS, Newton FC, Shah PM. Digital image processing of two-dimensional echocardiography: Identification of the endocardium. Am J Cardiol 1981;48:479–486.

Sutherland GR, Stewart MJ, Groundstroem KWE, et al. Color Doppler myocardial imaging: A new technique for assessment of myocardial function. J Am Soc Echocardiogr 1994;7:441–458.

Tardiff JC, Cao QL, Pandian NG, Esakof DD, Pollard H. Determination of cardiac output using acustic quantification in critically ill patients. Am J Cardiol 1994;74:810–813.

Uematsu M, Miyatake K, Tanaka N, et al. Myocardial velocity gradient as a new indicator of regional left ventricular contraction: Detection by two-dimensional tissue Doppler imaging technique. J Am Coll Cardiol 1995;26:217–223.

Heart 1997;78:382–389

Assessment of atrial septal defect morphology by transthoracic three dimensional echocardiography using standard grey scale and Doppler myocardial imaging techniques: comparison with magnetic resonance imaging and intraoperative findings

Aleksandra Lange, Mohammed Walayat, Colin M Turnbull, Przemyslaw Palka, Pankaj Mankad, George R Sutherland, Michael J Godman

Abstract

***Objective*—To determine whether transthoracic three dimensional echocardiography is an accurate non-invasive technique for defining the morphology of atrial septal defects (ASD).**

***Methods*—In 34 patients with secundum ASD, mean (SD) age 20 (17) years (14 male, 20 female), the measurements obtained from three dimensional echocardiography were compared to those obtained from magnetic resonance imaging (MRI) or surgery. Three dimensional images were constructed to simulate the ASD view as seen by a surgeon. Measured variables were: maximum and minimum vertical and horizontal ASD dimension, and distances to inferior and superior vena cava, coronary sinus, and tricuspid valve. In each patient two ultrasound techniques were used to acquire three dimensional data: standard grey scale imaging (GSI) and Doppler myocardial imaging (DMI).**

***Results*—Good correlation was found in maximum ASD dimension (both horizontal and vertical) between three dimensional echocardiography and both MRI (GSI r = 0.96, SEE = 0.05 cm; DMI r = 0.97, SEE = 0.04 cm) and surgery (GSI r = 0.92, SEE = 0.06 cm; DMI r = 0.95, SEE = 0.06 cm). The systematic error was similar for both three dimensional techniques when compared to both MRI (GSI = 0.40 cm (27%); DMI = 0.38 cm (25%)) and surgery (GSI = 0.50 cm (29%); DMI = 0.37 cm (22%)). A significant difference was found in both horizontal and vertical ASD dimension changes during the cardiac cycle. This change was inversely correlated with age. These findings were consistent for both DMI and GSI technique. In children (age ≤ 17 years), the feasibility of detecting structures and undertaking measurements was similar for both echo techniques. However, in adult ASD patients (age ≥ 18 years) this feasibility was higher for DMI than for GSI.**

***Conclusions*—Transthoracic three dimensional imaging using both GSI and DMI accurately displayed the varying morphology, dimensions, and spatial relations of ASD. However, DMI was a more effective technique than GSI in describing ASD morphology in adults.**

(*Heart* 1997;78:382–389)

Keywords: atrial septal defect; morphology; three dimensional echocardiography; magnetic resonance imaging

Department of Cardiology, Western General Hospital, Edinburgh, UK
A Lange
P Palka
G R Sutherland

Department of Cardiology, Royal Hospital for Sick Children, University of Edinburgh, Edinburgh, UK
M Walayat
P Mankad
M J Godman

Department of Radiology, Western General Hospital, Edinburgh, UK
C M Turnbull

Correspondence to:
Dr Lange, Department of Cardiology, Western General Hospital, Crewe Road, Edinburgh EH4 2XU, UK.

Accepted for publication 17 June 1997

Secundum atrial septal defect (ASD) accounts for between 7% and 10% of all congenital heart disease and for between 30% and 40% of congenital heart diseases seen in adults.[1] Each year approximately 300 to 400 patients in the United Kingdom undergo surgical closure of an ASD using standard sternotomy.[2] The development of new techniques of ASD closure including minimal access surgery[3 4] and percutaneous catheter closure[5–8] has increased the need for accurate assessment not only of ASD size but also ASD morphology and its spatial relations.[7 9 10] Currently, several techniques are used to image or size ASDs: echocardiography,[11–14] magnetic resonance imaging (MRI),[15 16] or balloon sizing during heart catheterisation. Cross sectional echocardiography is probably the most commonly used imaging technique and with standard precordial imaging the sensitivity in detecting secundum and primum ASDs is more than 90%.[14 17] However, anatomically the atrial septum is a concave convex structure and therefore an ultrasound beam can cut the defect in different planes and may not reflect its true size. A potentially superior role for three dimensional echocardiography in ASD sizing was claimed recently in a comparative investigation of guided three dimensional studies and conventional cross sectional examinations.[18]

Previous studies on three dimensional ASD reconstruction have been carried out using standard grey scale images.[10 19 20] In these reports, because of poor transthoracic image quality grey scale images were often acquired from a transoesophageal approach. In this study, therefore, we looked not only at the potential of transthoracic three dimensional grey scale image reconstruction but at the additional value of three dimensional reconstruction using the Doppler myocardial imaging technique. Doppler myocardial imaging is based on a colour Doppler principle in which

special algorithms are applied to detect myocardial wall motion instead of intracardiac blood flow.[21] As the quality of cross sectional Doppler myocardial imaging is not directly affected by the chest wall attenuation, as it is in grey scale images, it should provide better quality images than the standard grey scale for transthoracic three dimensional echocardiography.

Methods

A prospective study of the transthoracic three dimensional echocardiographic definition of ASD morphology and its dynamic changes during the cardiac cycle was performed. Two different imaging techniques, grey scale imaging and Doppler myocardial imaging, were used to acquire three dimensional datasets from each patient. The information obtained from three dimensional Doppler myocardial imaging and grey scale images was compared with that obtained by phase contrast cine magnetic resonance imaging or surgery.

PATIENT SELECTION

Forty seven consecutive patients with a known or suspected ASD underwent cross sectional and three dimensional echocardiographic examination to determine the defect size and location. In five patients, the interatrial septum appeared to be intact on both magnetic resonance imaging and ultrasound. In seven patients no correlative measurements of the defect could be obtained because neither magnetic resonance imaging nor surgery was performed. In one patient the surgery was done elsewhere and the correlative measurements were unavailable. Therefore 34 patients, mean (SD) age 20 (17) years, with secundum ASD were suitable for study. In 18 patients, aged 23 (18) years, three dimensional grey scale images and Doppler myocardial imaging measurements were correlated with phase contrast cine magnetic resonance imaging, and in the remaining 16 patients, aged 10 (7) years, the three dimensional measurements were correlated with these taken during surgical ASD repair. The three dimensional echocardiogram and magnetic resonance imaging scans were performed on the same day in 16 patients, and in two patients there was a four day interval between the three dimensional echocardiogram and magnetic resonance imaging scan. The average time between three dimensional echocardiogram and surgery was 30 (25) days. All but two patients were in sinus rhythm. These two patients were excluded from the analysis of changes in ASD size during the cardiac cycle. All patients were informed about the purpose of the study and gave informed consent to be enrolled in the study.

THREE DIMENSIONAL ECHOCARDIOGRAPHY

The instrumentation used for the three dimensional imaging protocol consisted of an ultrasound scanner (Acuson XP10 Mountain View, California, USA) with implemented Doppler myocardial imaging software and a three dimensional acquisition system (TomTec Echo-Scan, TomTec Imaging Systems, Munich, Germany). We have described the scanner modifications which enable Doppler myocardial imaging to be acquired.[21] Figure 1 shows schematically how the three dimensional

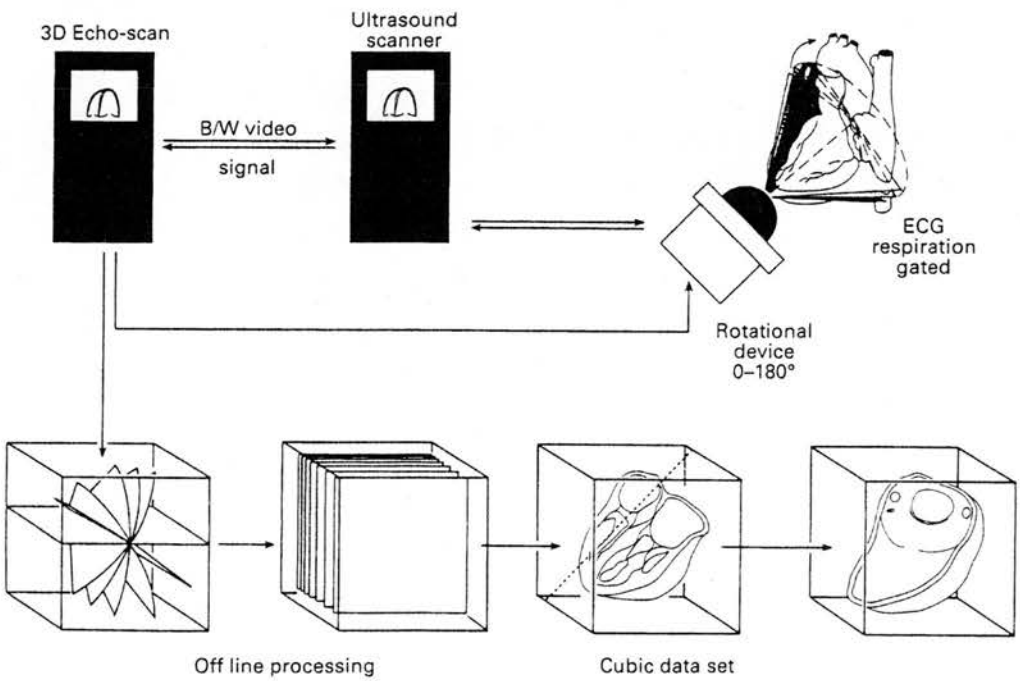

Figure 1 Steps taken to acquire three dimensional dataset. Diagram shows an ECG and respiration gated acquisition of two dimensional cross sections obtained from the apical window by rotating the transducer by the mechanical device at 2° steps over 180°. Once the acquisition was completed, off-line processing based on the interpolation of the missing information between the acquired two dimensional images at 2° steps and conversion of the images from polar to Cartesian coordinates was carried out.

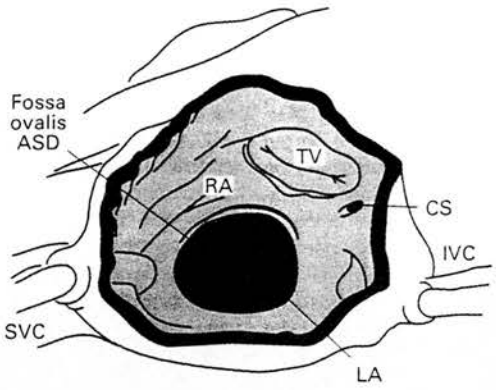

Figure 2 The schematic presentation of the atrial septal defect (ASD) as seen by the surgeon. CS, coronary sinus; IVC, inferior vena cava; LA, left atrium; RA, right atrium; SVC, superior vena cava; TV, tricuspid valve.

images were acquired. The three dimensional acquisition system consisted of a 486, 66 MHz computer with 64 megabytes of storage system memory, and steering logic for image acquisition, processing, and presentation. The ultrasound images were obtained using a 2.5–4.0 MHz phased array transducer steered by the transducer mechanical rotational device supplied with the Echo-Scan. In each patient the appropriate transducer frequency was selected to obtain the best quality cross sectional grey scale images. Each Doppler myocardial imaging dataset was acquired using a transducer frequency of 2.5 MHz. During the acquisition, the Echo-Scan was connected to the ultrasound video output of the Acuson scanner by a black/white video cable. Thus when Doppler myocardial images were acquired, the colour Doppler signal was transferred as a black and white video signal to the Echo-Scan. During the acquisition electrocardiographic and respiration gating was used. A standard three lead electrocardiogram cable was used to monitor the electrocardiogram while the patient's respiration was monitored by measuring skin impedance. Using this information the system created an on-line histogram based on the patient's heart rate and respiration. This enabled the setting of a gating window based on the RR intervals of the electrocardiogram. The expiratory phase was used for gating respiration. During the acquisition procedure, the transducer was placed in the standard apical position and was rotated by the mechanical rotational device at 2° steps over 180°. Based on the gating parameters, the computer acquired one complete cardiac cycle at the acquisition start position and recorded it at 25 frames per second. When one cardiac cycle had been stored in the computer's RAM, the steering control advanced the transducer by one step. A total of 90 cardiac cycles was stored during one acquisition. The same acquisition protocol was used for the acquisition of grey scale images and Doppler images. In each patient the acquisition started with grey scale image data and then Doppler imaging data were collected. The acquisition time was approximately three minutes for both grey scale and Doppler imaging. As the patient needs to be immobile during the image acquisition, seven patients (age between two and three and a half years) required mild sedation using Triclofos Elixir BP (triclofos sodium).

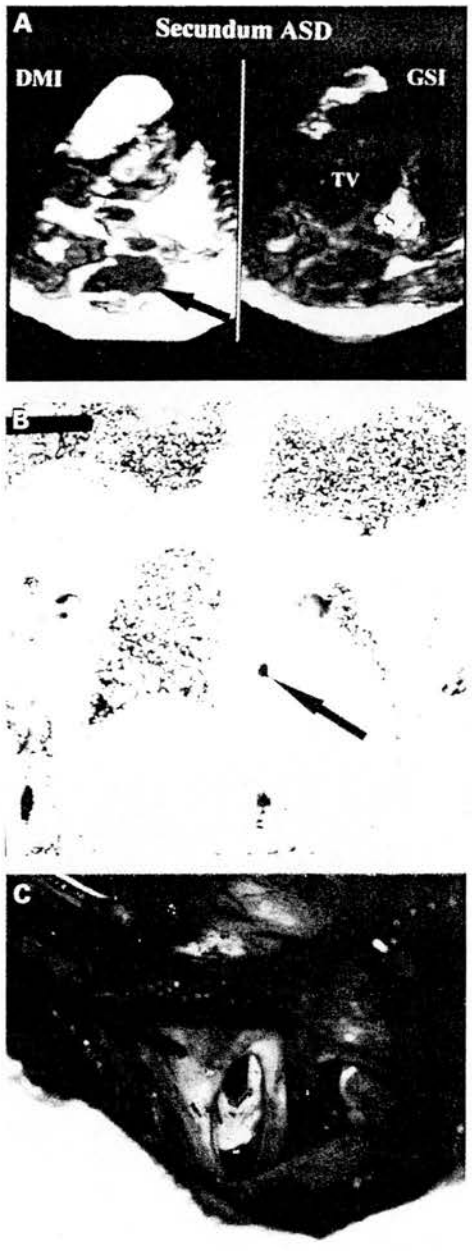

Figure 3 Maximum orifice of an atrial septal defect (ASD) as defined by three dimensional echocardiography (A), phase contrast cine magnetic resonance imaging (B), and surgery (C). CS, coronary sinus; DMI, Doppler myocardial imaging; GSI, grey scale imaging; IVC, inferior vena cava; SVC, superior vena cava; TV, tricuspid valve.

After acquisition, the data were stored on the system hard drive and then analysed off-line. In each patient, three dimensional reconstruction of the ASD was carried out from the right atrium. First, an apical four chamber view was reconstructed. Second, the acquired dataset was cut vertically by a longitudinal plane through the right atrial free wall, tricuspid valve, and anterior right ventricular free wall. Finally, the reconstruction was orientated anterior to posterior. These manoeuvres provided us with an en face view of the ASD from which the following variables were measured: minimum and maximum of horizontal and

vertical ASD dimensions during the cardiac cycle, distances to: coronary sinus, inferior vena cava, superior vena cava, and tricuspid valve during late left ventricular systole (maximum ASD dimension) (fig 2).

Although the Doppler information is angle dependent, the angle of insonation needs to be taken into account when measuring myocardial velocities only.[22] In previously reported cases where Doppler myocardial imaging was used as an acquisition technique to visualise cardiac structures, the incident angle of the ultrasonic beam did not affect the completeness of the image. This is because even very low myocardial velocities with approximate values of around 0 to 0.2 m/s are also colour coded by Doppler myocardial imaging as a mosaic of red and blue colour.[23 24]

Out of the 34 defects which were reconstructed using both grey scale and Doppler images, 30 were single secundum defects and four were multiple (from two to four defects).

From all three dimensional ASD reconstructions, the feasibility of detecting right atrial structures and undertaking measurements was assessed for both Doppler myocardial imaging and grey scale imaging.

MAGNETIC RESONANCE IMAGING

The magnetic resonance imaging studies were performed on a 1.5 T Siemens Magneton SP system. Fast acquisition "Turboflash" localiser images (repetition time (TR) 4.9 ms, time to echo (TE) 2 ms, flip angle (FA) 8°) were obtained in the coronal and transverse planes through the ventricles, followed by a single angulated plane through the ventricles, and then by a single angulated plane through the interventricular and interatrial septa to give a right anterior oblique (RAO) two chamber plane localiser. Multiple contiguous, 6 mm slice width, 16 cardiac phases, gated cine gradient echo images (TR 560 ms, TE 6 ms, FA 30°) were then obtained perpendicular to the interatrial septum in the four chamber projection, using the angulated RAO two chamber localiser.

Gated, velocity encoded, phase contrast imaging with a maximum velocity sensitivity of 120 cm/s was then performed using four chamber cine image with the imaging plane proscribed to lie parallel to, and contiguous with, the right atrial side of the interatrial septum, to provide an en face view of the defect. The maximum dimensions of the defects were measured from the images on an independent operating console using electronic calipers.

SURGICAL DATA

All operations were performed by one surgeon. The surgery was performed either through a midline sternotomy or through a right thoracotomy, with induced ventricular fibrillation. The aorta was not cross clamped and thus the heart was not arrested in diastole using cardioplegic solution in any of the patients. Once the heart was fibrillated and the right atrium opened, a pump sucker was left in the coronary sinus and intermittent suction was performed through the ASD into the left atrium to achieve a bloodless field. The various measurements, as described above, were taken by the single observer using a string of black silk suture material which was cut at an appropriate measured point from the margin of the defect. The length of the suture was measured on a ruler and the findings were noted down by the member of the team. Two independent measurements were taken for each dimension in the first six patients. No difference was observed between the two readings and therefore in the later part of the study only one measurement was obtained in the remaining 10 patients.

STATISTICAL ANALYSIS

The data are expressed as mean (SD). A paired t test was used to compare the maximum to minimum ASD dimensional change during the cardiac cycle, as measured by three dimensional echocardiography. Least square regression analysis was performed to test the correlation

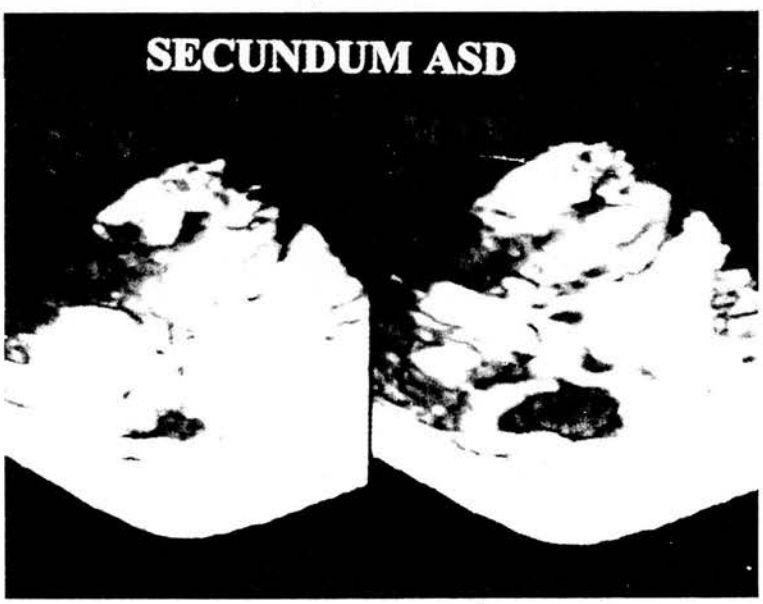

Figure 4 Changes in atrial septal defect (ASD) dimension during a cardiac cycle as seen by three dimensional Doppler myocardial imaging echocardiography.

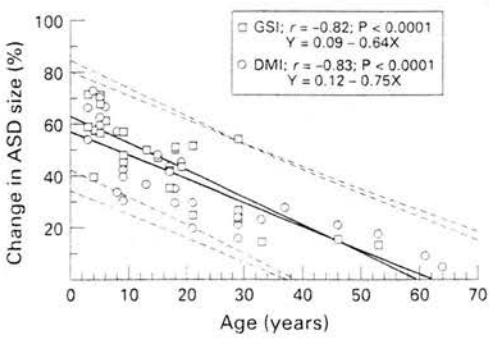

Figure 5 Linear regression analysis of the correlation between the patient's age and the dynamic changes in atrial septal defect (ASD) dimension during the cardiac cycle. The differences in ASD dimension changes were calculated as follows: [(HED - HES) + (VED - VES) / (HED + VED)] × 100%, where HED = horizontal end diastolic dimension, HES = horizontal end systolic dimension, VED = vertical end diastolic dimension, and VES = vertical end systolic dimension. Circles, Doppler myocardial imaging; squares, grey scale imaging. The dotted lines indicate the 95% predictive interval.

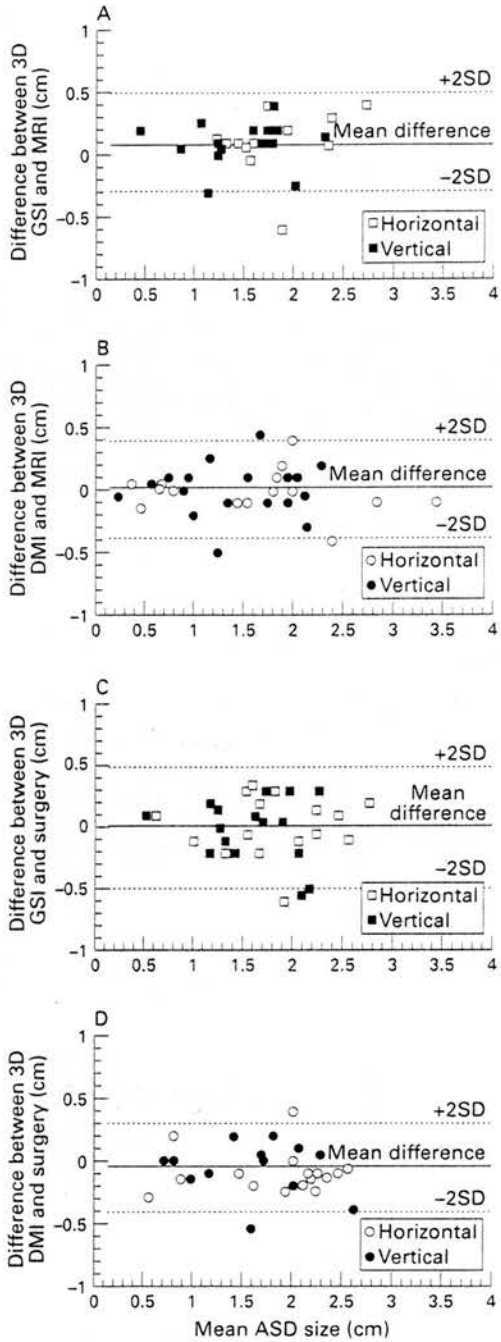

Figure 6 Bland and Altman analysis of the accuracy of atrial septal defect (ASD) dimension measurements by three dimensional echocardiography using both grey scale images and the Doppler myocardial imaging technique against phase contrast cine magnetic resonance imaging (A, B) or surgery (C, D). Empty squares, horizontal dimensions of ASDs by grey scale images; filled squares, vertical dimensions of ASDs by Doppler myocardial imaging; empty circles, horizontal dimensions of ASDs; filled circles, vertical dimensions of ASDs. The solid line shows the mean difference between the techniques used; the dotted lines show the 95% limit of agreement.

between the horizontal and vertical dimension of an ASD, and the distances from the ASD rim to inferior vena cava, superior vena cava, coronary sinus, and tricuspid valve, measured by grey scale imaging, Doppler myocardial imaging, magnetic resonance imaging, and surgery. Linear regression analysis was performed to assess the correlation between the changes in ASD size during the cardiac cycle and age. Finally, the Bland and Altman test was used to assess: (1) the bias (systematic error) between the two ultrasound techniques and magnetic resonance imaging or surgery; (2) how the studied techniques relate to each other (underestimation or overestimation); and (3) reproducibility.[25 26] Statistical analysis was performed using the statistical package UNISTAT 4 for Windows. A p value of < 0.05 was considered significant.

INTEROBSERVER AND INTRAOBSERVER VARIABILITY

In 10 randomly selected ASD patients, all the measurements acquired from three dimensional Doppler myocardial imaging and grey scale image reconstructions pertaining to the maximum and minimum (horizontal and vertical) ASD dimensions, and distances to inferior vena cava, superior vena cava, coronary sinus, and tricuspid valve were analysed by two independent observers. Additionally, in six randomly selected ASD patients, a three dimensional echocardiographic study was performed twice within an average period of 28 (4) days. Analysis of variance was used to assess the differences between the measurements of ASD morphology obtained by two observers (interobserver variability) and between measurements taken from the same subjects at different times (intraobserver variability). Both intraobserver and interobserver variability in ASD morphology are presented as the mean (SD).

The interobserver variability for three dimensional echocardiography for grey scale images was at 0.08 (0.09) cm (systematic error 16%) and for Doppler myocardial imaging, 0.07 (0.08) cm (systematic error 13%).

The intraobserver variability for grey scale images was at 0.07 (0.08) cm (systematic error 15%) and for Doppler myocardial imaging 0.06 (0.08) cm (systematic error 12%).

Results

Figure 3 shows the maximum ASD orifice as defined by three dimensional echocardiography using both techniques (Doppler myocardial imaging and grey scale images), magnetic resonance phase contrast cine imaging, and surgery.

Table 1 presents the measurements of ASD dimensions and the distances from the ASD rim to other structures of the right atrium by three dimensional echocardiography, magnetic resonance imaging, and surgery. A significant difference was found in changes of both horizontal and vertical ASD dimensions during the cardiac cycle (table 1, fig 4). The maximum dimension of ASDs was found in late ventricular systole and the minimum in late ventricular diastole. Stepwise multivariate regression analysis showed that the changes in ASD size are not dependent on the defect size but are inversely related to patient age. Figure 5 presents the linear regression analysis of the relation between the changes in ASD size and patient age.

A good correlation was obtained between maximum horizontal and vertical ASD dimensions by three dimensional echocardiography

Table 1 The measurements of atrial septal defect (ASD) dimensions and the distances from the ASD rim to other structures of the right atrium

	Dimension							
	Maximum		*Minimum*		*Distance to*			
Mean (SD) (cm)	*HD*	*VD*	*HD*	*VD*	*IVC*	*SVC*	*CS*	*TV*
GSI	1.9 (0.8)*	1.6 (0.6)*	1.2 (0.7)	0.9 (0.5)	1.4 (0.5)	1.1 (0.5)	0.9 (0.5)	2.1 (0.6)
DMI	1.8 (0.7)*	1.6 (0.6)*	1.2 (0.7)	0.9 (0.6)	1.5 (0.8)	1.0 (0.4)	1.0 (0.5)	2.3 (0.7)
MRI	1.7 (0.8)	1.4 (0.6)	N/A	N/A	N/A	N/A	N/A	N/A
Surgery	1.9 (0.6)	1.7 (0.5)	N/A	N/A	1.3 (0.6)	0.8 (0.3)	0.9 (0.4)	1.9 (0.7)
Mean	1.8 (0.8)*	1.6 (0.6)*	1.2 (0.7)	0.9 (0.5)	1.4 (0.7)	1.0 (0.4)	0.9 (0.5)	2.2 (0.6)

CS, coronary sinus; DMI, Doppler myocardial imaging; GSI, grey scale imaging; HD, horizontal dimension; IVS, inferior vena cava; MRI, magnetic resonance imaging; SVC, superior vena cava; TV, tricuspid valve; VD, vertical dimension.
*$p < 0.001$ *v* minimum.

Table 2 Correlation between the measurements obtained by three dimensional echocardiography and surgery

	GSI				*DMI*			
	r	*Coefficient*	*Standard error (cm)*	*p value*	*r*	*Coefficient*	*Standard error (cm)*	*p value*
IVC	0.84	0.82	0.19	0.0025	0.92	0.96	0.12	0.0001
SVC	0.64	0.57	0.21	0.0198	0.73	1.03	0.27	0.0023
CS	0.68	1.39	0.50	0.0223	0.96	0.98	0.08	0.0001
TV	0.82	0.75	0.15	0.0004	0.86	0.94	0.15	0.0001
Mean (SD)	0.75 (0.08)	0.88 (0.31)	0.26 (0.14)	0.0113 (0.001)	0.87 (0.09)	0.98 (0.03)	0.16 (0.07)	0.0007 (0.001)

CS, coronary sinus; DMI, Doppler myocardial imaging; GSI, grey scale imaging; IVC, inferior vena cava; SVC, superior vena cava; TV, tricuspid valve.

and magnetic resonance imaging (grey scale images: $r = 0.96$ cm, SEE = 0.05, $p < 0.001$; Doppler myocardial imaging: $r = 0.97$ cm, SEE = 0.04, $p < 0.001$) or surgery (grey scale images: $r = 0.92$ cm, SEE = 0.06, $p < 0.001$; Doppler myocardial imaging: $r = 0.95$, SEE = 0.06, $p < 0.001$). Figure 6 shows the difference in ASD size as determined by three dimensional echocardiography and magnetic resonance imaging or surgery using the Bland and Altman analysis. The systematic error (bias) between three dimensional echocardiography and magnetic resonance imaging was low at 0.40 cm (27%) for grey scale images and 0.38 cm (25%) for Doppler myocardial imaging. For surgery the systematic error was at 0.50 cm (29%) and 0.37 cm (22%) respectively. Good correlation was also obtained between the distances from the defect rim to inferior vena cava, superior vena cava, coronary sinus, and tricuspid valve in its maximum opening by three dimensional echocardiography and surgery (table 2).

In children (from three to 17 years of age; 19 patients) the feasibility of detecting structures and undertaking measurements was similar for both Doppler myocardial imaging and grey scale imaging. In adult ASD patients (from 18 to 61 years of age; 15 patients), the feasibility was better for Doppler myocardial imaging than for grey scale imaging (table 3).

Table 3 Feasibility of detecting structures and undertaking measurements from three dimensional atrial septal defect (ASD) reconstructions by grey scale imaging (GSI) and Doppler myocardial imaging (DMI)

	Group 1, mean age 8 (5) years (n=19)				*Group 2, mean age 35 (15) years (n=15)*			
	GSI		*DMI*		*GSI*		*DMI*	
	n	*%*	*n*	*%*	*n*	*%*	*n*	*%*
Maximum dimension	19	100	19	100	12	80	15	100
Minimum dimension	16	84	18	95	11	73	14	93
SVC	13	68	15	79	10	67	12	80
IVC	14	74	16	84	11	73	12	80
CS	12	63	16	84	8	53	12	80
TV	19	100	19	100	12	80	15	100
Mean (SD)	15 (3)	82 (15)	17 (2)	90 (8)	11 (1)	71 (9)	13 (1)	89 (9)

CS, coronary sinus; IVC, inferior vena cava; SVC, superior vena cava; TV, tricuspid valve.

Discussion

With the growing interest in new techniques of ASD closure, precise assessment of ASD is crucial for optimal patient selection. Cross sectional echocardiography and magnetic resonance imaging are the two most commonly used techniques to assess ASD size and morphology. The accuracy of magnetic resonance imaging is well established.[27 28] It is claimed to have a sensitivity and specificity greater than 90% in the identification of ostium secundum ASD and to be superior to standard transthoracic and transoesophageal cross sectional echocardiography for ASD sizing.[16]

During the last 15 years dynamic research has been conducted in the development of three dimensional echocardiography which may become a bedside diagnostic technique in the assessment not only of ASD size and morphology but also of spatial relations of the defect to other cardiac structures.[29-31] This seems to be particularly important in selecting patients for percutaneous ASD closure by transcatheter device placement.[12] Preliminary studies have been carried out by others showing the ability of three dimensional echocardiography to reconstruct en face the dynamic morphology of ASDs using transthoracic or transoesophageally acquired ultrasound data.[19 20 32] However, no comparison has been made to define the accuracy of these reconstructions. It was reported that the quality of transthoracic standard ultrasound images was not satisfactory in all cases and the transthoracic three dimensional en face reconstruction of ASD was feasible in 81% of a study group of children.[20]

In our study we therefore looked not only at the potential accuracy of transthoracic three dimensional grey scale image reconstruction but also at the additional value of three dimensional reconstruction using the Doppler myocardial imaging technique. We have shown that the feasibility of detecting right atrial structures and undertaking measurements by the two techniques studied was different with age. In children ($\leq$ 17 years of age) all the required anatomical structures were reconstructed in a similar percentage of patients. However, in patients over 18 years old, the feasibility of detecting anatomical structures was greater with Doppler imaging. For both age groups, superior vena cava and coronary sinus were the hardest to reconstruct by either ultrasound technique.

We have also shown that all the ASDs studied changed significantly in dimension during the cardiac cycle, with maximum size in late left ventricular systole and minimum in late left ventricular diastole. Although, this difference was present in all patients, it was inversely correlated with age. A similar finding of a significant difference in ASD area during the cardiac cycle has been reported by others.[32] This could provide new information about the natural history of secundum ASD which may be taken into account when assessing a patient for percutaneous ASD occlusion using a device placement.

The relation between measurements by three dimensional echocardiography and magnetic resonance imaging or surgery was good and within acceptable limits for clinical application. The maximum ASD dimension measured by three dimensional echocardiography correlated well with both magnetic resonance imaging and surgery. The systematic error for the group as a whole was slightly lower for Doppler imaging than for grey scale imaging when compared to both magnetic resonance imaging (25% *v* 27%, respectively) and surgery (22% *v* 29%). This was not verified for the two age subgroups (table 2) because of the relatively small sample size. Correlation of the distances from the ASD rim to inferior vena cava, superior vena cava, tricuspid valve, and coronary sinus measured by three dimensional echocardiography and surgery in late ventricular diastole was also good, and again slightly favoured Doppler myocardial imaging over grey scale imaging.

LIMITATIONS

Technical limitations

Despite growing interest and extensive research in developing real time three dimensional echocardiography, current three dimensional reconstructions are available off-line only. In this particular study time was of minor importance as the information on ASD morphology was needed as a baseline to plan the repair strategy. The average acquisition time of a single dataset is approximately two to three minutes. The time required for the off-line processing of the ultrasound data may take up to 20 minutes. Finally, the time required to reconstruct the data in three dimensions differs according to the quality of the acquired ultrasound images and may take from two minutes to 20 minutes, and sometimes in a complicated case even longer.

Using this three dimensional system, the position of the ultrasound transducer during the data acquisition is calculated according to the mechanical steering logic and not according to the transducer spatial coordinates. Therefore the three dimensional system does not record unexpected changes in the transducer position which may create a rotational artefact. In such cases any attempt at taking measurements from the reconstructed three dimensional image should be abandoned. In this study to avoid problems related to the rotational artefact, each dataset was acquired twice, thus extending the acquisition time.

Care also needs to be taken during the adjustment of image gain settings. The three dimensional system is sensitive enough to reconstruct the ultrasound noise if such is left on the image. This will result in insufficiently clear three dimensional reconstruction.

Methodological limitations

In this study the information on ASD sizing was compared to that obtained from magnetic resonance imaging or surgery. Taking measurement from magnetic resonance imaging phase contrast images, one has to make sure that the shunt flow is orthogonal to the cine imaging plane. This is because the technique depends on flow related enhancement and phase contrast effects. In most cases the shunt orifice is best seen at end systole or early diastole only. It is difficult to assess the dynamic change in ASD size during the cardiac cycle reliably. Therefore, in this study only the maximum ASD dimensions (horizontal and vertical) were measured from magnetic resonance images. One might also expect the defect size to be overestimated if measured from images acquired upstream of the orifice where the jet converges, as well as downstream where it diverges.

Surgical closure of an ASD is usually performed using a cardioplegic solution achieving diastolic arrest of the heart. This unfortunately does not reflect the in vivo situation of the beating heart. The relaxed state of the heart tends to overestimate the size of the defect and the various distances measured. In this study, we elected to perform the surgical closure in a fibrillating heart, thus maintaining the cardiac tone. The measurements taken at surgery were therefore a more accurate reflection of the in vivo situation. In order to avoid interobserver variability, all measurements at surgery were undertaken by a single surgeon. Two independent measurements were obtained initially to avoid interobserver variability. However, it soon became apparent that there was little difference in the two observations.

CONCLUSIONS

Transthoracic three dimensional grey scale images and Doppler myocardial imaging both accurately displayed the varying morphology,

dimensions, and spatial relations of ASDs. For the group as a whole there was no difference between the two ultrasound techniques in the accuracy of the reconstructed three dimensional images. However, in adult ASD patients, Doppler myocardial imaging was more effective than grey scale imaging in reconstructing a surgical view of ASDs. This study shows that a dynamic en face three dimensional image of an ASD is no longer restricted to the one seen only by a surgeon during an ASD repair, but may be reconstructed through the closed chest before closure of the defect. This should help to plan the surgical strategy or, where applicable, facilitate the selection of patients for percutaneous device closure.

This study was supported by the Chest, Heart and Stroke Association (196RR33163).

1 Dickinson DF, Arnold R, Wilkinson JL. Congenital heart disease among 160 480 liveborn children in Liverpool 1960 to 1969. Implications for surgical treatment. *Br Heart J* 1981;**46**:55–62.
2 Ward C. Secundum atrial septal defect: routine surgical treatment is not of proven benefit. *Br Heart J* 1994;71:219–23.
3 Burke RP, Michielon G, Wernovsky G. Video-assisted cardioscopy in congenital heart operations. *Ann Thorac Surg* 1994;**58**:864–8.
4 Schwartz DS, Ribakove GH, Grossi EA, Stevens JH, Siegel LC, St Goar FG, *et al.* Minimally invasive cardiopulmonary bypass with cardioplegic arrest: a closed chest technique with equivalent myocardial protection. *J Thorac Cardiovasc Surg* 1996;111:556–66.
5 Rome JJ, Keane JF, Perry SB, Spevak PJ, Lock JE. Double-umbrella closure of atrial defects. Initial clinical applications. *Circulation* 1990;**82**:751–8.
6 Das GS, Voss G, Jarvis G, Wyche K, Gunther R, Wilson RF. Experimental atrial septal defect closure with a new, transcatheter, self-centering device. *Circulation* 1993;**88**: 1754–64.
7 Boutin C, Musewe NN, Smallhorn JF, Dyck JD, Kobayashi T, Benson LN. Echocardiographic follow-up of atrial septal defect after catheter closure by double-umbrella device. *Circulation* 1993;**88**:621–7.
8 Lloyd TR, Rao S, Beekman RH, Mendelsohn AM, Sideris EB. Atrial septal defect occlusion with the buttoned device (a multinstitutional US trial). *Am J Cardiol* 1994;73:286–91.
9 Chan KC, Godman MJ. Morphological variations of fossa ovalis atrial septal defects (secundum): feasibility for transcutaneous closure with the clam-shell device. *Br Heart J* 1993;**69**:52–5.
10 Magni G, Hijazi ZM, Marx G, Das G, Delabays A, Levine J, *et al.* Utility of 3-D echocardiography in patient selection and guidance for atrial septal defect (ASD) closure by the new Das-angel wings occluder device [abstract]. *J Am Coll Cardiol* 1996;27(**suppl**):769–5.
11 Schapira JN, Martin RP, Fowles RE, Popp RL. Single and two-dimensional echocardiographic features of the interatrial septum in normal subjects and patients with an atrial septal defect. *Am J Cardiol* 1979;**43**:816–19.
12 Morimoto K, Matsuzaki M, Tohma Y, Shiro O, Tanaka N, Michishige H, *et al.* Diagnosis and quantitative evaluation of secundum-type atrial septal defect by transoesophageal Doppler echocardiography. *Am J Cardiol* 1990;**66**:85–91.
13 Hellenbrand WE, Fahey JT, McGowan FX, Weltin GG, Kleinman CS. Transesophageal echocardiographic guidance of transcatheter closure of atrial septal defect. *Am J Cardiol* 1990;**66**:207–13.
14 Mehta RH, Helmcke F, Nanda NC, Pinheiro L, Samdarshi TE, Vinod KS. Uses and limitations of transthoracic echocardiography in the assessment of atrial septal defect in the adult. *Am J Cardiol* 1991;**67**:288–94.
15 Holmvang G, Palacios IF, Vlahakes GJ, Dinsmore RE, Miller SW, Liberthson RR, *et al.* Imaging and sizing of atrial septal defects by magnetic resonance. *Circulation* 1995;**92**:3473–80.
16 Diethelm L, Dery R, Lipton MJ, Higgins CB. Atrial level shunts: sensitivity and specificity of MR diagnosis. *Radiology* 1987;**162**:181–6.
17 Reeder GS, Hagler DJ, Tajik AJ. Sensitivity of two-dimensional echocardiography in direct visualization of atrial septal defect utilizing the subcostal approach: experience with 154 patients. *J Am Coll Cardiol* 1983;2: 127–35.
18 King DL, Harrison MR, King DL, Gopal AS, Martin RP, DeMaria AN. Improved reproducibility of left atrial and left ventricular measurements by guided three-dimensional echocardiography. *J Am Coll Cardiol* 1992;**20**:1238–45.
19 Belohlavek M, Foley DA, Gerber TC, Greenleaf JF, Seward JB. Three-dimensional ultrasound imaging of the atrial septum: normal and pathologic anatomy. *J Am Coll Cardiol* 1993;**22**:1673–8.
20 Marx GR, Fulton DR, Pandian NG, Vogel M, Cao Q-L, Ludomirsky A, *et al.* Delineation of site, relative size and dynamic geometry of atrial septal defects by real-time three-dimensional echocardiography. *J Am Coll Cardiol* 1995;**25**:482–90.
21 Lange A, Wright RA, Al-Nafusi A, Sang C, Palka P, Sutherland GR. Doppler myocardial imaging: a potential better method of data acquisition for three-dimensional echocardiography. *J Am Soc Echocardiogr* 1996;**9**:918–21.
22 Fleming AD, McDicken WN, Sutherland GR, Hoskins PR. Assessment of colour Doppler tissue imaging using test-phantoms. *Ultrasound Med Biol* 1994;**20**:937–57.
23 Azevedo J, Garcia-Fernandez M, Puerta P, Moreno M, San-Roman D, Torrecilla E, *et al.* Dynamic 3-Dimensional echocardiographic reconstruction of the left ventricle using color Doppler myocardial tissue imaging technique. In vivo experimental and clinical study [abstract]. *J Am Coll Cardiol* 1996;**27(suppl A)**:901–47.
24 Lange A, Anderson T, Bouki KP, Fenn LN, Palka P, McDicken WN, *et al.* Validation of volume measurements by 3-dimensional echocardiography using Doppler myocardial imaging technique: in vitro and in vivo study [abstract]. *Circulation* 1995;**92(suppl)**:I-798.
25 Altman DG, Bland JM. Measurement in medicine: the analysis of method comparison studies. *Statistician* 1983; **32**:307–17.
26 Bland JM, Altman DG. Statistical methods for assessing agreement between two methods of clinical measurement. *Lancet* 1986;i:307–10.
27 Dinsomore RE, Wismer GL, Guyer D, Thompson R, Liu P, Stratemeier E, *et al.* Magnetic resonance imaging of the interatrial septum and atrial septal defects. *Am J Roentgenol* 1985;**145**:697–703.
28 Sakakibara M, Kobayashi S, Imai H, Watanabe S, Masuda Y, Inagaki Y. Diagnosis of atrial septal defect using magnetic resonance imaging. *J Cardiol* 1987;17:817–29.
29 Sheikh KH, Smith SW, von Ramm OT, Kisslo J. Real-time, three-dimensional echocardiography: feasibility an initial use. *Echocardiography* 1991;**8**:119–25.
30 Pandian NG, Nanda NC, Schwartz SL, Fan P, Cao Q-L, Sanyal R, *et al.* Three-dimensional and four-dimensional transesophageal echocardiographic imaging of the heart and aorta in humans using a computed tomographic imaging probe. *Echocardiography* 1992;9:677–87.
31 Roelandt JRTC, ten Cate FJ, Vletter WB, Taams MA. Ultrasonic dynamic three-dimensional visualization of the heart with a multiplane transoesophageal imaging transducer . *J Am Soc Echocardiogr* 1994;7:217–29.
32 Franke A, Rulands D, Kuhl HP, Breithardt OA, Erena C, Grabitz RG, *et al.* Changes of the atrial septal defect area during the cardiac cycle: evaluation by dynamic transoesophageal three-dimensional echo [abstract]. *Eur Heart J* 1996;17**(suppl)**:2317.

Three-dimensional echocardiographic evaluation of left ventricular volume: Comparison of Doppler myocardial imaging and standard gray-scale imaging with cineventriculography—an in vitro and in vivo study

Aleksandra Lange, MD, Przemystaw Palka, MD, Andrzej Nowicki, PhD, Robert Olszewski, MD, Thomas Anderson, MSc, Jerzy Adamus, MD, George R. Sutherland, MD, and Keith A.A. Fox, MD
Edinburgh, United Kingdom, and Warsaw, Poland

Background Standard gray-scale imaging (GSI), three-dimensional (3D) echocardiography has been shown to be superior to two-dimensional echocardiography in measuring left ventricular volume. However, the often relatively poor quality of transthoracic gray-scale data can limit the potential application of this technique. Doppler myocardial imaging (DMI) is a new ultrasound technique that potentially offers higher-quality 3D images with a transthoracic approach than the 3D GSI technique. This study was designed to compare the accuracy of standard GSI and DMI 3D left ventricular volume measurements in vitro and in vivo.

Methods and Results In vitro, the minimum and maximum volume of the contracting single-chamber, tissue-mimicking phantom was calculated by using both techniques. In vivo, GSI and DMI 3D left ventricular volume measurements were performed in 16 patients. End-diastolic and end-systolic left ventricular volumes were computed for both techniques and compared with those calculated by cineventriculography. In vitro, both methods tended to underestimate the true phantom volume, but the systematic error was smaller for DMI than for GSI (-1.2% ± 1.5% vs. -4.3% ± 3%; $p < 0.01$) and was more constant in the case of DMI over the range of different sizes of true volume. In vivo, for GSI the end-diastolic volume mean difference was -12.6 ml and the limits of agreement were ±18 ml, and for DMI the corresponding values were -4.2 and ±10.6 ml, respectively. The difference for end-systole was -6.5 ± 10.6 ml and -1.5 ± 10 ml for GSI and DMI, respectively. The magnitude of the difference in volume measurement between 3D echocardiography and cineventriculography was significantly smaller when using the Doppler technique.

Conclusions The results of this in vitro and in vivo study indicate that DMI is superior to GSI as a transthoracic acquisition technique for 3D volume computation. (Am Heart J 1998;135:970-9.)

The initial absolute measurement and subsequent monitoring of left ventricular volume is an important clinical parameter in patients with cardiac disease. Although cineventriculography has been accepted as a clinical standard for left ventricular volume determination, the invasive nature of the technique and the inherent assumptions concerning the geometry of the left ventricle limit its application in repeated assessments.[1-4] Radionuclide methods offer an alternative noninvasive approach[5] but are subject to other limitations. These are mainly related to the detection of edges and end planes as well as the determination of the level of background activity.[6] Previous attempts with standard two-dimensional echocardiographic techniques have also demonstrated several important limitations, particularly in patients with regions of left ventricular asynergy. Factors contributing to the low predictive accuracy of two-dimensional echocardiographic volume measurements include geometric assumptions, image plane positioning errors, and

From the Department of Cardiology, Western General Hospital, Edinburgh; Polish Academy of Sciences, Warsaw; Department of Cardiology, Central Clinical Hospital, Military Medical School, Warsaw; the Department of Medical Physics and Medical Engineering, Royal Infirmary, Edinburgh; and the Cardiovascular Research Unit, University of Edinburgh.
Supported by a grant from the Scottish Office Home and Health Department (No. K/MRS/50/C2357).
Submitted April 29, 1997; accepted Dec. 18, 1997.
Reprint requests: Dr. A. Lange, Department of Cardiology, Western General Hospital, Crewe Road, Edinburgh EH4 2XU, United Kingdom.

0002-8703/98/$5.00 + 0 **4/1/88877**

Figure 1

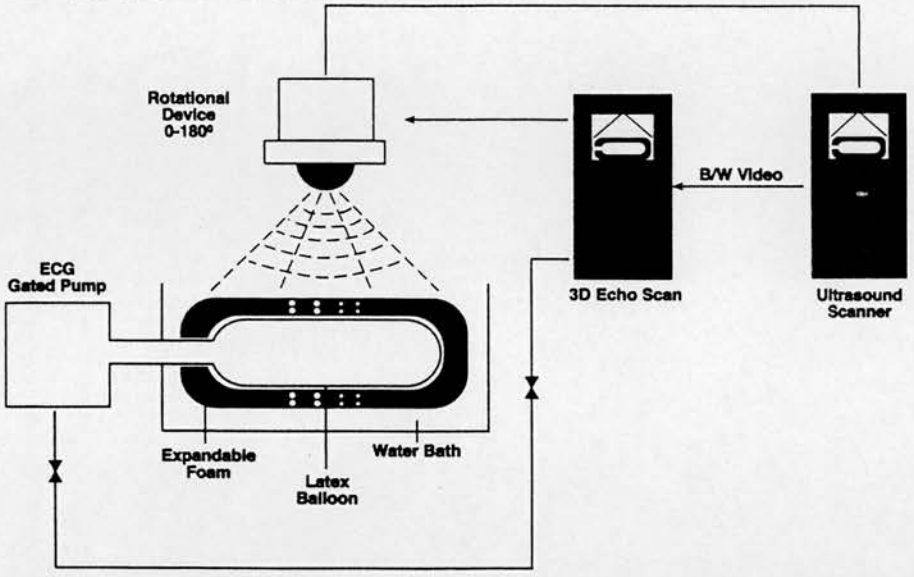

Schematic diagram presenting setup of in vitro study: Electrocardiographically gated acquisition of two-dimensional cross sections of phantom at 2 degree steps over 180 degrees. After completion of acquisition: Off-line processing based on the interpolation of missing information between acquired two-dimensional images at 2-degree steps and conversion of images from polar to cartesian coordinates.

imprecise endocardial boundary detection.[7,8] Recently, a number of three-dimensional (3D) echocardiographic scanners have been developed that address the issue of geometric assumptions.[9-13] These allow 3D images to be constructed from either transthoracic or transesophageal data sets. By using different 3D acquisition systems it has been shown that standard gray-scale imaging (GSI) 3D echocardiography is superior to two-dimensional echocardiography in measuring left ventricular volume[14,15] and that the 3D measurements correlate well with cineventriculography and magnetic resonance imaging.[16,17] However, a major limitation of the transthoracic approach to acquire a 3D data set is the poor quality of GSI images obtained in a substantial proportion of patients.[18,19] This is because the quality of a GSI image is related to the amplitude of the ultrasound signal returning from the interrogated myocardium, which is markedly attenuated by chest wall structures in a substantial number of patients. Doppler myocardial imaging (DMI) is a new ultrasound technique, based on Doppler principles, in which special algorithms are applied to detect myocardial wall motion instead of intracardiac blood flow.[20] The quality of DMI images is dependent on two factors as opposed to one factor in GSI: the amplitude of the returning signal, which is in turn directly dependent on the attenuation, and the frequency shift of this signal, which is relatively independent of the attenuation factor. Thus it is this latter factor that gives rise to the potential of the Doppler technique to provide more complete images of the myocardium than the standard gray-scale technique. The potential clinical application of DMI in quantifying regional left ventricular function[21-24] and in differentiating left ventricular hypertrophy of different causes[25,26] has been previously validated in a series of studies. Also, DMI has been reported to be a superior technique to GSI in displaying the endocardial boundary[27] and providing better-quality 3D reconstructions of heart structures when using the transthoracic approach.[18,19,28,29] This study was designed to compare the accuracy of standard GSI and DMI 3D left ventricular volume measurements in vitro and in vivo. In vitro, volume computations by both DMI and GSI were compared with the true volume of a dynamic tissue-mimicking phantom, and in vivo these were compared with the clinically accepted method of left ventricular volume measurement, cineventriculography.

Methods

In vitro studies

A one-chamber, contracting tissue–mimicking phantom was constructed to simulate left ventricle contraction (Fig. 1). The phantom consisted of a latex balloon (acting as endocardium) placed inside 1 cm thick, tissue-equivalent expandable foam (acting as myocardium) of a shape and size of the left ventricle. To mimic left ventricular contractions, the phantom was connected to the electrocardiogram-gated water pump, and degassed water was pumped into the phantom at a rate of 50 times per minute. A specially constructed valve between the phantom and the pump allowed the water from the phantom chamber to be returned back to the pump.

To validate the accuracy of the changes in volume measurements by both techniques, GSI and DMI, with changes in size of the measured volume, varying known amounts of water were pumped into the phantom (from 24 to 190 ml).

In addition, to define the minimum size of an isolated reflector that could be accurately identified in a 3D reconstruction by this system, rings of resin crystals of known differing dimensions were implanted on the surface of the scanned phantom (Fig. 1).

In vivo

Sixteen randomly selected patients with ischemic heart disease undergoing coronary angiography (eight women, mean age 63 ± 11 years) were studied. All of the 16 patients selected had localized regional wall motion abnormalities as assessed by standard two-dimensional echocardiography. Before entry into the study, informed consent was obtained from all volunteers.

Although computer tomography or magnetic resonance imaging would seem to be a more appropriate technique against which 3D echocardiographic volume measurements were compared, cineventriculography was chosen for practical reasons. All of our patients for whom surgical revascularization was planned had their left ventricles assessed by cineventriculography; therefore we used the results already available for the comparison with 3D echocardiographic measurements.

Three-dimensional imaging protocol

The instrumentation used for the 3D imaging protocol consisted of an ultrasound scanner (Acuson XP 10; Mountain View, Calif.) with DMI software connected to a 3D acquisition system (TomTec Echo-Scan; Munich, Germany). The scanner modifications enabling DMI have been described previously in our work.[24] The velocity range settings used to encode myocardial velocities (3 to 24 cm/sec) are lower than those typically used for blood flow. The display of Doppler information was achieved for tissue instead of blood, with the distinction being made on overall signal strength. No filters were used. Image persistence was turned off to eliminate blurring of the moving myocardium. Color Doppler gain control was also set to achieve maximum color Doppler information in the myocardium while limiting color information within the blood pool. Although the Doppler information is angle dependent, the angle insonation must be taken into account when measuring myocardial velocities only.[20] In previously reported cases in which DMI was used as an acquisition technique to visualize cardiac structures, the incident angle of the ultrasonic beam did not affect the completeness of the image.[18,19,27-29] This is because even very low myocardial velocities with approximate values of approximately 0 to 0.2 m/sec are also color coded by DMI as a mosaic of red and blue.[20] For GSI, the gain was adjusted to optimize the clarity of the phantom in vitro or the endocardial boundaries in the in vivo studies. In the GSI images, the endocardial boundary was defined as the "speckle line" near the myocardial borders. Often the lines were not continuous: In some instances, they would fade and then completely disappear. In such cases, the trace was terminated. However, should another speckle line be present at a slightly different depth that appeared to be the continuation of the first line, then the trace was continued from the first to the second line across the region of "dropout." In DMI, the endocardial boundary was defined as the line of interface between the myocardial wall and the blood pool.

The ultrasound images (both GSI and DMI) were obtained with a 2.5 MHz phased array transducer driven by the transducer mechanical rotational device supplied with the TomTec Echo-Scan. During acquisition, the TomTec Echo-Scan was connected to the ultrasound video output connector of the Acuson scanner with a black/white video cable. Thus when DMI images were acquired, the color Doppler signal was transferred as a black and white video signal to the TomTec Echo-Scan.

In the in vitro studies, consecutive imaging frames were acquired from the contracting phantom by electrocardiographic gating. A mechanical device rotated the transducer at 2 degree steps over 180 degrees (Fig. 1). By using a polyhedral volume algorithm, the minimum and maximum volumes (systolic and diastolic) of the contracting phantom were calculated from consecutive 1 mm thick short-axis slices. To validate the accuracy of both imaging techniques in 3D volume measurements, 17 different volumes of a tested object were measured during maximum and minimum contractions of the phantom. This was achieved by pumping differing known amounts of water into the chamber of the contracting phantom.

For the in vivo studies, electrocardiographic and respiration gating was used. The expiratory phase of breathing was used for gating respiration. During the acquisition procedure the transducer was placed in the standard apical position and was rotated by the mechanical rotational device at 2 degree steps over 180 degrees. On the basis of the gating

Figure 2

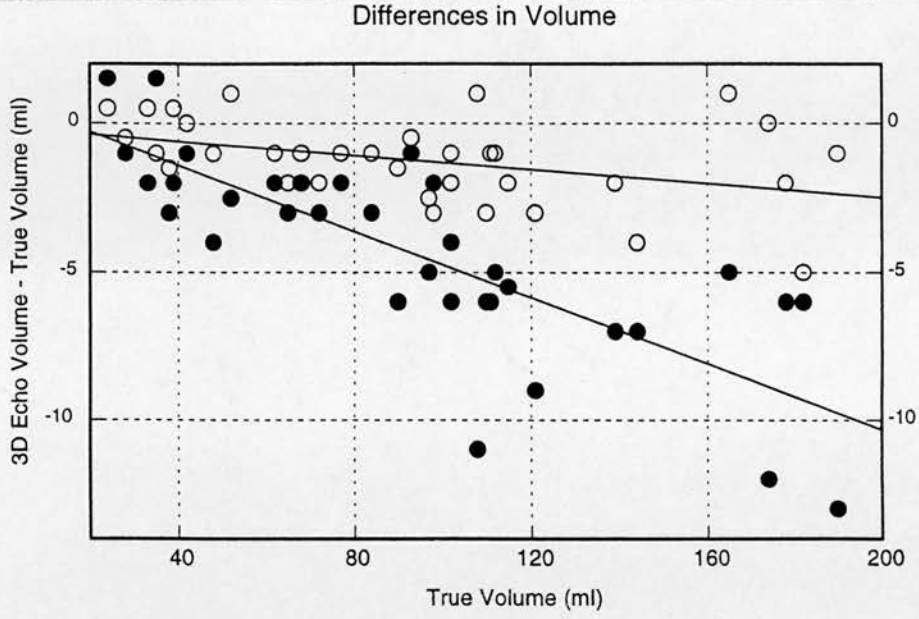

In vitro relation between magnitude and direction of systematic error (bias) and size of volume being measured. Difference between estimated and true volume is plotted against true volume. Systematic error for DMI (*open circles*) remains relatively constant over range of volumes measured, whereas for GSI (*solid circles*) it is greater at larger volumes.

parameters, the computer acquired one complete cardiac cycle at the acquisition start position and recorded it at 25 frames/sec. When one cardiac cycle had been stored in the computer's random access memory, the steering control advanced the transducer one step further. A total of 90 cardiac cycles were stored during one acquisition. To create the 3D data set, additional points needed to be interpolated (offline, after processing) between the acquired 2 degree step, two-dimensional images. The same protocol was used for GSI and DMI acquisition.

Left ventricular volumes were calculated at end-diastole and end-systole from both GSI and DMI data sets. The endocardial boundary was manually traced in a series of short-axis 5 mm thick images, which were acquired with reference to the predefined apical long axis of the image. Left ventricular volume was computed by using the same 3D polyhedral volume algorithm as used in the in vitro study. In assessing volumes, the papillary muscles were excluded from the chamber volume.

The results obtained from 3D ultrasound images were then compared with those obtained from cineventriculography.

Cineventriculography

Within 2 hours after the 3D echocardiograms were performed, the patients underwent diagnostic coronary angiography and cineventriculography. All cineventriculograms were recorded at 30 frames per second during the power injection of 30 to 40 ml of iopamidol at 10 ml/sec through a 6F pigtail catheter. In all patients, two views were obtained: 30 degree right anterior oblique (RAO) and 60 degree left anterior oblique (LAO). The first three sinus beats recorded after the contrast injection that did not follow a premature beat were used for volume calculation. Because of the lack of software to automatically calculate left ventricular volume from two views, we measured left ventricular volumes separately for 30 degree RAO and 60 degree LAO views and then the average value was taken from both measurements. Papillary muscles were excluded in the volume calculation. End-diastole was defined as the visually estimated largest silhouette and end-systole as the smallest silhouette of the left ventricle. The contours were then hand-traced and the volumes calculated by using the disk-summation method as previously described and validated by others.[1,30]

Statistical analysis

In vitro studies. The error of inaccuracy of both GSI and DMI 3D volume estimation was assessed by calculating two different parameters: bias (systematic error) and imprecision (random error).[31]

The differences between both GSI and DMI volume mea-

Figure 3

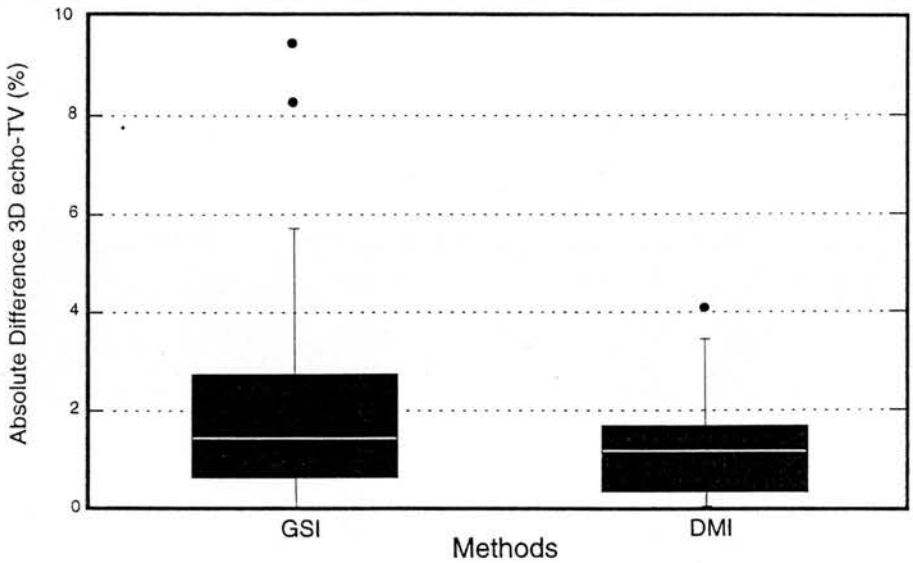

In vitro systematic error and imprecision of both ultrasound techniques. Position of box in relation to zero line is indicator of systematic error. Vertical height of box and its error bars are indicator of imprecision.

surements taken during minimum and maximum phantom contraction and true volume were compared with the true volume of the phantom. This allowed us to assess whether the two tested ultrasound techniques have a tendency to underestimate or overestimate the measured volume. To determine whether the changes in the magnitude of the systematic error varied according to the changes in the volume size, 17 different volumes were measured and these values were compared by linear regression analysis. The systematic error was also expressed as a percentage of the volume being measured [percentage error = (measured volume – true volume) / true volume × 100%], and the mean percentage error ± 1 SD was calculated for each method. Finally, the mean percent error was compared by nonparametric methods by using analysis of variance (Friedman ANOVA).

To assess the accuracy of each method, each measurement was adjusted for systematic error by applying a correcting factor based on the linear regression of the measured 3D GSI and DMI volumes with the respective true volume. In these calculations a predicted true volume was substituted for each measured volume. After this adjustment, the difference between the predicted true volume and the true volume was calculated, and the percentage error was expressed as an absolute value. The accuracy of each technique was compared by applying the Friedman ANOVA test.

In vivo studies. End-systolic and end-diastolic volumes of the left ventricle were assessed by both 3D echocardiography (GSI and DMI) and cineventriculography and are presented as mean ± SD. Because we did not have a true value of the measured left ventricular volume but a value obtained from an accepted clinical standard, both GSI and DMI 3D volume measurements were correlated, by using linear regression analysis, to the volumes obtained by cineventriculography. To assess the level of agreement between GSI versus cineventriculography and DMI versus cineventriculography and to test the reproducibility of both 3D ultrasound techniques, Bland and Altman's test[31] was used. The 95% limits of agreement were calculated as twice the standard deviation and the results were compared by Friedman ANOVA test. Interobserver variability and intraobserver variability were assessed in a group of 10 randomly selected patients. Finally, the endocardial boundary definition obtained by GSI and DMI was compared by using McNemars test for marginal homogeneity.[32] This expresses the percentage of a clearly defined endocardial boundary to the circumference of the inner dimension for each measured slice of the ventricle.[31] A value of $p < 0.05$ was considered to be significant.

Results

In vitro studies

Both 3D ultrasound techniques underestimated the true volume of the phantom, but the systematic error (bias) was significantly smaller for DMI than for GSI (–1.2% ± 1.5% vs –4.3% ± 3.1%; $p < 0.01$). Fig. 2 shows that the systematic error for 3D DMI was more constant ($r = –0.40$; $p < 0.02$) than GSI ($r = –0.79$; $p < 0.001$) over the range of different sizes of true volume.

Thus the magnitude of the bias was smaller in DMI than in GSI when the measurements were taken from bigger volumes.

Fig. 3 shows that random error was low in both 3D ultrasonic techniques: for GSI 2.1% ± 2.2% and for DMI 1.2% ± 1.0%; $p = 0.086$.

Finally, we have shown that a 1 mm isolated crystal may be correctly identified and measured in a 3D DMI reconstruction (see Fig. 4).

In vivo studies

The mean end-systolic volumes for 3D echocardiography were for GSI 70 ± 15 ml, for DMI 75 ± 18 ml; and for cineventriculography 77 ± 18 ml. For end-diastole these values were 127 ± 18 ml, 140 ± 20 ml, and 144 ± 22 ml, respectively.

There was a good correlation between both 3D ultrasonic techniques and cineventriculography (GSI $r = 0.98$, $p < 0.0001$; DMI $r = 0.99$, $p < 0.0001$). The standard error of estimates for GSI was ±7 ml and for DMI ±5 ml. In 3D echocardiography the mean difference for end-diastole by using GSI was –12.6 ml, the limits of agreement being ±18 ml. For end-systole these values were –6.5 ± 10.6 ml, respectively. By using DMI the mean difference for end-diastole was –4.2 and ±10.6 ml and for end-systole –1.5 ± 10 ml (see Fig. 5). The magnitude of the difference between 3D echocardiography and cineventriculography in volume measurement was significantly smaller for DMI than for GSI for both end-diastole and end-systole ($p < 0.01$).

Finally, DMI proved to be significantly more efficient than the standard GSI in endocardial boundary detection at both end-diastole (80% ± 8% vs 67% ± 16%, respectively, $p < 0.05$) and end-systole (85% ± 7% vs 71% ± 13%, respectively, $p < 0.05$) (McNemars test).

Table I shows the intraobserver and interobserver variability, which was slightly lower for DMI.

Figure 4

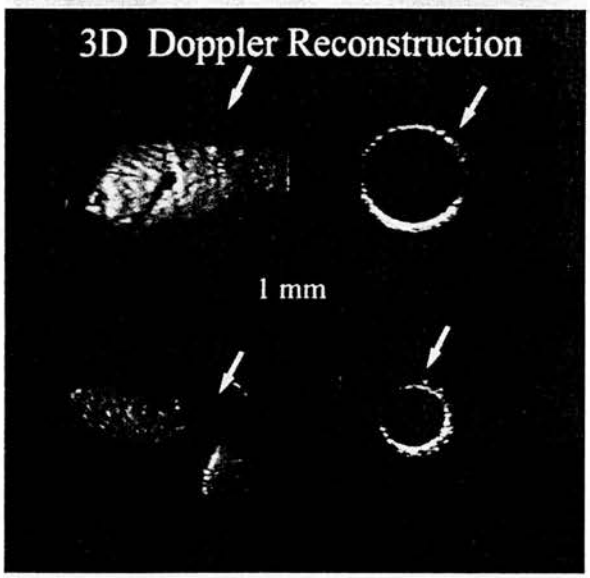

Three-dimensional reconstruction of tested tissue-mimicking phantom during minimum and maximum contractions. *Arrows* indicate reconstructed resin crystals of 1 mm dimension. From this reconstruction angle, 2 mm crystals are not visible.

Table I. Interobserver and intraobserver variability

	Interobserver variability		Intraobserver variability	
ml	**Mean ± SD**	**%**	**Mean ± SD**	**%**
EDV				
DMI	1.9 ± 5.8	9.7	1.2 ± 3.0	5.3
GSI	2.2 ± 5.9	10.9	1.8 ± 4.4	8.7
ESV				
DMI	0.9 ± 2.3	7.1	0.7 ± 2.0	6.8
GSI	1.3 ± 3.0	9.8	1.1 ± 2.9	9.2

EDV, End-diastolic volume; *ESV*, end-systolic volume.

Discussion

In vitro, 3D volumes were measured independently by the two techniques and the results were then correlated with the true volume of the tested object. In vivo, computation of left ventricular volumes by 3D GSI and DMI were compared with measurements obtained by using an accepted clinical method, cineventriculography. Previous studies that were based only on GSI have demonstrated a high degree of accuracy in in vitro 3D volume computation.[33-35] In vivo, although GSI 3D echocardiography slightly underestimates the measured volume, it has been found to be superior to GSI two-dimensional echocardiography.[14-16] A major potential problem in transthoracic GSI 3D echocardiography is the poor image quality obtained in a substantial number of patients.[36] Superimposed lungs and chest wall structures attenuate the ultrasound signal reducing the signal to noise ratio, making it difficult to acquire a sufficient number of clear images to represent the left ventricular cavity accurately. It is possible to overcome this problem by using

Figure 5

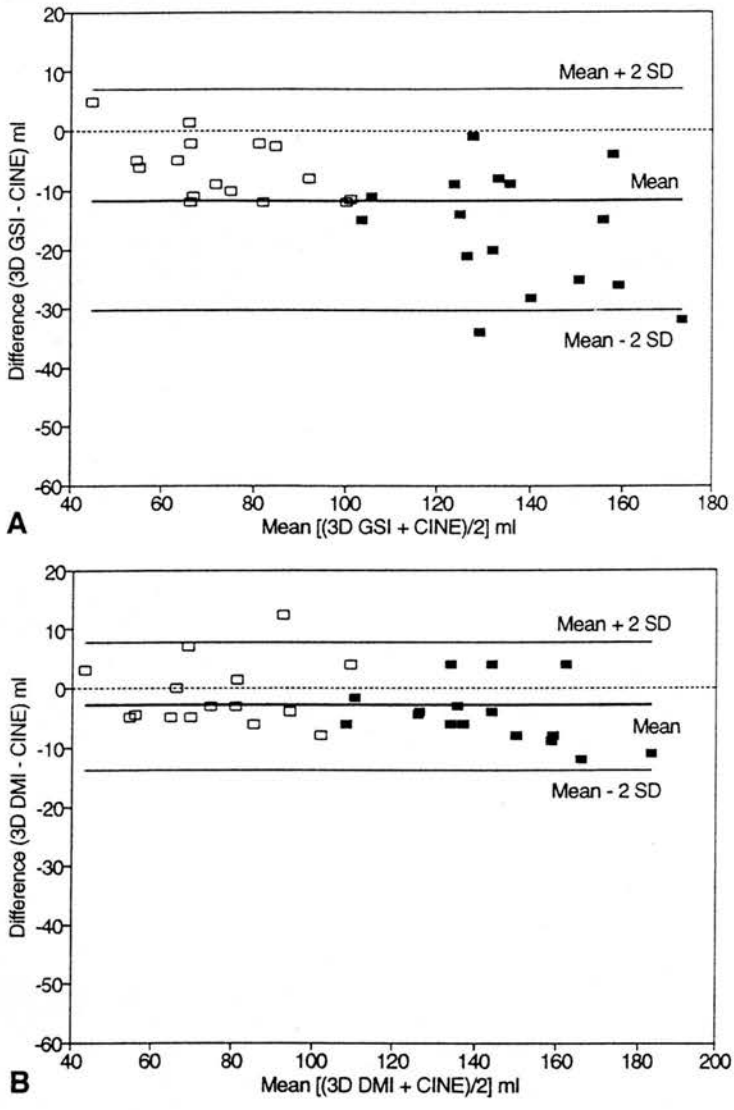

Difference between 3D GSI (A), DMI (B), and cineventriculography plotted against mean value. Results are shown for end-diastolic volumes (*solid squares*) and end-systolic volumes (*open squares*). *Lines* indicate mean of differences and limits of agreement ±2 SD from mean difference.

a transesophageal approach. Although it has been documented that this can be performed with a low level of accompanying risk, it still remains a semiinvasive technique, poorly tolerated by a significant number of patients.[37] DMI offers clear advantages over the standard GSI technique for transthoracic data acquisition. Unlike GSI, the quality of DMI images is dependent on two parameters: the amplitude of the ultrasound signal, which is directly affected by chest wall attenuation, and the frequency shift of ultrasound signal, which is relatively independent of the attenuation. Thus where ultrasound attenuation produced by overlying tissues is a problem, DMI could provide better quality transthoracic images in a substantial number of patients (see Fig. 6). This was confirmed in our recent study in which DMI was more a effective tech-

Figure 6

Example of transthoracic 3D reconstruction of left ventricle obtained from 54-year-old man. *Left,* DMI technique; *right,* GSI technique.

nique than GSI in 3D reconstructing of a surgical view of secundum atrial septal defects in older patients, in whom the attenuation of an ultrasound signal by chest wall structures is higher than that in children.[29] In this study, we have demonstrated that in vitro, both techniques slightly underestimated the true volume of tissue-mimicking phantom, and although there was no significant difference in the percentage of accuracy between the two, the systematic error was not only significantly smaller for DMI but also remained fairly constant over the range of volumes tested. Although a spatial resolution of two-dimensional DMI technique is slightly lower than a GSI technique,[20] we have shown that for all studied gain and depth settings, the minimum size of a relatively strong isolated reflector that may be correctly distinguished and measured in a three-dimensional DMI reconstruction is 1 mm. This gives a guide as to how accurate measurements taken from 3D images can be. In vivo, the correlation between volume measurements by 3D echocardiography and those obtained by cineventriculography was very good. However, 3D volume measurements obtained by DMI had significantly closer agreement with those generated by cineventriculography than did those from GSI. Additionally, by using McNemars test for marginal homogeneity, we have shown the superior boundary definition provided by DMI. This is also in agreement with our previous study in which we have shown that the endocardial boundary is more reliably displayed and visually easier to detect by using DMI than by using GSI.[27]

On the basis of our results, we can conclude that if 3D echocardiography is to be used to estimate left ventricular volume, DMI is the ultrasound technique of choice.

Limitations

A potential source of error in both the in vitro and in vivo studies was the small differences in frame rate of the studied techniques. This was approximately 20 frames per second for DMI as opposed to 25 frames per second for GSI and 30 frames per second for cineventriculography. As a consequence, end-systolic and end-diastolic volume measurements could have been measured in slightly different time periods of the heart cycle. Echocardiography and cineventriculography detect different endocardial outlines; additionally, cineventriculography still makes assumptions about left ventricular shape. Finally, the changes in the heart rate and expanded circulating volume during cineventriculography may have contributed to differences between the left ventricular volume measurements and 3D echocardiography.

We thank Mr. Bill Adams of the Department of Public Health Sciences, University of Edinburgh, for his advice on the statistical analysis and Mr. Paul Johnston of the Department of Medical Illustration, University of Edinburgh, for technical support. We give special thanks to Dr. Maria Dlugolecka for help in preparing the manuscript.

References

1. Dodge HT, Sandler H, Ballew DW, Lord JD Jr. The use of biplane angiocardiography for the measurement of left ventricular volume in man. Am Heart J 1960;60:762-76.
2. Vas R, Diamond GA, Forrester JS, Whiting JS, Swan HJC. Computer enhancement of direct and venous-injected left ventricular contrast angiography. Am Heart J 1981;102:719-28.
3. Wyme J, Green LH, Mann T, Levin D, Grossman W. Estimation of left ventricular volumes in man from biplane cineangiograms filmed in oblique projections. Am J Cardiol 1978;41:726-32.
4. Schnittger I, Fitzgerald PJ, Daughters GT, Ingels NB, Kantrowitz NE, Schwarzkopf A, et al. Limitations of comparing left ventricular volumes by two-dimensional echocardiography, myocardial markers and cineangiography. Am J Cardiol 1982;50:512-9.
5. Levy WC, Cerqueira MD, Matsuoka DT, Harp GD, Sheehan FH, Stratton JR. Four radionuclide methods for left ventricular volume determination: comparison of manual and an automated technique. J Nucl Med 1992;33:763-70.
6. Starling MR, Crawford MH, Sorensen SG, Levi B, Richards KL, O'Rourke RA. Comparative accuracy of apical biplane cross-sectional echocardiography and gated equilibrium radionuclide angiography for estimating left ventricular size and performance. Circulation 1981; 63:1075-84.
7. Wyatt HL, Heng MK, Meerbaum S, Hestenes JD, Cobo JM, Davidson RM, et al. Cross-sectional echocardiography, II: analysis of mathematic models for quantifying volume of the formalin-fixed left ventricle. Circulation 1980;61:1119-25.
8. Tortoledo FA, Quinones MA, Fernandez GC, Waggoner AD, Winters WL. Quantification of left ventricular volumes by two-dimensional echocardiography: a simplified and accurate approach. Circulation 1982; 67:579-84.
9. Geiser EA, Ariet M, Conetta DA, Lupiewicz SM, Chrisite LG Jr, Conti CR. Dynamic three-dimensional reconstruction of the intact human left ventricle: technique and initial observations in patients. Am Heart J 1982;103:1056-65.
10. Nixon JV, Saffer SI, Lipscomb K, Blomqvist CG. Three-dimensional echoventriculography. Am Heart J 1983;106:435-43.
11. Ghosh A, Nanda NC, Maurer G. Three-dimensional reconstruction of echocardiographic images using the rotation method. Ultrasound Med Biol 1982;8:655-61.
12. Sawada H, Fujii J, Kato K, Onoe M, Kuno Y. Three-dimensional reconstruction of the left ventricle from multiple cross sectional echocardiograms. Br Heart J 1983;50:438-42.
13. Snyder JE, Kisslo J, von Ramm OT. Real-time orthogonal mode scanning of the heart, I: system design. J Am Coll Cardiol 1986;7:1279-83.
14. Schroeder KM, Sapin PM, King DL, Smith MD, DeMaria AN. Three-dimensional echocardiographic volume computation: in vitro comparison to standard two-dimensional echocardiography. J Am Soc Echocardiogr 1993;6:467-75.
15. Gopal AS, Keller AM, Rigling R, King DL Jr, King DL. Left ventricular volume and endocardial surface area by three-dimensional echocardiography: comparison to two-dimensional echocardiography and magnetic resonance imaging in normal subjects. J Am Coll Cardiol 1993;22:258-70.
16. Sapin PM, Schroder KM, Gopal AS, Smith MD, DeMaria AN, King DL. Comparison of two- and three-dimensional echocardiography with cineventriculography for measurement of left ventricular volume in patients. J Am Coll Cardiol 1994;24:1054-63.
17. Pini R, Giannazzo G, Bari MD, Innocenti F, Rega L, Casolo G, et al. Transthoracic three-dimensional echocardiographic reconstruction of left and right ventricles: in vitro validation and comparison with magnetic resonance imaging. Am Heart J 1997;133:221-9.
18. Lange A, Anderson T, Bouki KP, Fenn LN, Palka P, McDicken WN, et al. Validation of volume measurements by 3-dimensional echocardiography using Doppler myocardial imaging technique: in vitro and in vivo study [abstract]. Circulation 1995;92[suppl I]:I-798.
19. Azevedo J, Garcia-Fernandez M, Puerta P, Moreno M, SanRoman D, Torrecilla E, et al. Dynamic 3-dimensional echocardiographic reconstruction of the left ventricle using color Doppler myocardial tissue imaging technique: in vivo experimental and clinical study. J Am Coll Cardiol 1996;27[suppl A]:901-47.
20. Fleming AD, Palka P, McDicken WN, Fenn LN, Sutherland GR. Verification of cardiac Doppler tissue images using gray-scale M-mode images. Ultrasound Med Biol 1996;22:573-81.
21. Donovan CL, Armstrong WF, Bach DS. Quantitative Doppler tissue imaging of the left ventricular myocardium: validation in normal subjects. Am Heart J 1995;130:100-4.
22. Miyatake K, Yamagishi M, Tanaka N, Uematsu M, Yamazaki N, Mine Y, et al. New method for evaluating left ventricular wall motion by color coded tissue Doppler imaging: in vitro and in vivo studies. J Am Coll Cardiol 1995;25:717-24.
23. Gorcsan J III, Gulati VK, Mandarino WA, Katz WE. Color-coded measures of myocardial velocity throughout the cardiac cycle by tissue Doppler imaging to quantify regional left ventricular function. Am Heart J 1996;131:1203-13.
24. Palka P, Lange A, Fleming AD, Fenn LN, Bouki KP, Shaw TRD, et al. Age-related transmural peak mean velocities and peak velocity gradients by Doppler myocardial imaging in normal subjects. Eur Heart J 1996;17:940-50.
25. Rodriguez L, Garcia M, Ares M, Griffin BP, Nakatani S, Thomas JD. Assessment of mitral annular dynamics during diastole by Doppler tissue imaging: comparison with mitral Doppler inflow in subjects without heart disease and in patients with left ventricular hypertrophy. Am Heart J 1996;131:982-7.
26. Palka P, Lange A, Fleming AD, Donnelley JE, Dutka DP, Starkey IR, et al. Differences in myocardial velocity gradient measured throughout the cardiac cycle in patients with hypertrophic cardiomyopathy, athletes and patients with left ventricular hypertrophy due to hypertension. J Am Coll Cardiol 1997;30:760-8.
27. Lange A, Palka P, Caso P, Fenn LN, Olszewski R, Ramo MP, et al. Doppler myocardial imaging vs. B-mode gray-scale imaging: a comparative in vitro and in vivo study into their relative efficacy in endocardial boundary detection. Ultrasound Med Biol 1997;23:69-75.
28. Lange A, Wright RA, Al-Nafusi A, Sang C, Palka P, Sutherland GR. Doppler myocardial imaging: a new method of data acquisition for three-dimensional echocardiography. J Am Soc Echocardiogr 1996;9: 918-21.
29. Lange A, Walayat M, Turnbull CM, Palka P, Mankad P, Sutherland GR, et al. Assessment of atrial septal defect morphology by transthoracic three dimensional echocardiography using standard gray scale and Doppler myocardial imaging techniques: comparison with magnetic resonance imaging and intraoperative findings. Heart 1997;78: 382-9.
30. Erbel R, Schweizer P, Lambertz H, Henn G, Meyer J, Krebs W, et al. Echoventriculography: a simultaneous analysis of two-dimensional echocardiography and cineventriculography. Circulation 1983;67: 205-15.

31. Bland JM, Altman DG. Statistical methods for assessing agreement between two methods of clinical measurement. Lancet 1986;1:307-10.
32. Bishop YMM, Fienberg SE, Holland PW. Discrete multivariate analysis. Theory and practice. In: Analysis of square tables: symmetry and marginal homogeneity. Cambridge, Mass./London, England: The MIT Press; 1975. p. 281-310.
33. Gopal AS, Keller AM, Shen Z, Sapin PM, Schroeder KM, King DL Jr, et al. Three-dimensional echocardiography: in vitro and in vivo validation of left ventricular mass and comparison with conventional echocardiographic methods. J Am Coll Cardiol 1994;24:504-13.
34. Kuroda T, Kinter TM, Seward JB, Yanagi H, Greenleaf JF. Accuracy of three-dimensional volume measurement using biplane transesophageal echocardiographic probe: in vitro experiment. J Am Soc Echocardiogr 1991;4:475-84.
35. Sapin PM, Schroeder KD, Smith MD, DeMaria AN, King DL. Three-dimensional echocardiographic measurement of left ventricular volume in vitro: comparison with two-dimensional echocardiography and cineventriculography. J Am Coll Cardiol 1993;22:1530-7.
36. Pearlman AS. Measurement of left ventricular volume by three-dimensional echocardiography: present promise and potential problems [editorial]. J Am Coll Cardiol 1993;22:1538-40.
37. Daniel WG, Erbel R, Kasper W, Visser CA, Engberding R, Sutherland GR, et al. Safety of transesophageal echocardiography: a multicenter survey of 10,419 examinations. Circulation 1991;83:817-21.